Palacky University in Olomouc
Faculty of Science
Department of Botany

Ph.D. thesis

Role of Vacuolar Cation Exchanger In Leaf Development

Dejana Jurišić-Knežev

Study program P1501 Biology

Supervisor: doc. RNDr. Martin Fellner, Ph.D.
Co-supervisor: Véronique Bergougnoux, Ph.D.

Olomouc, 2013

I hereby declare that this Ph.D. thesis has been fully worked out by me with the use of cited references.

Olomouc, 2013 Dejana Jurišić-Knežev

Bibliographical Identification

Author's first name and surname: Mgr. Dejana Jurišić-Knežev

Title: Role of Vacuolar Cation Exchanger in Leaf Development

Type of thesis: Ph.D. thesis

Department: Department of Botany

Supervisor: Doc. RNDr. Martin Fellner, Ph.D.

Co-supervisor: Véronique Bergougnoux, Ph.D.

The year of presentation: 2013

Abstract: Growth of plants is regulated by a complex interplay between internal and external factors, such as hormones and light. Plant hormone auxin performs its action via at least two auxin receptors: TIR1 and ABP1 (Auxin-Binding-Protein 1). It has been shown that during auxin signalling transduction a level of calcium (Ca^{2+}) in the cytoplasm increases. This elevation is partially regulated by Cation eXchangers (CAXs), specifically by Ca^{2+}/H^{+} antiporters. Since ABPs are putative auxin receptors it can be assumed that auxin via ABPs increases the level of Ca^{2+} in the cell. In this thesis, maize loss-off-function mutants in *ABP1* and/or *ABP4* genes were used in order to unravel the relationship between auxin, Ca^{2+}, ABP1, ABP4 and CAXs in maize. Phenotype analysis of single *abp1* and *abp4* and double *abp1/abp4* mutants revealed that ABP1 and ABP4 are involved in maize leaf development as well as in the growth of coleoptile, mesocotyl and primary root of maize seedling. Moreover, ABP1 and ABP4 mediate the sensitivity of maize seedlings to exogenous auxin and are involved in auxin-regulated growth under different light conditions (blue and red light). Two putative Ca^{2+}/H^{+} exchangers in maize, homologs of *Arabidopsis AtCAX1*, designated as *ZmCAX2* and *ZmCAX3*, were cloned and characterized and their relationship with ABP1 and ABP4 was assessed through Ca^{2+}/auxin-induced expression of *ZmCAXs*. The results presented in this work contribute to the understanding of the role of ABP1 and ABP4 in maize development and suggest that the relationship between auxin, Ca^{2+}, ABPs and CAXs occurs at different levels of maize leaf and whole seedling development.

Keywords: auxin, Auxin-Binding Proteins (ABPs), calcium (Ca^{2+}), CAtion eXchanger (CAX), light, maize (*Zea mays* L.), plant development.

Number of pages: 116

Number of appendices: 1

Language: English

Bibliografická identifikace

Jméno a příjmení autora: Mgr. Dejana Jurišić-Knežev

Název práce: Úloha vakuolárního kationtového přenašeče ve vývoji listů

Typ práce: dizertační práce

Pracoviště: Katedra botaniky

Vedoucí práce: Doc. RNDr. Martin Fellner, Ph.D.

Školitel specialista: Véronique Bergougnoux, Ph.D.

Rok obhajoby: 2013

Abstrakt: Růst rostlin je regulován složitou interakcí vnitřních a vnějších faktorů, jako jsou např. hormony a světlo. Rostlinný hormon auxin účinkuje prostřednictvím nejméně dvou receptorů: TIR1 a ABP1 (Auxin-Binding-Protein1). Bylo ukázáno, že během přenosu auxinového signálu se zvyšuje hladina vápníku (Ca^{2+}) v cytoplazmě. Toto zvýšení je částečně regulováno kationtovými přenašeči CAXs (Cation eXchangers), specifickými Ca^{2+}/H^{+} antiporty. Protože ABP jsou domnělé auxinové receptory, je možno předpokládat, že auxin, prostřednictvím ABP, zvyšuje hladinu Ca^{2+} v buňce. K tomu, aby bylo možné odhalit vztah mezi auxinem, Ca^{2+} a proteiny ABP1, ABP4 a CAX, byly k experimentům použiti mutanti kukuřice, vykazující ztrátu funkce genů *ABP1* a/nebo *ABP4*, Fenotypová analýza jednoduchých mutantů *abp1* a *abp4* a dvojitého mutanta *abp1/abp4* odhalila, že ABP1 a ABP4 jsou zapojeny v regulaci vývoje listu kukuřice a v růstu kukuřičné koleoptile, mezokotylu a primárního kořene. Bylo dále zjištěno, že ABP1 a ABP4 zprostředkují citlivost rostlin kukuřice k exogennímu auxinu, a že jsou zapojeny v auxinem-regulovaném růstu rostlin na světle (modrém a červeném). Výsledkem dizertační práce je rovněž klonování a charakterizace dvou domnělých Ca^{2+}/H^{+} přenašečů, *ZmCAX2* a *ZmCAX3*, homologních k *AtCAX1* u *Arabidopsis*. Vztah obou přenašečů k ABP1 a ABP4 byl studován pomocí exprese *ZmCAX2* a *ZmCAX3* v mutantech *abp* indukované Ca^{2+} a auxinem. Výsledky práce přispívají k porozumění úlohy ABP1 a ABP4 při vývoji kukuřice a naznačují, že interakce mezi auxinem, Ca^{2+}, ABP a CAX se děje na různých úrovních vývoje listů i celých rostlin.

Klíčová slova: auxin, Auxin-Binding Proteiny (ABPs), vápník (Ca^{2+}), CAtion eXchanger (CAX), světlo, kukuřice (*Zea mays* L.), vývoj rostliny.

Počet stran: 116

Počet příloh: 1

Jazyk: anglický

Acknowledgement

The work described in this Ph.D. thesis was carried out in the group of Dr. Martin Fellner, at the Department of Cell Biology and Genetics, Palacky University in Olomouc. I am particularly thankful to Martin for accepting me as a Ph.D. student in his laboratory and for giving me the opportunity to work on this exciting project. I would like to express my gratitude for his ideas, support, patience, attention and motivation during my Ph.D. thesis.

I am especially grateful to Dr. Véronique Bergougnoux, my co-supervisor, for her invaluable help, advices, objections, patience and support during my Ph.D. studies. Many thanks to all the present and former members of the Martin's lab: Renáta Plotzová, Marie Karlická, Věra Chytilová, Jana Bořucká, Jan Humplík, David Zalabák, Tereza Vaclová, Mária Čudejková, Jiří Řehulka, Marta Hlobilová and Zdeněk Svoboda for their help, nice working atmosphere and for making my stay in the Czech Republic unforgettable!

Thanks to all the colleagues at the department who have helped with scientific advices or by providing the necessary infrastructure. I would especially like to thank Mrs. Zdeňka Sladká for her precious help and excellent technical support! I also thank professor Alan M. Jones (University of North Carolina, USA) for providing the maize *abp* mutant seeds and Dr. David Milde (Palacky University, Department of Analytical Chemistry) for the calcium content analysis.

This work was financially supported by the European EU FP6 Marie Curie Research Training Network VaTEP (www.vatep.eu) (grant No. MRTN-CT-2006-035833). My special thanks go to the members of the VaTEP project management (Potsdam University, Germany), Dr. Katrin Czempinski and Dr. Regina Gerber, for their patience and invaluable help in dealing with bureaucratic issues during my Ph.D.

Lastly, I would like to thank my family. Without their constant and unconditional support I would not have been able to reach this final step and this is why they deserve a big THANK YOU! I am also grateful to my parents-in-law for their support. The last, but not the least, I would like to thank my husband Zoran and our adorable daughter Milica. Thank you for supporting me, believing in me and being there whenever I needed you!

To my mother...

Content

1 Introduction

Auxin is a hormone involved in many aspects of plant growth and development such as embryogenesis, lateral root formation, vascular development, tropism, apical dominance and senescence (reviewed in Kepinski and Leyser, 2005a). At the cellular level, auxin is involved in the regulation of cell elongation, cell division and cell differentiation.

The most abundant naturally occurring auxin is indole-3-acetic acid (IAA) (Figure 1.1). Many synthetic auxins, such as α-naphthalene acetic acid (α-NAA) and 2,4-dichlorophenoxyacetic acid (2,4-D) (Figure 1.1) are available and are used both in experimental approaches and commercially, mostly as herbicides.

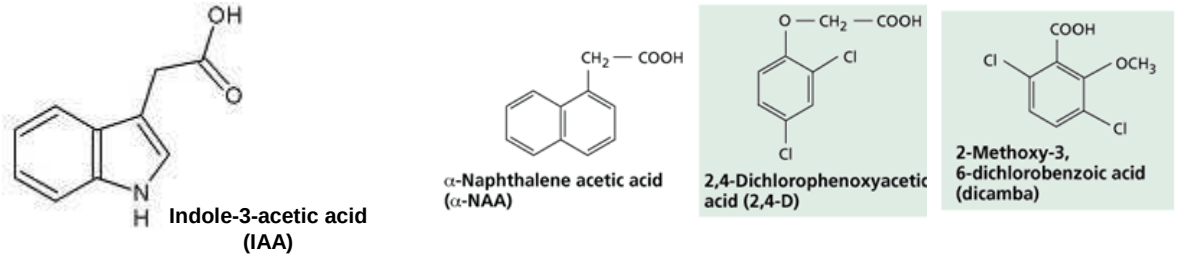

Figure 1.1 Indole-3-acetic acid (IAA), the most abundant naturally occurring auxin and the structure of some synthetic auxins.

Most of these synthetic auxins are used as herbicides in horticulture and agriculture. The most widely used are probably dicamba and 2,4-D, which are not subject to breakdown by the plant and are very stable (Photo taken from Plant Physiology online, 4th edition and adapted).

1.1 Auxin perception

One of the first steps of a hormone action is its binding to a receptor. Beside the described function of auxin receptors from the TRANSPORT INHIBITOR RESPONSE 1/AUXIN-BINDING F-BOX PROTEIN (TIR1/AFB) family, putative auxin receptor, the AUXIN-BINDING PROTEIN 1 (ABP1) has been identified (reviewed in Tromas and Perrot-Rechenmann, 2010; Shi and Yang, 2011; Sauer and Kleine-Vehn, 2011, and Scherer, 2011).

TIR1 is an F-BOX protein, which is located in the nucleus and allows the recognition and the degradation of repressors of auxin-regulated genes. Once the repressors are degraded, transcription of early auxin response genes can occur directly and leads to auxin responses. *TIR1* encodes a member of large family of F-box proteins involved in regulated proteasome-mediated protein degradation (Kepinski and Leyser, 2005b; Dharmasiri et al, 2005).

ABP1 has been shown to participate in fast auxin responses at the plasma membrane, to mediate auxin control of cell division and cell elongation, and lately, to modulate regulation of early auxin response genes (reviewed in Tromas et al, 2010). All these functions support its role as an extracellular receptor for auxin.

1.1.1 Auxin-Binding Proteins (ABPs)

Auxin binding proteins (ABPs) are components of auxin signalling pathways. They were identified relatively early in the crude fractions of etiolated maize (*Zea mays* L.) coleoptiles (Hertel et al, 1972), and so far, at least five ABPs (in the literature also found as Zm-ERabp (*Zea mays* endoplasmic reticulum auxin-inding protein), 22kDaABP or ABPzm1) have been identified in maize (Schwob et al, 1993). However, their function in maize growth is still poorly understood. In contrast to maize, in *Arabidopsis ABP* gene family is represented by the only one member, *ABP1* (Palme et al, 1992).

1.1.1.1 Structure and localization of ABPs

First sequence data of ABP were obtained in 1990s (Hesse et al, 1989; Tillmann et al, 1989). Hesse et al. (1989) purified three maize ABPs (ABP1, ABP2 and ABP3) from crude coleoptile membrane fractions. Few years later, Schwob et al. (1993) cloned, sequenced and compared three maize genes encoding ABP1, ABP4 and ABP5. In the predicted amino acid sequences four key features were found:

1) a transit peptide,
2) a C-terminal KDEL sequence thought to be involved in retaining proteins in the endoplasmic reticulum (ER),
3) the HRHSCE sequence thought to be responsible for auxin binding (Venis et al, 1992) and
4) an NXT glycosilation site.

ZmABP1 forms homodimer of 20-22 kDa (Hesse et al, 1989). The mature proteins of ZmABP1 and ZmABP4 are 85% identical and the mature protein of *Arabidopsis* ABP1 is 63% and 64% identical to ZmABP1 and ZmABP4 proteins, respectively (Schwob et al, 1993). Despite the presence of the KDEL sequence at the C-terminus (Pelham, 1990; Napier et al, 1992), a fraction of ABP1 reaches the plasma membrane (Leblanc et al, 1999; Diekman et al, 1995). Indeed, in maize, ZmABP1 is mainly located in the ER, with less than 5% exported to the plasma membrane (Henderson et al, 1997; Feckler et al, 2001). In *Arabidopsis* and tobacco, the relative amount of ABP1 in the ER or at the plasma membrane is much more equally distributed than in maize (Shimomura et al, 1999). Therefore, it has been proposed that ABP1 cycles between the ER and the plasma membrane (Jones, 1990; Cross, 1991). The optimal pH binding of NAA is 5.5 with essentially no binding around pH7, which supports the concept that in the ER the ABP1 behaves as a very low affinity auxin binding site, whereas the optimal conditions for its binding are at the plasma membrane (Löbler and Klämbt, 1985).

In maize, ABP1 was detected in roots, mesocotyls, coleoptiles, ears and tassels (reviewed in Jones, 1994). Its abundance correlated with growing regions of etiolated seedling, i.e. apical regions of mesocotyl, basal regions of coleoptiles and young leaves. Using reverse genetic approach and Robertson's *Mutator* transposable element system, Im et al. (2000) isolated and characterized three maize loss-of-function mutants in *ZmABP1* and/or *ZmABP4* genes. Analysing the phenotype of *abp* mutants they observed no significant differences between the single *abp1* and *abp4* and double *abp1/abp4* mutants, suggesting the functional redundancy of these gene family in maize. However, they did observe that the amount of ABP1 protein in *abp4* mutant was 4-7 times higher than in WT, whereas the *ABP1* transcript level did not differ among WT and individual *abp4* mutants. This data indicate that the elimination of the *ABP4* gene activates *ABP1* expression post-transcriptionally. The expression analysis of *ZmABP* genes *1* and *4* revealed that *ZmABP4* gene showed highest expression in male floral tissue while *ZmABP1* was most expressed in female flower parts (Im et al, 2000). In addition, both genes were higher expressed in the coleoptile compared to primary leaves of etiolated *Zea mays* seedlings (Hesse et al, 1993; Schwob et al, 1993). In *Arabidopsis*, ABP1 is crucial for the embryogenesis because its loss-of-function in the null *abp1* mutant causes embryo lethality already at the globular stage (Chen et al, 2001). In

contrast, plants heterozygous for the mutation in the single *Arabidopsis ABP1* gene do not exhibit any phenotype (Chen et al, 2001).

1.1.1.2 Auxin-dependent responses mediated by ABP1

In *Arabidopsis thaliana*, ABP1 is involved in numerous auxin-dependent responses including early responses at the plasma membrane, regulation of gene expression, cell division and cell expansion (reviewed in Tromas et al, 2010).

Auxin induces the decrease of the cytosolic pH (Felle et al, 1986, 1991; Felle, 1988; Shishova and Lindberg, 1999) by promoting proton secretion into the cell wall (Rayle and Cleland, 1980; Cleland et al, 1991) inducing the hyperpolarizaton of the plasma membrane (Ephritikhine et al, 1987). Acidification of the extracellular space can activate cell wall expansins, the major agent for cell wall loosening, thus facilitating future expansion of the cell wall (Cosgrove, 2000). Activation of a voltage-dependent inward rectifying K^+ channels (Figure 1.2) contributes to the water uptake, which is necessary for cell expansion (Rück et al, 1993; Philippar et al, 1999; Philippar et al, 2004).

ABP1 is involved in the binding of auxin at the plasma membrane (Goldsmith, 1993; Timpte, 2001; Napier et al, 2002) and polyclonal antibodies directed against maize ABP1 inhibit auxin-mediated hyperpolarizaton of the plasma membrane (Barbier-Brygoo et al, 1989) and cell division of tobacco mesophyll protoplasts (Fellner et al, 1996). In addition, maize ABP1 added to the tobacco protoplasts enhances the auxin-mediated hyperpolarizaton (Barbier-Brygoo et al, 1989). Taken together, these results suggest that the auxin-induced processes are mediated by ABP1 at the outer face of the plasma membrane (Barbier-Brygoo et al, 1989; Barbier-Brygoo et al, 1991). Since the ABP1 protein has no putative transmembrane region in its sequence, the existence of a “docking protein” has been proposed (Figure 1.2). Auxin is perceived by ABP1, which binds to the docking protein, allowing the transduction of the signal inside the cell (Klämbt, 1990). The C-terminal peptide-binding protein (CBP1) is a potential candidate as docking protein (Shimomura, 2006). However, the direct interaction of CBP1 with ABP1 protein has not been demonstrated yet.

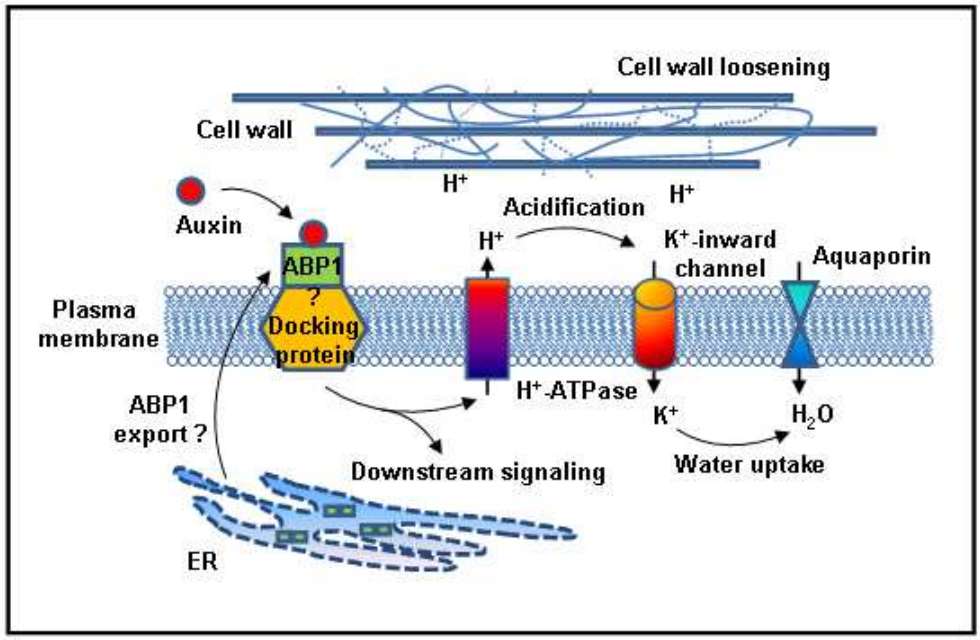

Figure 1.2 Rapid auxin responses mediated by ABP1.

Auxin is perceived at the outer face of the plasma membrane by ABP1, which interacts with an unknown membrane-associated protein or protein complex (docking protein). Binding of auxin to ABP1 activates a cascade of events including activations of the plasma membrane proton pump ATPase (H^+-ATPase) and potassium (K^+) inward rectifying channels. The activation of the H^+-ATPase induces hyperpolarization of the plasma membrane and acidification of the extracellular space which contributes to cell wall loosening. The increase of intracellular K^+ contributes to the uptake of water which is essential for cell expansion. It is not known whether these early events are part of a signalling cascade controlling downstream ABP1-mediated cellular responses (scheme adapted from Tromas et al, 2010)

Chen et al. (2001) proposed a model in which ABP1 is a high-affinity auxin receptor mediating auxin-regulated cell elongation at low auxin levels, whereas another unknown low-affinity auxin receptor exists, which is involved in auxin-regulated cell division. The work of David et al. (2007) with the functional inactivation of ABP1 in tobacco BY2 cells or in tobacco and *Arabidopsis* plants demonstrated that ABP1 is crucial for auxin regulation of the cell cycle, acting at both the G1/S transition and G2/M transition.

The involvement of ABP1 in auxin-induced cell expansion has been reported in maize coleoptile protoplasts and *Arabidopsis* hypocotyls (Steffens et al, 2001) as well as in protoplasts of pea (*Pisum sativum*) stem epidermal cells (Yamagami et al, 2004). ABP1 is involved in the regulation of early auxin response genes. Indeed, the accumulation of 10 of the 14 *Aux/IAA* transcripts rapidly reduced in shoots tissues of young seedlings after a short-

term ABP1 inactivation. In addition, the responsiveness of the same genes to auxin was also affected with an increased response in shoot, whereas a reduced response in roots (Braun et al, 2008). ABP1 is involved in the auxin-dependent stimulation of cell expansion in leaves and acts as a negative regulator of cell expansion in roots as observed for auxin itself (reviewed in Tromas et al, 2010). Recently, evidences were provided that ABP1 is involved in the regulation of polar auxin transport (PAT), thus affecting local auxin concentration and cell expansion (Braun et al, 2008; Robert et al, 2010; Xu et al, 2010; Effendi et al, 2011).

1.2 Relationship between auxin and calcium

Auxin action causes different effects on the cellular level. Auxin induces increase in the cytosolic free calcium (Ca^{2+}) concentrations (Felle, 1988; Shishova and Lindberg, 2004). In addition, as a response to auxin, a cytosolic alkalinization and a transient increase of cytosolic Ca^{2+} concentrations in guard cells have also been reported (Fricker et al, 1994; Gehring et al, 1998)

1.2.1 Role of calcium in plant growth and development and the regulation of calcium homeostasis in plant

Ca^{2+} is an important divalent cation, which plays many essential roles in plants. It is one of the most essential macronutrients for plants as it acts also as a second messenger mediating a wide range of cellular responses (Sanders et al, 2002). Beside its role as a second messenger, it is an essential plant nutrient required for growth and development, especially for the root and shoot, which meristematic regions are very active in cell divisions. Ca^{2+} helps in the formation of microtubules that are essential in the anaphase of mitotic division. Ca^{2+} plays a role in strengthening the cell wall by cross-linking the carboxyl groups of the pectic polymers (Cleland et al, 1990) as well as in maintaining the structural and functional integrity of the outer surface of the plasma membrane (Clarkson and Hanson, 1980). Ca^{2+} is also an important counterion for inorganic and organic anions in the vacuole.

Ca^{2+} concentration in the cytosol fluctuates in response to growth, development and environmental perturbations (Sanders et al, 1999; Curran et al, 2000). Although an elevated

cytosolic Ca^{2+} concentration is necessary for signal transduction, a prolonged increase in Ca^{2+} in cytosol is lethal. Sustained high cytosolic Ca^{2+} concentration is implicated in apoptosis, both during normal development and in hypersensitive responses to pathogens (Levine et al, 1996). Different biotic (the hormones abscisic acid, auxin and giberellin, pathogen elicitors, bacterial and fungal signals and nodulation factors) and abiotic signals (light, low and high temperature, touch, hyperosmotic stress and oxidative stress) can change the free Ca^{2+} concentration in the cytosol (Sanders et al, 2002). The free cytosolic Ca^{2+} is maintained at very low concentrations ranging from 100 to 200 nM (Bush, 1995). However, the pool of cytosolic Ca^{2+} is much higher due to the presence of Ca^{2+}-binding proteins with high affinity for Ca^{2+}. In contrast, cell wall and cellular compartments such as vacuole, ER and mitochondria, contain mM concentrations of Ca^{2+}, making large concentration gradients across the plasma membrane and endomembranes. The vacuole serves as a primary pool of Ca^{2+} ions in plant cells (Ueoka-Nakanishi et al, 1999). During biological responses, Ca^{2+} can be mobilized from and to the vacuole to act as an intracellular signalling molecule (Marty, 1999).

As a second messenger, Ca^{2+} is involved in different signalling pathways including auxin signalling pathway. Two signalling pathways have been proposed to participate in auxin-induced internode growth in pea (*Pisum sativum*): an ABP1-independent pathway, which is dependent on extracellular Ca^{2+} and an ABP1-dependent pathway, and not dependent on extracellular Ca^{2+} (Yamagami et al, 2004). However, latter case does not exclude the involvement of intracellular Ca^{2+} in auxin response through ABPs.

As a consequence of concentration gradients across membranes, Ca^{2+} passively enters the cytosol through Ca^{2+} channels (Chung et al, 2000) either from apoplast or from intracellular organelles (vacuole, ER and mitochondria). The control of Ca^{2+} homeostasis can be achieved through four mechanisms: Ca^{2+} channels, Ca^{2+}-binding proteins (calmodulin, CaM-like proteins, calcineurin B-like proteins and Ca^{2+}-dependent protein kinases), Ca^{2+}-ATPases and Ca^{2+}/H^{+} exchangers (CAtion eXchangers, CAXs) (Sanders et al, 2002; Pittman and Hirschi, 2003).

The channel type, their cellular location and their abundance altogether influence the spatial characteristics of Ca^{2+} intracellular signal. The opening of Ca^{2+} channel influences

local biochemical processes since the diffusion of Ca^{2+} within the cytoplasm is very low (Clapham, 1995) and buffering of Ca^{2+} in the cytoplasm is very high (Malhó et al, 1998; Trewavas, 1999). The opening of Ca^{2+} channel produces a local increase in cytosolic Ca^{2+} concentration that dissipates rapidly after the channel has closed. Trewavas (1999) suggested that the local elevation of Ca^{2+} concentration might generate soluble second messengers, such as inositol trisphosphate or cyclic ADP ribose, that diffuse through the cytoplasm to activate a relay of spatially separated Ca^{2+}-channels. This activation of Ca^{2+} channels produces 'waves' within the cytoplasm by the successive recruitment of receptive Ca^{2+} channels.

The binding of Ca^{2+} to Ca^{2+}-binding proteins changes their structural and/or enzymatic properties and provokes their subsequent interaction with target proteins, which can alter solute transport and enzymatic activities, cytoskeletal orientation, protein phosphorylation cascades and gene expression. The type of specific physiological response is determined not only by the cytosolic Ca^{2+} perturbations, but also by the expression of Ca^{2+}-binding proteins, their affinities for both Ca^{2+} and target proteins and the abundance and activity of the target proteins (reviewed in White and Broadley, 2003).

Ca^{2+} is removed from the cytosol by Ca^{2+}-ATPases and Ca^{2+}/H^{+} exchangers which activity is energized by the pH gradient established by proton pumps, such as H^{+}-ATPase or H^{+}-pyrophosphatase (H^{+}-PP-ase). The stoichiometry of the vacuolar CAX has been estimated to be $3H^{+}/1Ca^{2+}$ (Blackford et al, 1990). Ca^{2+}-ATPases and Ca^{2+}/H^{+} exchangers insure a low cytosolic Ca^{2+} concentration in the cell appropriate for the cytoplasmic metabolism. They provide Ca^{2+} in the ER for the secretory system to function (Blatt, 2000; Ritchie et al, 2002) and remove divalent cations, such as Mg^{2+}, Mn^{2+}, Ni^{2+} or Zn^{2+}, from the cytosol, to support the specialized biochemistry of particular organelles and to prevent mineral toxicities (Hirschi, 2001; Wu et al, 2002). The relative importance of Ca^{2+}-ATPases and Ca^{2+}/H^{+} exchangers in each of these functions is still unclear. Hirschi (2001) suggested that Ca^{2+}-ATPases, which have high affinity (K_m=1-10 μM; Evans and Williams, 1998) but low capacity for Ca^{2+} transport, are responsible for maintaining Ca^{2+} homeostasis in the cytosol of the resting cell, whereas the Ca^{2+}/H^{+} exchangers, which have lower affinities (K_m=10-15 μM) but high capacities for Ca^{2+} transport, are likely to remove Ca^{2+} from the cytosol during Ca^{2+} signals and thereby modulate Ca^{2+} perturbations in the cytosol.

1.2.2 CAtion eXchangers (CAXs)

As mentioned earlier, CAXs belong to the group of proteins that mediate the cations extrusion from the cytosol out of the cell or to the storage compartments maintaining optimal cytosolic ionic concentrations (Shigaki et al, 2006). They can function as Ca^{2+}/H^{+} and/or heavy metal (Cd^{2+} and Mn^{2+})/H^{+} exchangers (Hirschi et al, 1996; Hirschi et al, 2000). Several Ca^{2+}/H^{+} antiporters have been isolated from bacteria, fungi and plants (Ivey et al, 1993; Cunningham and Fink, 1996; Hirschi et al, 1996). The phenotypes of *cax* mutants suggest the involvement of CAXs and Ca^{2+} signalling in several processes such as plant development, hormonal responses or cold acclimation (Catala et al, 2003; Cheng et al, 2003, 2005). In plants, they can be localized at the tonoplast, the plasma membrane or the thylakoid membrane (Hirschi, 2001; Cheng et al, 2003; Kasai and Muto, 1990; Ettinger et al, 1999). However, the localization of most of the CAXs is still unknown. First plant *CAXs*, *AtCAX1* and *AtCAX2*, were isolated from *Arabidopsis thaliana* by their ability to sequester Ca^{2+} into vacuoles of *Saccharomyces cerevisiae* mutants deficient in Ca^{2+} vacuolar transport (Hirschi et al, 1996). The high-affinity, high-capacity Ca^{2+}/H^{+} transporter *AtCAX1* is highly expressed in response to exogenous Ca^{2+} in plants, whereas the low affinity Ca^{2+}/H^{+} transporters *AtCAX2* and *AtCAX4* are not induced by exogenous Ca^{2+} (Shigaki and Hirschi, 2000; Hirschi, 2001). Up to date several CAXs were isolated from different plant species (Table 1.1).

Species	Gene name	Reference
Arabidopsis thaliana	*AtCAX1*	Hirschi et al, 1996
	AtCAX2	
	AtCAX3	Shigaki et al, 2002
	AtCAX4	Cheng et al, 2002
	AtCAX5	Mäser et al, 2001
	AtCAX6	
Oryza sativa	*OsCAX1a*	Kamiya et al, 2005
	OsCAX1b	
	OsCAX1c	
	OsCAX2	
	OsCAX3	
Vigna radiata	*VCAX1*	Ueoka-Nakanishi et al, 1999
Capsella bursa-pastoris	*CbCAX51*	Lin et al, 2008
Hordeum vulgare	*HvCAX2*	Edmond et al, 2008
Lycopersicon esculentum	*LeCAX2*	
Zea mays	*ZmHCX1*	Shigaki & Hirschi, 2000

Table 1.1 List of known *CAX* sequences in different plant species.

Shigaki and Hirschi (2000) identified the first monocot *CAX-like* gene in maize named *ZmHCX1*. Despite the high homology to the previously characterized CAXs, ZmHCX1 could not overcome the Ca^{2+} growth defect in yeast mutant defective in Ca^{2+} vacuolar transport suggesting that this gene does not encode for the vacuolar Ca^{2+}/H^{+} transporter in maize (Hirschi et al, 1996; Ueoka-Nakanishi et al, 1999, 2000; Shigaki and Hirschi, 2000).

All of the CAXs characterized so far share some common features. They are approximately 400 amino acids long and are predicted to have 11 transmembrane domains (Kamiya and Maeshima, 2004). They contain a central hydrophilic motif, rich in acidic amino acid residues (the acidic motif), that bisects the polypeptide into two groups of five or six transmembrane spans (Hirschi, 2001). Two domains modulate CAX activity: the N-terminal regulatory region (NRR) (Pittman and Hirschi, 2001) and the Ca^{2+} domain (CaD) (Shigaki et al, 2001). The NRR of AtCAX1 is 36 amino acids long. Whereas the NRR must be removed to ensure a proper Ca^{2+} transport across the tonoplast in *Saccharomyces cerevisiae* (Pittman and Hirschi, 2001), in *Arabidopsis*, the presence of the NRR is necessary to get the active antiporter (Cheng et al, 2003). The NRR is predicted to be present in all *Arabidopsis* CAX-like transporters. This region controls AtCAX1 activity as well as other CAX transporters including VCAX1 and AtCAX2 (Pittman and Hirschi, 2001; Pittman et al, 2002, 2004). The CaD region is 9 amino acids long and in AtCAX1 it is located between amino acids 87 and 95 (Figure 1.3).

Shigaki et al. (2001) have shown that expression of *AtCAX3* in yeast does not induce changes in Ca^{2+} transport and transgenic tobacco expressing *AtCAX3* did produce any alteration in its ion sensitivity. However, when the CaD region of AtCAX1 was introduced into AtCAX3 the expression of the chimeric protein induced in yeast an increased transport of Ca^{2+} and ion sensitivity of transgenic tobacco plants similar to those of tobacco plants over-expressing *AtCAX1* (Hirschi, 1999). When the CaD of AtCAX1 was fused to AtCAX2, which besides Ca^{2+} transports also Cd^{2+} and Mn^{2+}, this resulted in an increase in vacuolar transport of Ca^{2+} with no noticeable change in the transport of other ions. Shigaki et al. (2002) have shown that the Ile residue at the position 87 within the CaD is necessary for the Ca^{2+} transport.

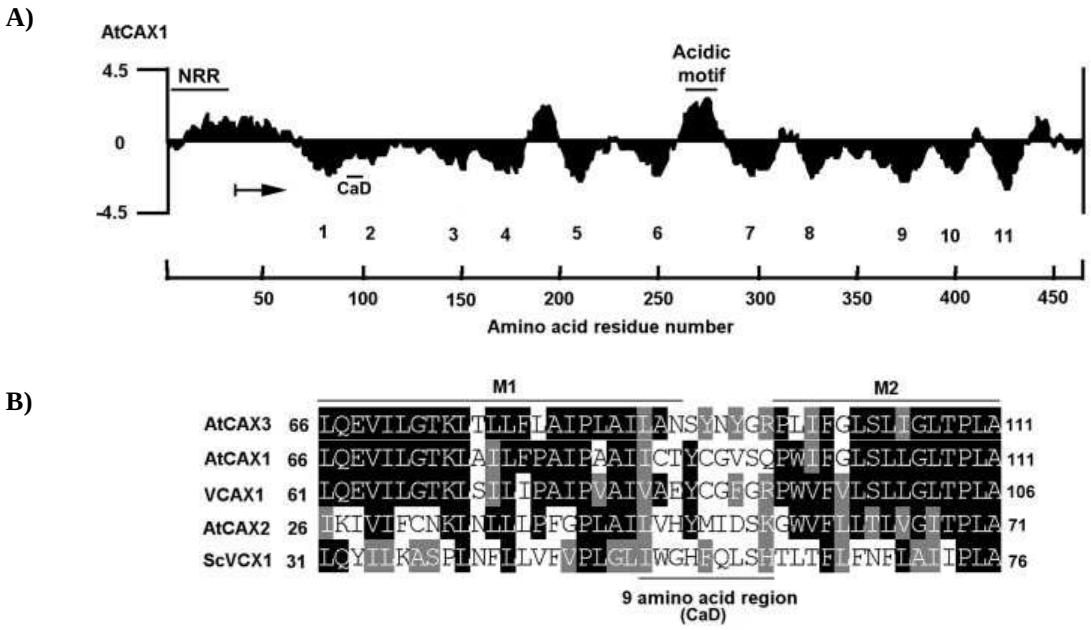

Figure 1.3 Ca^{2+} domains in the CAX-like genes.

(**A**) The region shown is put into context of the entire CAX open reading frame with a hydropathy plot of AtCAX1 (Shigaki and Hirschi, 2000). The positions of the 36-amino acid N-terminal regulatory region (*NRR*), the Ca^{2+} domain (*CaD*), and the acidic motif are *highlighted.*

(**B**) Alignment of deduced amino acid sequences between the deduced first and second membrane-spanning domains (M1 and M2) of polypeptides encoded by *A. thaliana* (*At*) CAX1, CAX2, and CAX3, mung bean VCAX1, and *S. cerevisiae* (*Sc*) VCX1. Alignments were performed by using CLUSTAL W 1.8 program (Baylor College of Medicine; Thompson et al, 1994). Consensus amino acid residues are *boxed* in *black* (identical) or *gray* (similar). (Adapted from Shigaki et al, 2001)

The plant CAX family can be divided into two clusters based on their different substrate specificity: type I-A (transports predominantly Ca^{2+}) includes AtCAX1, AtCAX3, AtCAX4 from *Arabidopsis* and OsCAX1a, b and c from rice, whereas type I-B (transports multiple cations such as Ca^{2+}, Cd^{2+}, Mn^{2+}) contains AtCAX2, AtCAX5 and AtCAX6 from *Arabidopsis* and OsCAX2, 3 and 4 from rice (Shigaki et al, 2006).

1.2.3 Relationship between auxin, Ca^{2+}, ABPs and CAXs

In plants, the cytosolic pH is slightly alkaline and is regulated by the H^+-pumps on the plasma membrane (P-ATPase) and tonoplast (V-ATPase and H^+-PP-ase). CAX-mediated transport may alter the cytosolic Ca^{2+} concentration and pH, as well as intracellular Ca^{2+} gradients (Barkla et al, 2008). Any slight alteration in pH has the potential to significantly reduce Ca^{2+} loading to the vacuole and thus dramatically alter the cytosolic Ca^{2+} levels

(Pittman et al, 2005). The overexpression of *AtCAX1* in *Arabidopsis* resulted in an increased V-ATPase activity, whereas mutations in *AtCAX1* caused a decrease in the measured V-ATPase activity (Cheng et al, 2003). In *Arabidopsis cax1* mutant, the Ca^{2+}-pump (Ca^{2+}-ATPase) is upregulated as a compensatory mechanism to correct the perturbations in the Ca^{2+} gradient (Cheng et al, 2003). In turn, the P-ATPase could be activated in order to restore the normal cytoplasmic content of H^+ (Barkla et al, 2008; Zhao et al, 2008). However, not all CAX mutants show this complex feedback.

Since *cax1* mutant in *Arabidopsis* shows typical symptoms of auxin deficiency (i.e. reduction of the number of lateral roots and branching shoots), it can be assumed that AtCAX1 is involved in the auxin transduction pathway, as well as in the mobilization of the intracellular Ca^{2+} (Cheng et al, 2003). Moreover, these mutants showed alterations in auxin-mediated growth responses and altered expression of auxin-regulated promoters, reinforcing the idea that CAXs are important components of the auxin signalling pathway. Very recently, it was demonstrated that vacuolar CAX1 and CAX3 in *Arabidopsis* influence auxin transport in guard cells via regulation of apoplastic pH (Cho et al, 2012). The authors also showed that *cax1* and *cax3* mutants are less responsive than WT to the IAA-induced inhibition of hypocotyl elongation.

Up to date, no information is available concerning the possible interaction between ABP1 and CAXs. On the base of literature data, it can be assumed that auxin action, mediated via ABP1 could change the cytosolic Ca^{2+} concentration via the regulation of Ca^{2+} transport by both AtCAX1 and AtCAX2, which are sensitive to and regulated by cytosolic pH (Pittman et al, 2005). However, the involvement of auxin in the regulation of *CAX* expression in maize and the role of ABPs in this possible relationship has not been investigated yet. Moreover, maize CAX homologs of AtCAX1 still remain to be identified and characterized.

Shishova and Lindberg (2010) proposed a hypothetical model of auxin perception, which explains the possible interplay among ABP1, P-ATPase and cytosolic Ca^{2+} (Figure 1.4). The extrapolation of this model could also explain the relationship between auxin, ABP1 and the vacuolar Ca^{2+} uptake provided by CAX.

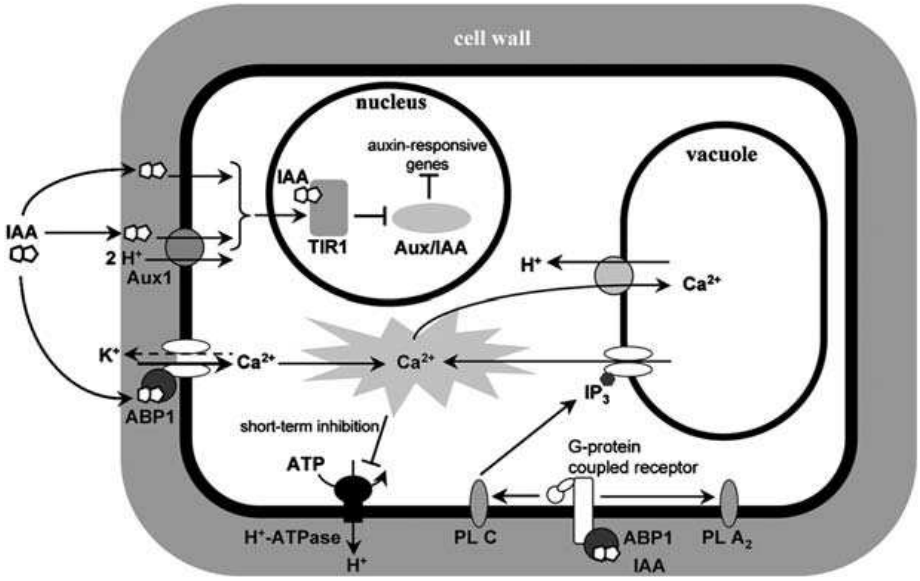

Figure 1.4 A hypothetical model of auxin perception, summarizing different mechanisms at the plasma membrane of a plant cell.

Auxin perception is processed by a TIR1 receptor within the nucleus and results in rapid expression of auxin-induced genes. A possible perception of auxin at the plasma membrane might appear through the 2-subunitreceptor. The external subunit is provided by ABP1, while the transmembrane domain is still under discussion. It might be coupled with a G-protein and lead to an activation of phospholipases, and a subsequent elevation of cytosolic free Ca^{2+} concentration through receptor-operated IP3-regulated channels. The receptor transmembrane domain might also represent a Ca^{2+}-channel, which manages fast shifts in Ca^{2+} concentration via extracellular Ca^{2+}. In both cases the rise in free Ca^{2+} concentration results in short inhibition of H^{+}-ATPase, which causes a number of physiological effects, including cytosol acidification. (Figure taken from Shishova, and Lindberg, 2010)

1.3 Functional interplay between auxin and light

As it was mentioned before, auxin, as an internal factor, has multiple effects on the growth of plants including cell enlargement required for stem elongation, leaf expansion and tropic growth. Auxin also inhibits lateral shoot growth and promotes lateral root formation. On the other side, light, as an external factor, regulates numerous developmental events including seed germination, stem elongation, apical hook opening, leaf expansion, phototropism, chloroplast movement. These overlapping functions of auxin and light indicate a functional interplay between them (reviewed in Tian and Reed, 2001; Halliday et al, 2010). However, mechanisms of a cross-talk between auxin and light are still not fully understood (reviewed

in Halliday at al, 2009). In addition, it is still not completely known how auxin could be involved in the light-induced growth inhibition.

It has been shown that light affects auxin biosynthesis (Iino, 1982a; Iino, 1982b; Nishimura et al, 2006), homeostasis (Tanaka et al, 2002; Hoecker et al, 2004), transport (Jones et al, 1991; Jensen et al, 1998; Nagashima et al, 2008) and signalling/response (Galston and Baker, 1953; Kondo et al, 1969). Numerous studies have shown the existence of a correlation between light responses and auxin content or polar auxin transport (PAT). For example, light reduced the intensity of PAT in etiolated coleoptile segments (Huisinga, 1964, 1967; Naqvi, 1975; Fellner et al, 2003) and reduced the concentration of free IAA in etiolated maize seedlings (Briggs, 1963; Bandurski et al, 1977; Iino, 1982a). Several studies have implicated the importance of light and PAT in mesocotyl photomorphogenesis (Van Overbeek, 1936; Vanderhoef and Briggs, 1978; Iino, 1982b; Jones, 1990; Barker-Bridgers et al, 1998). It has been shown that auxin distribution can be modified by light which controls the abundance of auxin efflux carriers, P-glycoproteins (PGPs) and PIN-FORMED proteins (PINs) (Sidler et al, 1998; Friml et al, 2002; Nagashima et al, 2008). In addition, several studies provided the evidence of light controlling auxin-regulated genes (reviewed in Halliday et al, 2010)

Several hypotheses have been made about the involvement of ABP1 in the light-regulated growth (Walton and Ray, 1981; Napier et al, 1988; Jones et al, 1989; Jones and Venis, 1989). For example, Jones et al. (1991) showed that the red light (RL) reduced the growth rate of maize mesocotyl by decreasing the content of IAA and the abundance of ABP1. In addition, Im et al. (2000) reported that expression of *ABP1* in maize seedlings was much less in light- than in dark-grown plants. By contrast, Fellner et al. (2006) showed that the expression of *ABP4*, another member of ABP family, was up-regulated in mesocotyl of RL- and far red light (FR)-grown maize seedlings. Interestingly, Bořucká and Fellner (2012) showed that functional *ABP1* and *ABP4* are required for normal expression of *PHYB* gene and that expression of *PHYB* is not reduced by white light when *ABP1* or *ABP4* are knockout.

1.3.1 Interaction between auxin and light in the regulation of shoot and leaf growth

The interaction between auxin and light in the regulation of shoot and leaf growth was intensively reviewed (Tian and Reed, 2001; Chen, 2001; Dengler and Kang, 2001; Casal et al, 2003). In leaves, auxin and light promote cell expansion (Cosgrove, 1994; Jones et al, 1998). Leaf growth is regulated by light acting via phytochrome and other photoreceptor signalling pathways (Downs, 1955; Dale, 1988; Van Volkenburgh and Cleland, 1990). Cellular mechanisms of light-stimulated leaf expansion involve enhanced proton efflux from mesophyll and epidermal cells. In epidermal cells, blue and red light increase the proton efflux by two different mechanisms (Van Volkenburgh et al, 1990; Van Volkenburgh, 1999). Elzenga (1997) proposed that the blue light stimulates proton efflux by a direct interaction between the blue light receptor and the proton pump, whereas the red light-induced stimulation of proton pump may involve an indirect modulation of calcium and potassium channels (Staal et al, 1994; Elzenga, 1997). However, it is still unknown how light and auxin interact in the regulation of the leaf angle development.

One of the interesting phenotypic characters of modern maize hybrids is their more upright leaf position in comparison with the older, density sensitive varieties. It is assumed that upright leaves are responsible for the observed tolerance of modern maize hybrids to neighbours and higher yield in dense planting (Duvick, 2001). Previous results obtained from the analysis of maize hybrids led to the hypothesis that the development of upright leaves in the modern maize hybrids is a consequence of their reduced responsiveness to auxin, light, and increased expression of *ABP4* compare to old hybrid (Fellner et al, 2003, 2006). The authors further showed that in both hybrids (old and modern), light (white, red and blue) can increase the leaf declination from the vertical, whereas N-1-naphthylphthalamic acid (NPA), an inhibitor of PAT, reduced the leaf declination in old, but not in modern maize hybrids. Their results further support the hypothesis that auxin and PAT are involved in the elongation of maize seedlings and that light interacts with auxin or PAT in the regulation of the leaf declination.

1.3.2 Morphology of maize leaf

The maize leaf has three major axes along which morphological differentiation occurs: proximodistal, mediolateral, and adaxial-abaxial (dorsoventral) (Bennetzen et al**,** 2009; Figure 1.5).

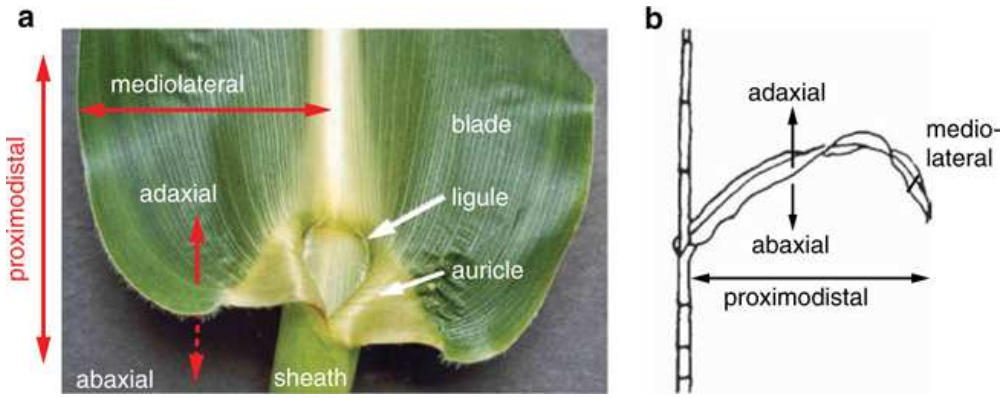

Figure 1.5 The anatomy and major growth axes of the maize leaf.

a) Image of the adaxial (upper) surface of the maize leaf showing distal blade and proximal sheath, separated by the ligule/auricle region. (b) Scheme illustrating the axes of the maize leaf relative to the main axis of the plant. Photo taken from Handbook of Maize: Its Biology, Springer New York, 2009, ISBN978-0-387-79417-4 (Print) 978-0-387-79418-1 (Online), page: 162.

The proximodistal axis lies along the length of the leaf and is the primary axis of growth. The mediolateral axis is defined as midrib to margin and can also permit an extensive growth. By contrast, the adaxial-abaxial axis, which extends across the leaf from the upper to the lower surface, comprises only few distinct cell layers.

The maize leaf, typical for the grasses, is divided into three regions: the proximal sheath, the distal blade and the central ligular region that connects these two parts (Figure 1.5). The sheath wraps around the stem, providing mechanical support for the blade, which projects outwards to catch the light and is optimized for photosynthesis. Ligular region consists of the ligule and auricles, specialized triangular structures that allow the blade to bend outwards thus describing leaf angle (Figure 1.6). Fellner et al. (2003) proposed that the length of the auricles is proportionally associated with the leaf angle declination in maize.

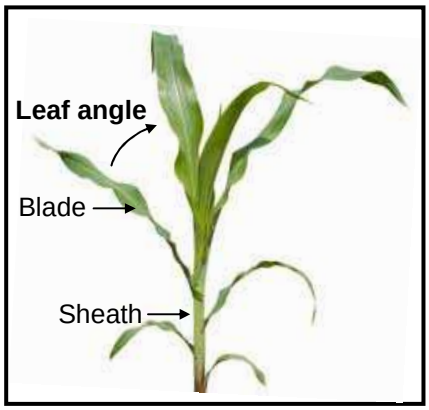

Figure 1.6 A schematic representation of maize leaf angle.

The sheath (proximal part of maize leaf) wraps around the stem, providing mechanical support for the blade (distal, free part of maize leaf), which projects outwards describing the leaf angle.

1.4 Maize mutants in *ABP* genes as a model of study

Maize is the most productive grain crop in the world. Archaeological and molecular data indicate that modern maize was domesticated from its wild grass ancestor teosinte (*Zea mays ssp. parviglumis*) in southern Mexico (Mesoamerica) between 6.600 and 9.000 years ago (Figure 1.7).

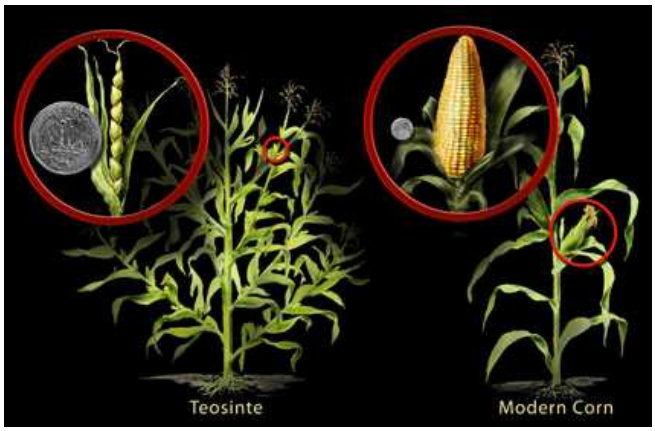

Figure 1.7 An example of maize ancestor Teosinte (*Zea mays ssp. parviglumis*) and modern maize plant (*Zea mays* L.).

The suppression of branching from the stalk of Teosinte resulted in a lower number of ears per plant but allows each ear to grow larger. The hard case around the kernel disappeared over time. Today, maize has just a few ears of maize growing on one unbranched stalk (source: National Science Foundation).

Maize plant can be used for many purposes - every part of the plant has commercial value. Maize is used both as human and livestock food as well as feedstock for many industrial products including maize oil, sweeteners, maize starch, alcohol for beverages and ethanol as a car fuel. In addition, new bioproducts such as amino acids, antibiotics and biodegradable chemicals and plastics are increasingly being synthesized using maize as a raw material.

Maize is also very important plant as an experimental model both for fundamental and applied research. For example, it was the maize plant where Hertel et al. (1972) detected first ABP activity from the crude membrane fraction of etiolated coleoptiles. The maize loss-of-function mutants made by the means of Robertson's mutator transposable element (Bennetzen, 1996) represent a very good research tool. Using reverse genetic approach, Im et al. (2000) isolated and characterized three maize loss-of-function mutants in *ABP1* and/or *ABP4* genes. They observed no obvious phenotypic differences between single maize mutants *abp1* and *abp4*, double mutant *abp1/abp4* and wild type (WT), suggesting the redundancy of ABPs in maize. In contrast to Im et al. (2000), Fellner et al. (2006) observed that the same *abp* mutants developed leaves with altered declination compared to WT suggesting that ABPs may play a role in the auricle growth and the leaf angle development. Therefore, the maize loss-of-function mutants in *ABP* genes *1* and *4* are good experimental models which can help in elucidating the mechanism(s) by which auxin (via ABPs or not) may regulate the auricle growth and consequently the leaf angle in maize.

2 The aims of this Ph.D. thesis

Up to date, no information is available concerning the possible involvement of CAX transporters during the leaf angle development in maize; especially as no maize vacuolar Ca^{2+}/H^{+} antiporter has been isolated and characterized so far. Considering the fact that auxin influences the level of Ca^{2+} during the signalling transduction events, it can be hypothesized that vacuolar CAXs can also be involved in one of the steps in this auxin signalling cascade.

The aim of this work was to determine, by use of maize loss-of-function mutants in *ABP1* and/or *ABP4* genes, whether auxin, Ca^{2+}, ABPs and CAXs play a role in the leaf angle development in mature plant and in the seedling development. For this purpose, three questions were addressed:

1) Do ABP1 and ABP4 play a role during maize seedling development? Are they regulated by the light quality?
2) Can maize seedling development be altered by modifying Ca^{2+} and auxin status?
3) Are CAXs important in the leaf angle development or during the maize seedling development?

.

3 Material and Methods

3.1 Plant material

The loss-of-function mutants in *ABP1* and *ABP4* genes in maize (*Zea mays* L.) were used for all experiments (Im et al, 2000). The *abp* mutants contained the Robertson's *Mutator* transposable elements (Bennetzen, 1996) in *ABP1* and/or *ABP4* genes. Seeds of the single *abp1* and *abp4* mutants, double *abp1/abp4* mutant and a near isogenic line (inbred line A619, here called WT) were kindly provided by Alan M. Jones (The University of North Carolina, Chapel Hill, NC). All mutants were tested for the lack of *ABP1* and/or *ABP4* gene expression, and they showed stable phenotypes.

3.2 Growth conditions *in vitro*

3.2.1 Seeds handling

For the experiments *in vitro*, seeds were first washed with 70% ethanol for 3 min, rinsed with distilled sterile water and then soaked in Savo® original solution (~5% sodium hypochlorite; Bochemie, s.r.o, Czech Republic) supplemented with a drop of Tween®20 (Calbiochem, USA), shaken on a stirrer for 30 min and then rinsed extensively with sterile distilled water. Seeds germinated on 0.7% (w/v) agar medium in Magenta GA7 boxes (77x77x196 mm; Sigma-Aldrich, Prague, Czech Republic) (6 to 9 seeds per box) at the temperature of 23°C and different light conditions (dark, blue light and red light) described below.

3.2.2 Medium

The basal medium (BM) contained Murashige and Skoog salts (MS medium; Sigma-Aldrich, Prague, Czech Republic) (Murashige and Skoog, 1962), 1% (w/v) sucrose and 1 mM MES (2-(N-morpholino)-ethanesulfonic acid; pH adjusted to 6.1 before autoclaving).

In experiments with auxin, BM was supplemented or not with 1-Naphthaleneacetic acid (NAA) in various concentrations. Medium without Ca^{2+} was prepared using the components of the BM excluding $CaCl_2$ (41.2 mM, NH_4NO_3, 18.8 mM KNO_3, 1.5 mM $MgSO_4x7H_2O$, 1.25 mM KH_2PO_4, 100 μM H_3BO_3, 100 μM $MnSO_4x4H_2O$, 30 μM $ZnSO_4x7H_2O$, 5 μM KI, 1 μM $Na_2MoO_4x2H_2O$, 0.1 μM $CuSO_4x5H_2O$, 0.1 μM $CoCl_2x6H_2O$, 0.2 mM $Na_2EDTAx2H_2O$, 0.1 mM $FeSO_4x7H_2O$, 1% sucrose (w/v) and 1 mM MES). The pH was adjusted to 6.1 before autoclaving. In the experiments with Ca^{2+}, the prepared medium without Ca^{2+} was supplemented with $CaCl_2$ in various concentrations (3 mM and 10 mM).

3.2.3 Light and temperature conditions

Seeds in the Magenta boxes (Sigma-Aldrich, USA) were placed in a growth chamber (Microclima MC1000E, Snijders Scientific, The Netherlands) and incubated at a temperature regime of 23°C. For development of etiolated seedlings (D), the boxes were wrapped in aluminium foil. Maize seeds were also incubated under continuous blue light (BL) with maximum irradiance at 460 nm or in continuous red light (RL) with maximum irradiance at 660 nm at 23°C. BL as well as RL were provided by blue (Philips TLD-36W/18-Blue, Phillips, USA) and red fluorescent tubes (Philips TLD-36W/15-Red, Phillips, USA), respectively. Total photon fluence rates of BL and RL were 10 $\mu mol.m^{-2}.s^{-1}$. Fluence rate was measured with a portable spectroradiometer (model LI-1800; Li-Cor; Lincoln, NE) calibrated by the Department of Biophysics at Palacky University in Olomouc.

3.2.4 Measurement of seedling growth *in vitro*

In all conditions *in vitro* the size of various organs (coleoptile, mesocotyl, primary root) of five-day-old seedlings developed on BM was measured with a ruler in various light conditions (D, BL, RL). Coleoptile length was measured from coleoptilar node to the tip of the coleoptile. Mesocotyl length was measured from scutellar to the coleoptilar node and primary root length was measured from the scutelar node to the root tip. In each genotype, six to nine seedlings per treatment that germinated on the same day were measured in each experiment. When necessary, changes in growth (i.e. inhibition or stimulation) caused by an effector (light, exogenous auxin, etc.) in individual genotype were expressed in percents

based on the following formula:

$$X = 100 \times (A-B) / A,$$

where "X" is the change in growth (in %), "A" and "B" stand for growth (in mm) in the absence and presence, respectively, of the effector.

3.3 Growth conditions *in vivo*

For experiments *in vivo*, plants were grown in soil (Potgrond H, Klasmann Deilmann GmBH, Germany) in small pots (190x190 mm; one seed per pot; 1 cm deep) and regularly watered. In summer, plants grew under natural light conditions and temperatures of 15^{o}C and higher. In winter, plants grew under high-pressure sodium lamps PlantaStar E40/ES 400 W (Osram GmbH, Germany) to maintain 16-hour photoperiod. The temperature was adjusted from 15 to 27^{o}C.

3.3.1 Measurement of plant growth *in vivo*

For the study of the leaf characteristics, plants were grown in soil in the greenhouse as described above and watered regularly. The leaf angle (declination from the vertical plant's axis) (Figure 3.1) was measured with a protractor held at the base of the leaf blade in 5 to 10 intact seedlings of each genotype from 2 to 4 weeks after seed germination in 12 independent experiments.

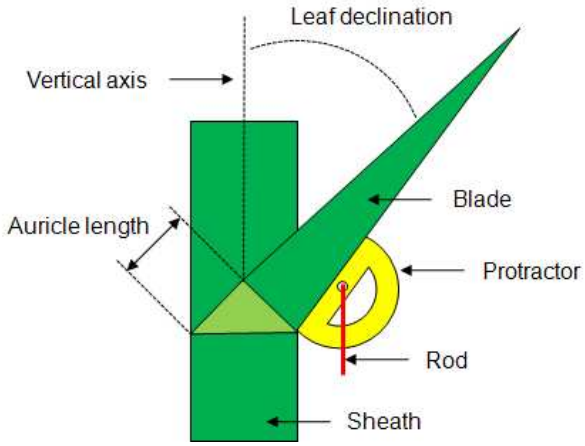

Figure 3.1 Schematic representations of leaf declination and auricle length measurement (adapted from Fellner et al, 2003).

The protractor was placed upside down along the midrib of the leaf blade closest to the plant's vertical axis. The size of the leaf angle was indicated by a freely swinging rod.

3.3.2 Microscopic analysis of the auricles

For the microscopic analysis, auricles were excised with a blade from leaves of plants grown in the greenhouse. They were mounted between a microscopic slide and a cover glass with a drop of water. The natural auto-fluorescence of lignin was used to monitor cell size as described by Nelson et al. (2002). Auricle region was observed on a microscope Olympus BX60 standard light microscope under epifluorescent illumination using a 372 nm excitation filter with a 456 nm long pass observation filter allowing a visualization of fluorescence as light blue signal. Images were captured using an Olympus DP71, CCD colour video camera and DPManager and DPController Software. Length of the auricle cells was determined using the ImageJ software.

3.3.3 Determination of the effects of exogenous auxin and calcium on the plants grown in the greenhouse

For determination of the effects of exogenous auxin and Ca^{2+} on plant growth, plants were sprayed every day, late in the afternoon in the period of 4 weeks from the moment of germination, with approximately 2 ml of solution (0.1 μM, 10 μM and 100 μM NAA or 10 μM, 50 μM, 100 μM, 1mM and 10mM solution of $CaCl_2$) per plant and the control plants were sprayed in the same time with the same volume of distilled water. Plant characteristic including plant height, blade length and leaf angle were determined in both controlled and treated plants in the way described above.

3.4 Calcium content determination

Calcium content was determined in the aerial parts (coleoptile and mesocotyl) of seedlings grown in the medium without Ca^{2+} or supplemented with 3 mM and 10 mM Ca^{2+}. Seeds in the Magenta boxes were wrapped in foil, placed in growth chamber and incubated at 23°C. Five-day-old seedlings were collected and freeze-dried in lyophilizer (Thermo, Electron Corporation, Heto, PowerDry, PL300, Freeze Dryer) for 24 hours.

Ca^{2+} content was determined by the Flame Atomic Absorption Spectrometry (FAAS) (Avanta Sigma, GBC, Australia) using acetylene-air flame at the wavelength 422.7 nm. Lanthanum oxide (2 $g.l^{-1}$) was used as releasing agent to overcome common chemical interferences caused by phosphates. External calibration in range 0.1-10.0 $mg.l^{-1}$ was used to evaluate Ca^{2+} concentration in samples. Prior to FAAS determination, all samples were digested by microwave digestion unit (Uniclever II, Plazmatronika, Poland) using mixture of nitric acid and hydrogen peroxide (EN ISO 7980:1986: Water quality-Determination of Ca^{2+} and magnesium (Mg^{2+}) -- Atomic absorption spectrometric method). Analysis of Ca^{2+} content in collected samples was performed by Dr. David Milde from the Department of Analytical Chemistry (Palacky University in Olomouc).

3.5 RNA extraction

Five days after germination, coleoptiles and mesocotyls were harvested, frozen immediately and ground in liquid nitrogen with a mortar and pestle. Total RNA was extracted from mesocotyl and coleoptile using the RNeasy Plant Mini Kit (Qiagen, Germany) according to the manufacturer instructions. An additional DNaseI treatment was performed using RQ1 RNA-free DNase (Promega, USA) for 60 min at 37ºC, followed by a subsequent phenol/chloroform/isoamylalcohol (25:24:1) purification. The absence of gDNA contamination was checked by PCR before cDNA synthesis using primers covering an intron sequence of *Zea mays Actin* gene (*ZmAct81*; accession number: U60511) (Table 3.1).

3.6 cDNA synthesis (reverse transcription)

The cDNA synthesis was performed from 1 μg of the total RNA with the SuperScript III reverse transcriptase (InVitrogen, USA) according to the instructions of manufacturer. The reaction contained 1X RT buffer, 0.5 mM dNTP, 5 mM DTT, 2.5 μM oligo(dT), 20u RNasin Plus RNase inhibitor (Promega, USA) and 200u SuperScriptIII reverse transcriptase. The reaction mixture was incubated at 50ºC for 60 min followed by heat-inactivation of the enzyme at 70ºC for 15 min. The RNA was digested by 5u RNaseH (New England Biolabs, USA) for 20 min at 37ºC. The obtained cDNA were subsequently diluted 50 times in RNase-free water before use for PCR analysis. Integrity of cDNA was confirmed by PCR using the

same actin primers as in the case of gDNA contamination (*ZmAct81*, accession number: U60511). In the case of cDNA, this primer combination gives a 350 bp long product. The 20 µl PCR reaction contained 1X GoTaq polymerase buffer, 1 µM of each primer, 1 mM dNTPs, 1u GoTaq polymerase and the cDNA matrix. For the amplification, the DNA was denatured at 94°C for 5 min followed by 35 cycles of amplification (30 sec at 94°C, 30 sec at 45°C, 45 sec at 72°C). A final extension step at 72°C for 7 min was performed. PCR products were visualized on 1.5 % (w/v) agarose gel containing 0.5 $\mu g.ml^{-1}$ ethidium bromide.

3.7 Database search and sequence analysis

Blast algorithm available at the National Center for Biotechnology Information (NCBI) was used to identify *Arabidopsis* CAX1 (*AtCAX1*) homologs in maize. The *AtCAX1* (accession number: AF461691) was used as a reference sequence for BlastT and BlastX analysis. Alignments were performed with CLUSTAL W 1.8 program (Larkin et al, 2007).

The full lengths sequence of *ZmCAX2* (accession number: AB044567) and *ZmCAX3* (accession number: AY108295) genes were amplified using specific primers (Table 3.1) designed based on the sequences available in the database. The PCR reaction was performed as previously described with the following program: the DNA was denatured at 95°C for 5 min followed by 35 cycles of amplification (30 sec at 95°C, 30 sec at 50/58°C, 1 min. at 72°C). The final incubation at 72°C was extended to 7 min.

3.8 Cloning, sequencing and sequence analyses

3.8.1 PCR reactions and PCR products purifications

The amplified *ZmCAX2* and *ZmCAX3* genes were sequenced in order to confirm their identity and more especially their sequence in the genotype used in this study. The PCR amplification of the full-length sequences of *ZmCAX2* and *ZmCAX3* was performed in the conditions already described. The amplification program was as follow: the DNA was denatured at 95°C for 5 min followed by 30 cycles of amplification (30 sec at 95°C, 30 sec at 57/56°C (*ZmCAX2*/*ZmCAX3*), 3/1.5 (*ZmCAX2*/*ZmCAX3*) min at 72°C). The final incubation at 72°C was extended to 7 min. However, in the case of *ZmCAX2* High Fidelity PCR Enzyme

Mix (Fermentas, Canada) was used. PCR products were size fractionated by electrophoresis on a 0.8% (w/v) agarose gel stained with ethidium bromide (0.5 µg.ml^{-1}). PCR products were excised from gel and subsequently extracted according the instructions of the manufacturer of the QIAquick Gel Extraction Kit (Qiagen, Germany). Elution was performed twice with 50 µl of EB. DNA concentration was quantified using NanoDrop ND-1000 spectrophotometer (Thermo Fisher Scientific Inc., USA).

In the case of *ZmCAX2*, amplified by the High Fidelity PCR Enzyme Mix, a subsequent A-tailing step was performed with GoTaq® polymerase in order to ensure a successful ligation into the pGEM® -T Easy Vector. For this purpose, 2 µl of 10 mM dATP, 6 µl of 5X GoTaq® polymerase buffer and 5 u of GoTaq® polymerase were added to the 21 µl of PCR product (final volume 30 µl). Samples were incubated 30 min at 72°C. Then, PCR products were again purified on QIAquick PCR Purification Kit following manufacturer's instructions. Elution was performed twice with 50 µl of EB. PCR products were precipitated by addition of 10 µl of 1M Acetic acid, 100 µl H_2O and 330 µl of 96% ethanol and incubated overnight at -20°C. Samples were centrifuged 30 min (13000 rpm; 4°C). Supernatant was removed and the pellet was washed by 500 µl of 70% ethanol and centrifuged 5 min again. Supernatant was removed and the pellet was washed by 500 µl of 96% ethanol and centrifuged 5 min again. Finally, supernatant was removed and the pellet was air dried and subsequently dissolved in 6 µl of DEPC water.

3.8.2 Ligation, *E.coli* DH5α transformation and plasmid isolation

The ligation into the pGEM®-TEasy Vector (Promega, USA) was performed overnight at 4°C as followed: 1X T4 DNA ligase buffer, 25 ng of vector, 3 u of T4 DNA ligase and the PCR product (4 µl). The 10 µl of ligation reaction was used to transform 100 µl of DH5α™ competent cells (Invitrogen, USA) by thermic shock. Cells were grown overnight at 37ºC in incubator and selected on LB agar medium containing 50 µg.ml^{-1} Ampicilin, 50 µg.ml^{-1} Xgal and 0.1 nM IPTG.

The pGEM®-Teasy vector allows a blue/white selection of vectors containing the gene of interest. Plasmid was isolated from several 2ml-overnight LB-Amp^{50} culture following the instructions of the Nucleospin® Plasmid Quick Pure kit (Macherey Nagel,

Germany). Elution was performed twice with 30 µl of EB. *Eco*RI restriction was performed on purified plasmids to verify presence of the insert. Vectors containing inserts were quantified and sent to the Macrogen Company for sequencing (Korea). Sequences were analysed with BioEdit (Hall, 1999) and BLAST analysis was performed to confirm identity of sequences.

3.8.3 Prediction of transmembrane topology

Prediction of transmembrane topology was done by the TMHMM program (Krogh et al, 2001). In addition, TMpred program (Hofmann and Stoffel, 1993) that makes a prediction of membrane-spanning regions and their orientation was also used.

3.9 Gene expression analyses

3.9.1 Plant material and growth conditions

Gene expression analyses were performed in the plants grown in both *in vivo* and *in vitro* conditions. *In vitro* plants grew in the dark (as described above) in two different conditions: in the BM supplemented with 50 µM NAA and in the BM supplemented with 3 and 10 mM Ca^{2+}. As a control condition plants grew in the BM. Analyses were performed in the coleoptile and mesocotyl of five-day-old maize seedlings. *In vivo*, the analyses were performed in the leaf bases of the third leaf, including auricles, which were harvested from the plants when the leaf emerged or was fully developed (one-month-old plants). These plants were grown in the greenhouse as described above.

Expression analysis of both genes was first studied by semiquantitative RT-PCR. Since the expression of *ZmCAX3* was very weak and almost no detectable by semiqRT-PCR, the expression analysis of *ZmCAX3* was further determined by quantitative RT-PCR (qRT-PCR). Primer combinations used and size of expected products are listed in Table 3.1.

Gene name and accession number	Forward (F) and reverse (R) primers		Product size (bp)
ZmAct81 (U60511)	F	5'-ACACAGTGCCAATCT-3'	316
	R	5'-ACTGAGCACAATGTTAC-3'	
ZmCAX2 fl (AB044567)	F	5'-AATCGAGATGGGCGGTTTCAAGG-3'	1338
	R	5'-AGGTATTTGACGCATTACTTACAG-3'	
ZmCAX3 fl (AY108295)	F	5'-CGGCGAAGGAGATGGATCGTCTGC-3'	1590
	R	5'-GACCGGATGCAAATTCGCTACCC-3'	
ZmCAX2	F	5'-ATCATTCTCCACTTCACGAC-3'	327
	R	5'-TGCCTTACTGAAGATTTGGT-3'	
ZmCAX3	F	5'- ATGAGCATCCAAGGCAGCAACG-3'	62
	R	5'-CATCAACCTTTGCACGGCATTG-3'	
GAPDH (Zm.3765)	F	5'-TGATCCGCCACATGTTCAAGACC-3'	79
	R	5'-CGGCATACACAAGCAGCAACC-3'	

Table 3.1 The list of primers used in CAX cloning.

3.9.2 Expression analyses of *ZmCAX2* by RT-PCR

The *ZmCAX2* expression analysis by semiquantitative PCR was performed in a 20 µl reaction as already described and according the following conditions: the DNA was denatured at 95°C for 5 min followed by 35 cycles of amplification (30 sec at 95°C, 30 sec at 50°C, 1 min. at 72°C). A final extension step at 72°C was performed for 7 min. PCR products were loaded into a 1.5% agarose gel containing 0.5 ug/ml EtBr and the picture was taken with a G-BOX Syngene Cold camera UV transiluminator (20x30 cm). The intensity of the signal was determined using ImageJ program. Normalization was assessed by the housekeeping gene actin and the gene expression was expressed as relative to the gene expression observed in WT. Results presented are average ± standard error (SE) of 3 independent biological repeats.

3.9.3 Expression analyses of *ZmCAX3* by quantitative Real Time-PCR

Amplification of the second target gene, *ZmCAX3,* and real-time detection of amplicon production were monitored on an Mx3000P sequence detector (Stratagene, USA). qRT-PCR reactions contained 80 nM of each primer, 5 µl of cDNA template (diluted 1/50), 12.5 µl of 2X absolute SYBR Green ROX Mix (ABGene, Epsom, UK). The volume was filled up to 25

µl with sterile RNase-free water. PCR cycling conditions required an initial HotStart activation of 15 min at 95 ºC, followed by 45 cycles of 95 ºC for 30 s and 60 ºC for 30 s. To confirm the product purity, a melting curve analysis was performed at the end of the PCR reaction. The SYBR green fluorescent signal was standardized with a passive reference DYE (ROX) included in the SYBR green PCR master mix. The target gene expression was quantified relative to the expression of the reference gene *GAPDH* (accession number: Zm3765) in the same sample. Differences in the cycle numbers during the linear amplification phase between the samples and the ΔΔCT method were used to determine the differential gene expression. Primers for qRT-PCR were designed using the program QuantPrime (Arvidsson et al, 2008). Gene expression in the *abp* mutants was expressed as relative to that obtained for WT plants. Results presented are average ± SE of 3 independent biological repeats.

3.10 Statistical analysis

When needed, statistical analysis was performed using the Student's t-test (MS Office Excel).

4 Results

4.1 Maize *abp* mutants as an experimental model

In this study maize mutants in *ABP* genes were used as an experimental model. Therefore, and extensive phenotypic analyses of these mutants was performed both in condition *in vivo* and in condition *in vitro*.

4.1.1 Phenotype of maize *abp* mutants *in vivo*

One-month-old plants developed in the greenhouse were analyzed for overall growth, leaf blade length and width, and leaf blade declination. Generally, during this period all experimental genotypes fully developed four leaves (Figure 4.1.1). The development of the leaves was the fastest in *abp1/abp4* mutant, whereas *abp1* mutant showed the slowest leaf development (data not shown).

Control plants grown in the greenhouse were approx. 60 cm tall. Plants with mutation in *ABP1* gene were about 20% shorter than WT plants, whereas *abp4* mutant was taller than WT. Plants of *abp1/abp4* mutant reached height similar to that of control plants (data not shown).

4.1.1.1 Leaf angle

Leaf angle was analyzed in fully developed leaves of 25-day-old plants for the 2nd leaf, 32-day-old plants for the 3rd leaf, and in 35-day-old plants for the 4th leaf. In one-month-old WT plants, declination of the 2nd and 3rd leaf reached approx. 25 degrees (Figure 4.1.1A). Mutation in *ABP1* gene led to the development of smaller leaf declination (approx. 20 degrees), whereas defect in *ABP4* gene led to development of less vertical leaves (leaf angle approx. 28 degrees) in comparison to WT. Finally, the loss-of-function in both

genes resulted in leaves with declination similar to that observed in *abp4* mutant (Figure 4.1.1A).

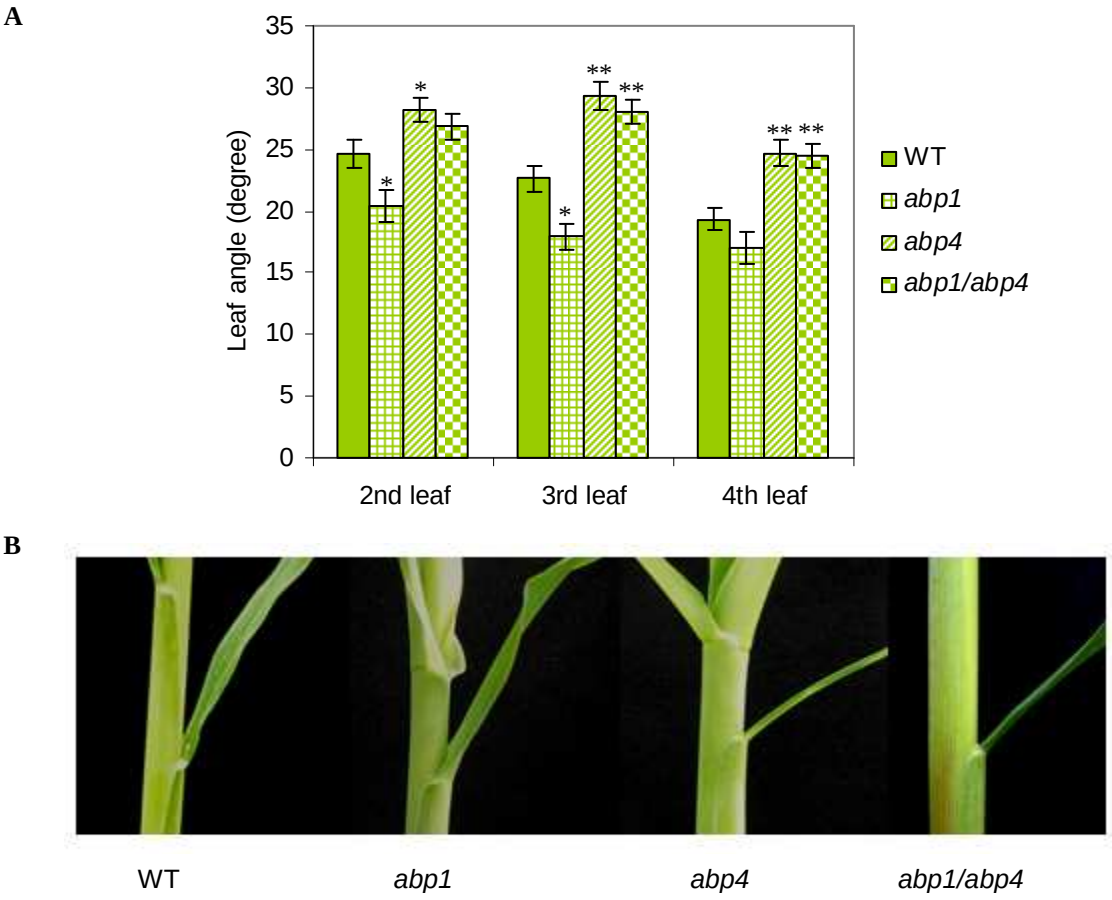

Figure 4.1.1 Leaf angle in single maize *abp1* and *abp4* mutants, double *abp1/abp4* mutant and the corresponding WT grown in the greenhouse.

Leaf angle, measured as a declination from vertical in 25-day old plants (2nd leaf), 32-day-old plants (3rd leaf), and in 35-day-old plants (4th leaf), was determined by a protractor to the nearest degree. For each genotype, four to ten seedlings were measured in each experiment. Values show leaf angle (mean ± SE) obtained in 12 independent experiments (**A**). WT and *abp* mutants show significant difference (*t*-test: $p \leq 0.05$ (*), $p \leq 0.01$ (**)). In (**B**), photography of angle of 3rd leaf is shown in one-month-old WT and *abp* mutant plants.

4.1.1.2 Blade length

Single *abp1* mutant developed blades of the first four leaves longer than WT. In *abp4* mutant 1st and 2nd leaves were of the same size as in WT plants, whereas 3rd and 4th leaf were longer than in WT (by approx. 25%). Interestingly, 1st and 2nd leaves of *abp1/abp4* mutant were

shorter than in WT plants, whereas 3rd and 4th leaf reached a length similar to that observed in control plants (Figure 4.1.2).

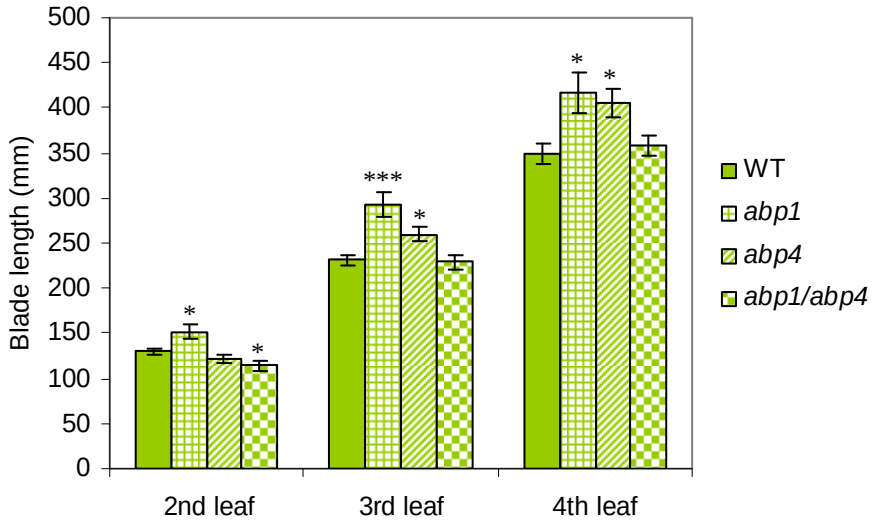

Figure 4.1.2 Length of the leaf blade in single maize *abp1* and *abp4* mutants, double *abp1/abp4* mutant and the corresponding WT grown in the greenhouse.

Blade length in 25-day-old plants (2nd leaf), 32-day-old plants (3rd leaf), and in 35-day-old plants (4th leaf) was measured by a ruler to the nearest millimetre. For each genotype, four to ten seedlings were measured in each experiment. Values show lengths of leaf blade (mean ± SE) obtained in 12 independent experiments. WT and *abp* mutants show significant difference (*t*-test: $p \leq 0.05$ (*), $p \leq 0.01$ (**), $p \leq 0.001$ (***)).

4.1.1.3 Blade base width

The loss-of-function in *ABP1* and/or *ABP4* genes led also to the development of different blade base width in comparison to WT (Figure 4.1.3). The base of the 2nd leaf blade in *abp1* and *abp1/abp4* mutant was wider than in WT plants, especially seen in 3rd and 4th leaf. The narrowest leaf blade base was found in *abp4* mutant especially in 2nd leaf (Figure 4.1.3A and B). The examples of blade base width in 2nd, 3rd and 4th leaf in WT and the mutants are shown on Figure 4.1.3B.

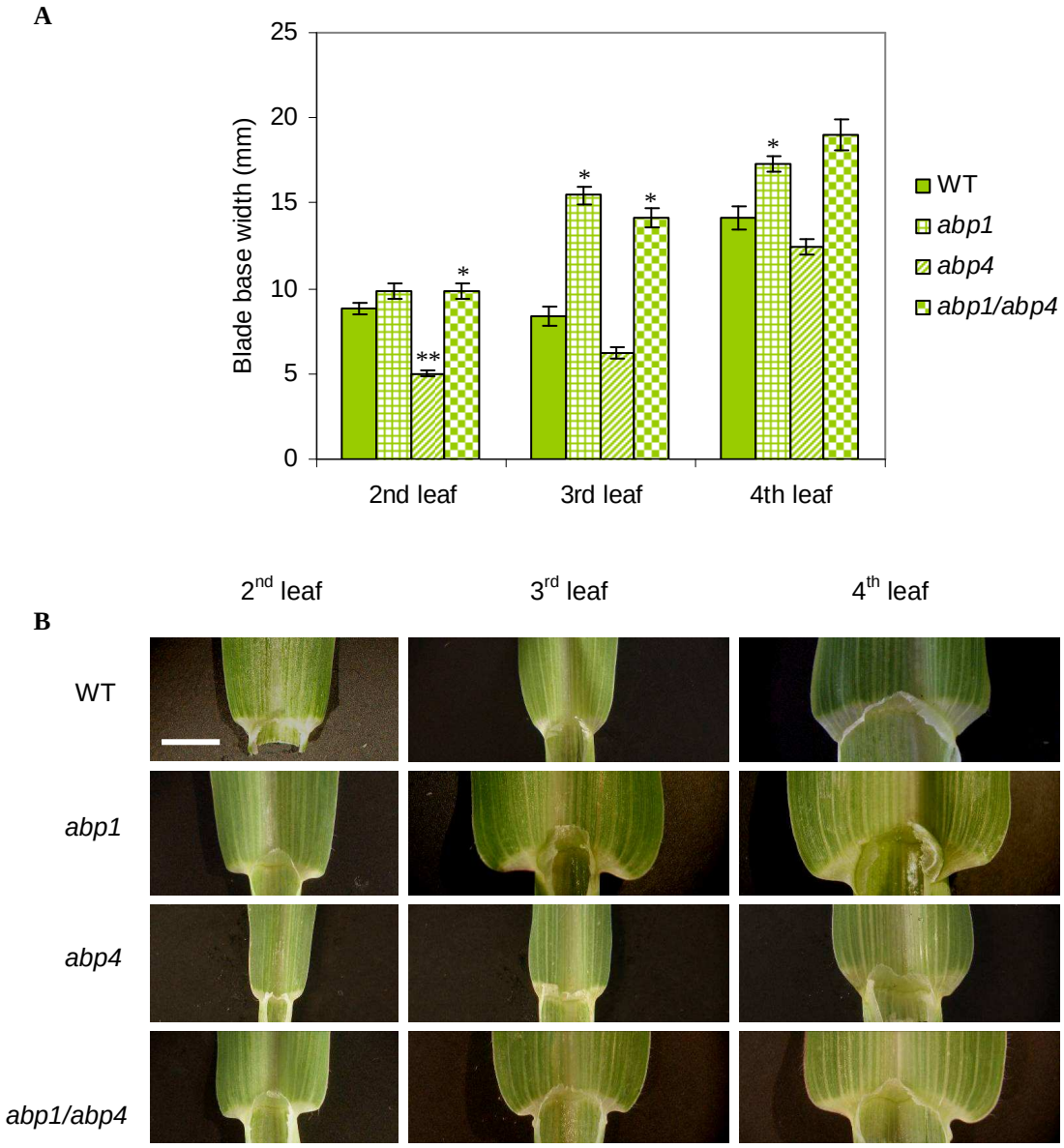

Figure 4.1.3 Width of the blade base in single maize *abp1* and *abp4* mutants, double *abp1/abp4* mutant and the corresponding WT grown in the greenhouse.

Blade base width in 25-day-old plants (2nd leaf), 32-day-old plants (3rd leaf), and in 35-day-old plants (4th leaf) was determined using ImageJ program. For each genotype, fifteen to twenty seedlings were measured in each experiment. Values show width of leaf base (mean ± SE) obtained in a single experiment (**A**). WT and *abp* mutants show significant difference (*t*-test: $p \leq 0.05$ (*), $p \leq 0.01$ (**)). In (**B**), photo of the widths of the bases of 2nd, 3rd and 4th leaf in one-month-old WT and *abp* mutant plants are shown. Bar = 5 mm.

4.1.1.4 Blade surface

The blade surface of 2nd, 3rd and 4th leaf was determined using ImageJ software. The analysis showed that the greatest blade surface was developed by the *abp1* mutant. The *abp1/abp4* mutant had blade surface greater than WT. The mutant *abp4* showed blade surface similar to that observed in WT plants with the exception of the 2nd leaf, where mutant blade surface was significantly smaller than that observed in the 2nd leaf of the WT plants (Figure 4.1.4).

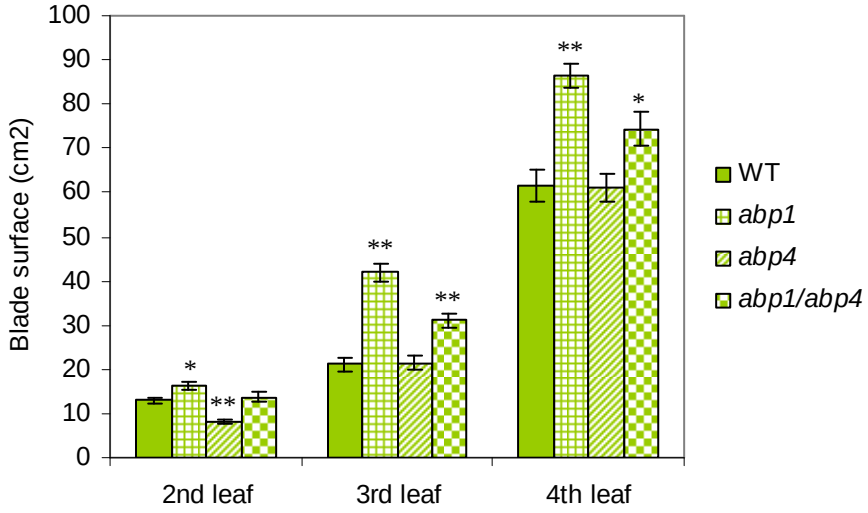

Figure 4.1.4 Leaf blade surface in single maize *abp1* and *abp4* mutants, double *abp1/abp4* mutant and the corresponding WT grown in the greenhouse.

Blade surface in 25-day-old plants (2nd leaf), 32-day-old plants (3rd leaf), and in 35-day-old plants (4th leaf) was measured by scanning the leaf blades and afterwards determined using ImageJ software. For each genotype, four to ten seedlings were measured in each experiment. Values show leaf surfaces (mean ± SE) obtained in 12 independent experiments. WT and *abp* mutants show significant difference (*t*-test: $p \leq 0.05$ (*), $p \leq 0.01$ (**)).

4.1.1.5 Auricle length

The *abp1* mutant developed auricles longer than WT for all leaves measured, whereas the auricle length did not differ between WT and the *abp4* mutant. The *abp1/abp4* mutant developed auricles shorter than WT plants (Figure 4.1.5).

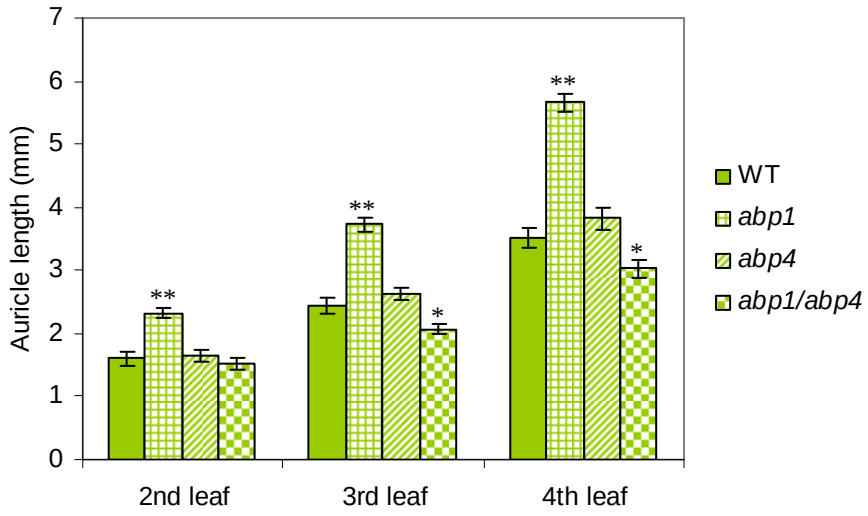

Figure 4.1.5 Auricle length of the 2nd, 3rd and 4th leaf in single *abp1* and *abp4* mutants, double *abp1/abp4* mutant and the corresponding WT.

For each genotype 35 to 45 auricles were measured. Values represent mean ± SE. WT and *abp* mutants show significant difference (*t*-test: $p \leq 0.05$ (*), $p \leq 0.01$ (**)).

4.1.1.6 Microscopic analysis of auricles

The microscopic analysis based on the autofluorescence of the lignin was used to study the epidermal auricle cells that are believed to be responsible for leaf angle development (Figures 4.1.6 and 4.1.7).

The epidermal auricle cells of the second leaf in WT plants and in the a*bp1* and *abp1/abp4* mutants were approximately 150 µm long (Figures 4.1.6 and 4.1.7). In contrast, the auricle epidermal cells of the *abp4* mutant were shorter than those of the WT. In the third leaf, the epidermal auricle cells had approx. the same length as those of 2nd leaf. The single *abp1* and *abp4* mutants developed auricles with cells of the same length as the WT. In contrast, the *abp1/abp4* mutant developed 3rd leaf bearing an auricle with in comparison to WT. Interestingly, the length of the auricle cells of the 4th leaf was the same in the WT and the *abp4* mutant (approx. 200 µm), whereas the *abp1* mutant developed the auricle with cells of the same length as the *abp1/abp4* mutant (approx. 100 µm), i.e. two times shorter in comparison to WT.

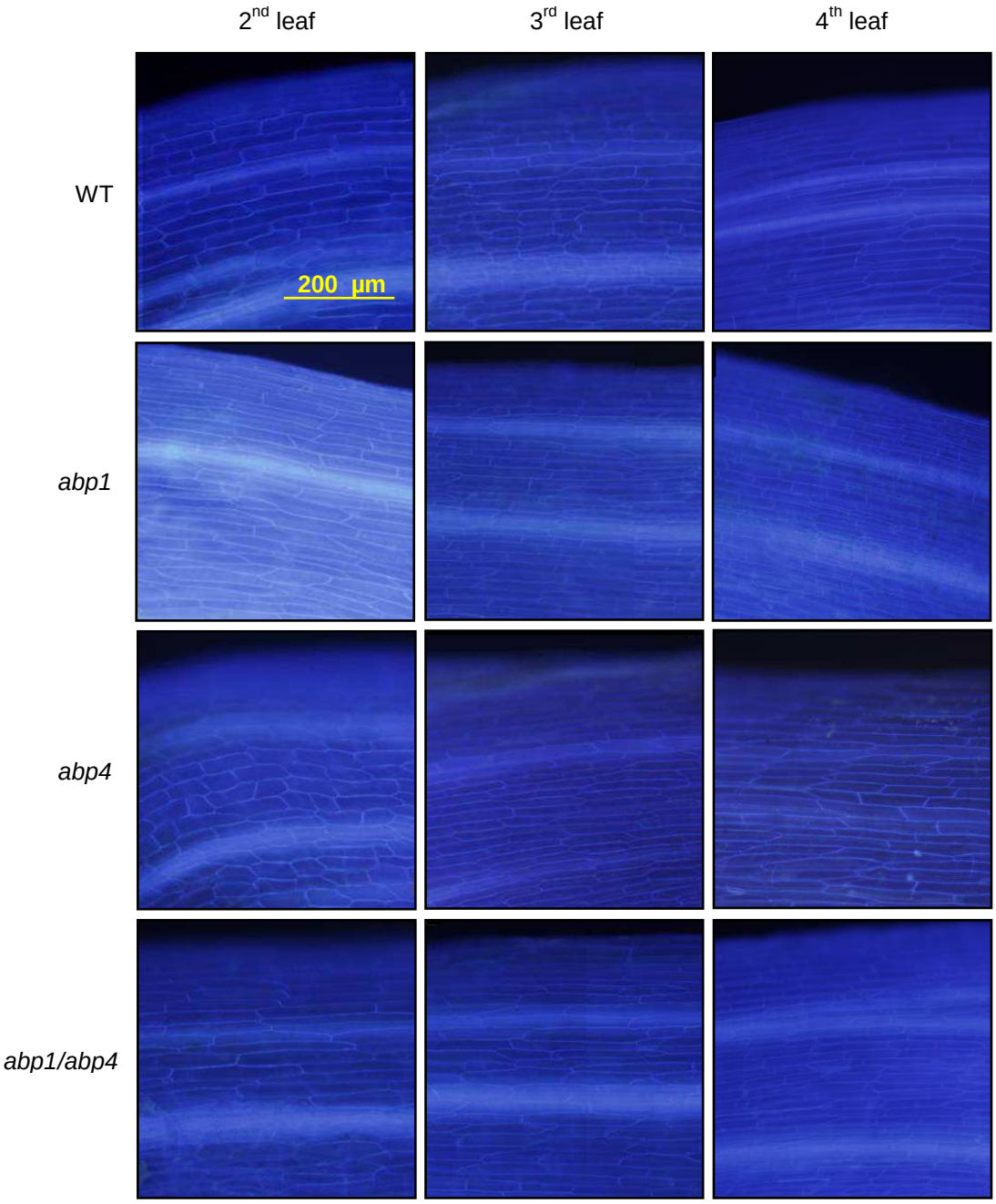

Figure 4.1.6 Micrographs of the adaxial auricle epidermis of the 2nd, 3rd and 4th maize leaf in single *abp1* and *abp4* mutants, double *abp1/abp4* mutant and the corresponding WT observed by fluorescent light using lignin autofluorescence.

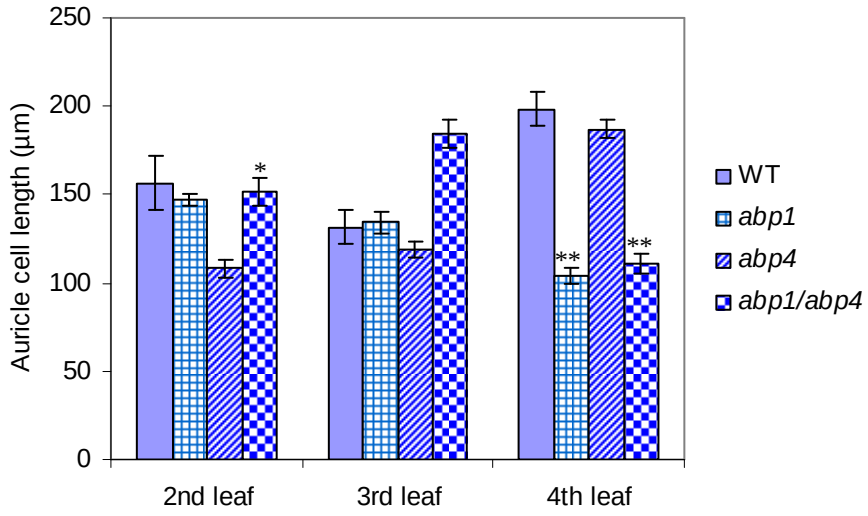

Figure 4.1.7 Length of the auricle cells of the 2nd, 3rd and 4th leaf in single *abp1* and *abp4* mutants, double *abp1/abp4* mutant and the corresponding WT.

30 to 50 cells in the region between the edge of the auricle and 2nd vain of 5 auricles were measured. Values represent mean ± SE. WT and *abp* mutants show significant difference (*t*-test: $p \leq 0.05$ (*), $p \leq 0.01$ (**)).

4.1.2 Phenotype of the *abp* mutants in conditions *in vitro*

In addition to the phenotype analysis *in vivo*, the phenotype of maize *abp* mutants was also analyzed in conditions *in vitro*. The analyses included the determination of the length of three different etiolated seedling's organs: coleoptile, mesocotyl and primary root in basal medium (Figure 4.1.8A). The size of these organs was measured with a ruler to the nearest millimetre in 5-day-old intact seedlings developed *in vitro* and germinated in the same day. Mesocotyl length was measured from scutellar to coleoptilar node and coleoptile length was measured from coleoptilar node to the tip of the coleoptile. Length of primary root was also measured.

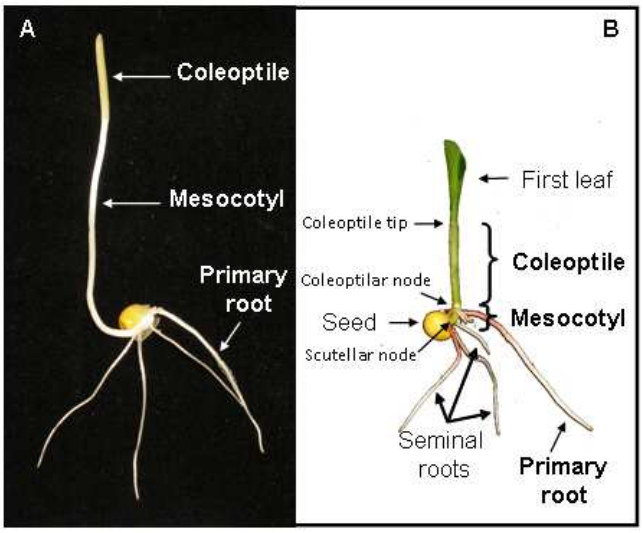

Figure 4.1.8 An example of etiolated (A) and light grown (B) maize seedling.

4.1.2.1 Length of etiolated organs

The single mutant *abp1* grown in the dark developed coleoptile slightly longer than that observed in the WT, while the coleoptile length of the *abp4* and double *abp1/abp4* mutants was almost 20 to 30% shorter than the coleoptile of the control plants (Figure 4.1.9).

Differences between the WT and *abp* mutants were also observed in the respect of mesocotyl growth (Figure 4.1.9). Whereas etiolated seedlings of the *abp1* mutant developed mesocotyl shorter than that in the WT, the length of the mesocotyl in the *abp4* mutants was identical to the WT plants. The etiolated double *abp1/abp4* mutant developed almost two third-length mesocotyl in comparison with that in control plants.

The primary root of etiolated seedlings (Figure 4.1.9) was the longest in the WT plants. The a*bp1* and *abp4* mutants developed primary root shorter than the WT. Interestingly, the double mutation led to even shorter primary root (almost 60% shorter) than in the WT.

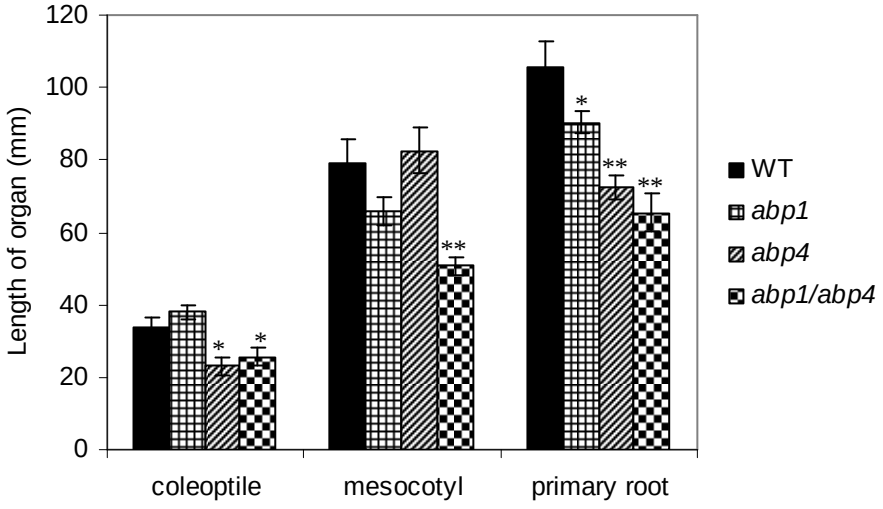

Figure 4.1.9 Elongation of the coleoptile, mesocotyl and primary root in 5-day-old WT and *abp* mutants in maize grown *in vitro* on the BM in the dark.

Elongation of organs was measured with a ruler to the nearest millimetre in 5-day-old seedlings. The results are the mean length ± SE obtained from 5 to 12 independent experiments. In each genotype, six to nine seedlings were measured in each experiment. WT and *abp* mutants show significant difference (*t*-test: $p \leq 0.05$ (*), $p \leq 0.01$ (**)).

4.2 Effect of auxin on the development of maize

4.2.1 Effect of auxin on the elongation of coleoptile, mesocotyl and primary root in condition *in vitro*

In order to investigate the role of exogenous auxin in the growth of maize *abp* mutant seedlings, plants were grown in condition *in vitro* in the dark in medium supplemented or not with different auxin concentrations (1-Naphthaleneacetic acid/NAA: 10^{-6}, 10^{-5}, $5x10^{-5}$, 10^{-4} M). The growth of all organs of etiolated seedlings of all genotypes was gradually inhibited by auxin in a concentration-dependent manner (Figure 4.2.1).

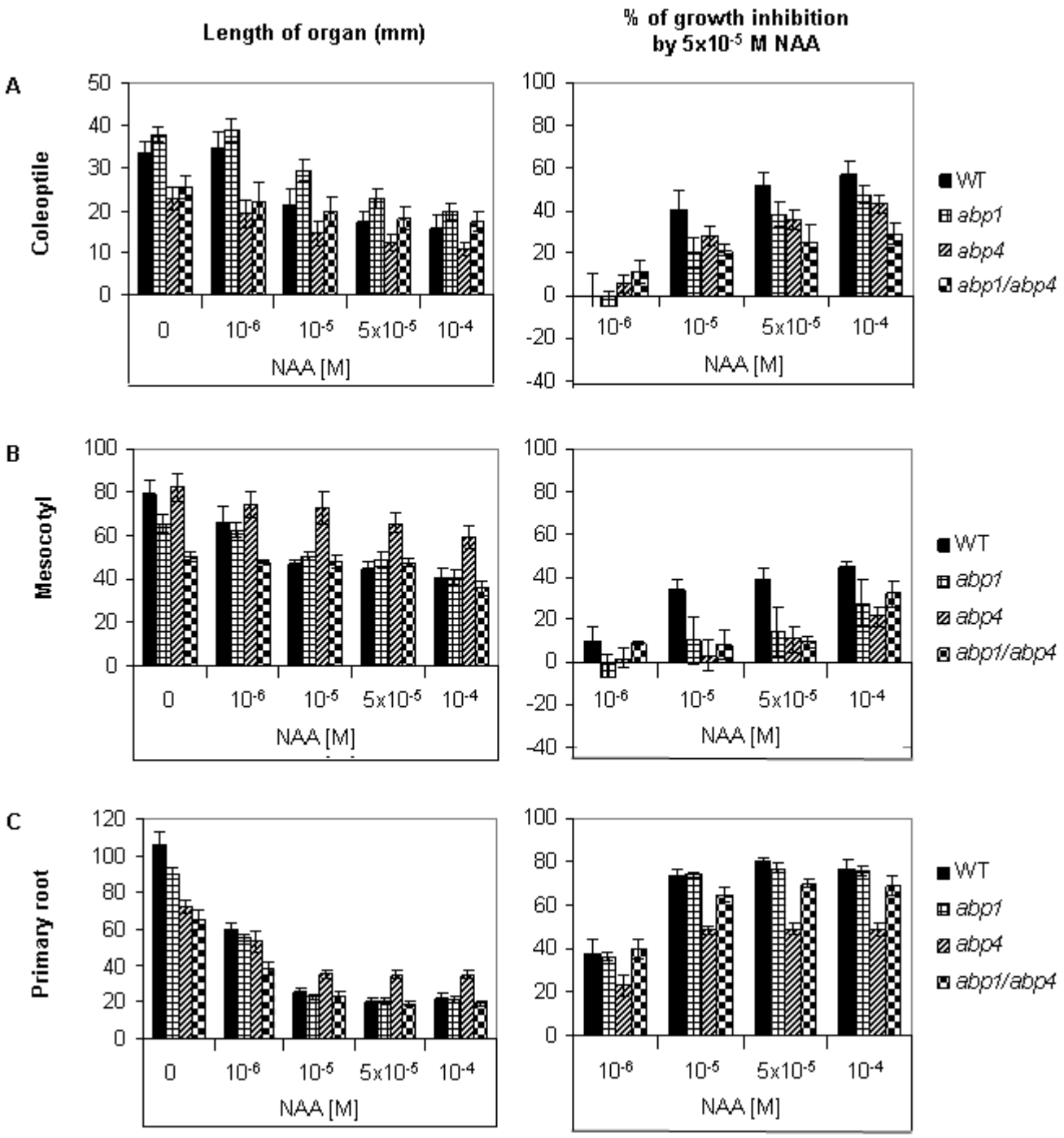

Figure 4.2.1 Elongation of coleoptile (A), mesocotyl (B) and primary root (C) in 5-day-old WT and *abp* mutants grown in the dark *in vitro* on the BM supplemented or not with auxin (NAA).

For each genotype and condition, organ length in six to nine seedlings was measured. Values represent mean organ length ± SE obtained from 5 to 12 independent experiments. Percent of inhibition ± SE of organ growth in etiolated seedlings is calculated from the mean values in 5 to 12 independent experiments.

The results showed that etiolated WT plants are more sensitive to exogenous auxinhan *abp* mutants. For example, the elongation of coleoptile of the WT plants was inhibited by 50% by 50 µM NAA whereas the *abp* mutants were less sensitive at the same concentration (Figure 4.2.1A). The coleoptile of etiolated a*bp1* and *abp4* mutants exhibited approx. the same sensitivity to exogenous NAA (inhibition approx. 35%), but remained essentially lower compared to WT plants (Figure 4.2.1A). The etiolated double *abp1/abp4* mutant was the least sensitive to the inhibitory effect of exogenous auxin. Indeed the NAA-induced inhibition of coleoptile growth was half of those observed for the WT seedlings.

Like for the coleoptile, exogenous auxin inhibited the elongation of the mesocotyl in WT and *abp* etiolated seedlings in a concentration-dependent manner. All etiolated *abp* mutants were less responsive to the inhibitory effect of auxin than the WT (Figure 4.2.1B).

The strongest inhibitory effect of NAA on elongation was observed on the primary roots (Figure 4.2.1C). Whereas etiolated WT, *abp1* and double *abp1/abp4* mutant showed almost the same sensitivity to NAA (growth inhibition: approx. 80%), primary root growth of the *abp4* mutant was inhibited by only 50%.

4.2.2 Effect of exogenous auxin on the phenotype of WT plants and *abp* mutants developed in the greenhouse

In order to check the effects of exogenous auxin on the plants grown *in vivo* the growth of plants developed in the greenhouse was analysed for the overall growth (plant height), the leaf blade length and width, and the blade declination. For this purpose plants were sprayed every day with a solution of 0.1 µM, 10 µM or 100 µM NAA; the control group of plants was sprayed with the same amount of distilled water. Three independent experiments with each auxin concentration have been performed but no effects were observed in relation to any of the parameters being tested (data not shown).

4.3 Effects of light on the growth of maize seedlings

In order to further extend the phenotypic analysis of the maize mutants' seedlings, the effect of light on the growth of maize seedlings in conditions *in vitro* was also studied. Plants were

grown for 5 days under continuous blue (BL) and red light (RL) and the length of the three different organs, coleoptile, mesocotyl and primary root, was measured.

The results showed that BL had an inhibitory effect only on the elongation of the *abp1* mutant coleoptile, whereas it did not affect the length of the WT and the *abp1/abp4* double mutant coleoptile. However, it slightly stimulated the elongation of the *abp4* mutant coleoptile (Figure 4.3.1A). RL stimulated coleoptile elongation in WT, *abp4* and *abp1/abp4* double mutant, but not in the *abp1* mutant (Figure 4.3.1A).

In all genotypes tested, BL strongly inhibited the mesocotyl elongation in comparison to etiolated seedlings (Figure 4.3.1B). The mutation in *ABP1* and/or *ABP4* genes had no effect on the sensitivity of mesocotyl to BL. Similarly to BL, RL showed a strong inhibitory effect on the elongation of mesocotyl. Interestingly, under RL, the *abp4* mutant developed mesocotyl significantly longer compare to WT, *abp1* and *abp1/abp4* double mutants (Figure 4.3.1B). BL inhibited the elongation of the primary root of the WT and the *abp1/abp4* double mutant, but had no effect on the elongation of the primary root of the single *abp1* and *abp4* mutants (Figure 4.3.1C). In comparison to WT, under BL the length of primary root of the *abp1* mutant was longer, whereas the *abp4* mutant had primary root length similar to that of the WT. The mutation in both *ABP1* and *ABP4* genes led to development of essentially shorter primary root in the *abp1/abp4* double mutant compare to the WT. RL inhibited the primary root elongation of WT plants by approx. 30%, whereas it had no effect on the elongation of the primary roots of neither the single nor double *abp* mutants. Under RL, the *abp1* mutant developed primary roots slightly longer than WT, whereas, the *abp4* and *abp1/abp4* double mutants had primary roots of a similar length as observed in the WT (Figure 4.3.1C).

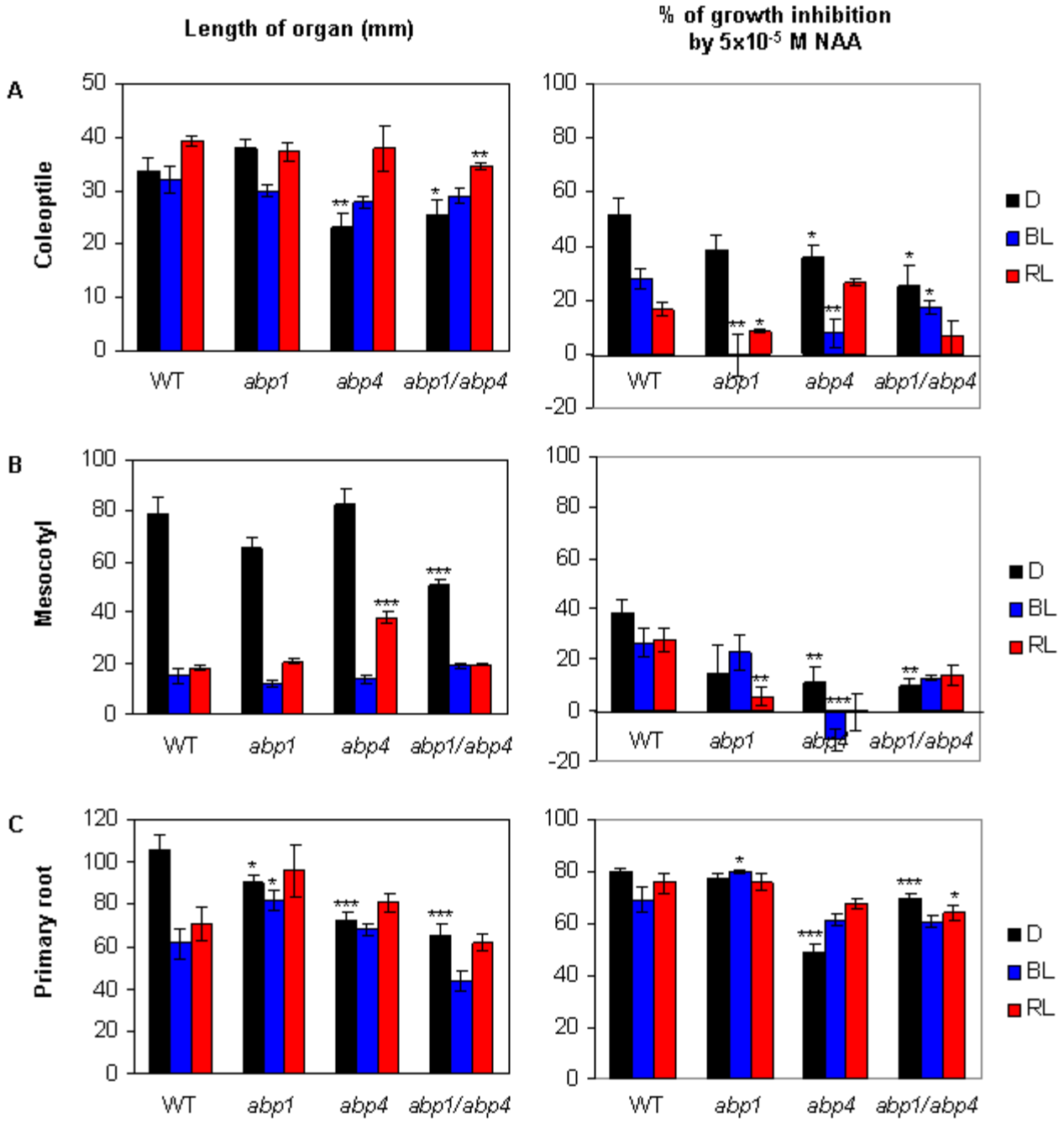

Figure 4.3.1 Comparison of seedling growth in single maize mutants *abp1* and *abp4*, double mutant *abp1/abp4* and corresponding WT, in response to dark and light.

Elongation of coleoptile (**A**), mesocotyl (**B**) and primary root (**C**) was measured with a ruler to the nearest millimetre in 5-day-old seedlings grown in condition *in vitro* in dark (D), blue light (BL), or in red light (RL) on the BM. The results are the mean length ± SE obtained from 5 to 12 independent experiments. In each genotype, six to nine seedlings were measured in each experiment. Comparison of NAA-induced growth inhibition of coleoptile (**A**), mesocotyl (**B**) and primary root (**C**) in seedlings developed in D, BL or RL at auxin concentration of 5.10^{-5} M. Values are mean growth inhibition ± SE calculated from the mean values in 5 to 12 independent experiments. WT and *abp* mutants under the same light condition show significant difference (*t*-test: $p \leq 0.05$ (*), $p \leq 0.01$ (**), $p \leq 0.001$ (***)).

4.3.1 Effects of auxin on the growth of maize seedlings under different light conditions

The effect of exogenous auxin on the growth of maize seedlings was assessed in different light conditions using several concentrations of NAA. For a clearer presentation of the results only data obtained with 50 μM NAA are shown (Figure 4.3.1).

Under BL, the coleoptile responsiveness to the inhibitory effect of auxin was markedly lower than that of etiolated seedlings. Like in the dark, BL-developed coleoptile of WT seedlings showed a higher sensitivity to exogenous auxin than the *abp* mutants (Figure 4.3.1A). Whereas the coleoptile of BL-grown *abp1* mutant showed almost no sensitivity to auxin, the coleoptiles of the *abp4* and *abp1/abp4* double mutants were three and two times, respectively, less sensitive than coleoptiles in WT. The mesocotyl of BL-grown *abp1* mutant showed almost the same sensitivity to exogenous auxin as mesocotyl of the WT seedlings (Figure 4.3.1B). Interestingly, whereas in WT seedlings grown under BL auxin inhibited mesocotyl elongation by approx. 25%, in the *abp4* mutant developed in BL mesocotyl growth was slightly stimulated by auxin. Mesocotyl of *abp1/abp4* double mutant was the least sensitive to auxin under BL. Primary root of BL-grown *abp1* seedlings showed almost the same sensitivity to auxin as WT plants, whereas roots of the *abp4* and *abp1/abp4* double mutants were slightly less responsive to exogenous auxin than WT grown in the same condition (Figure 4.3.1C).

Under RL, the responsiveness of coleoptiles to exogenous auxin was generally lower than the sensitivity of coleoptiles developed in the dark. In RL, coleoptiles of the *abp1* and *abp1/abp4* double mutants showed less sensitivity to exogenous auxin than WT (Figure 4.3.1A), whereas coleoptile of the *abp4* mutant was the most sensitive to exogenous auxin. Mesocotyl of RL-grown WT plants showed higher sensitivity to auxin than all *abp* mutants. Mesocotyl of the *abp4* mutant showed almost no sensitivity to exogenous auxin under RL (Figure 4.3.1B). The primary root of RL-grown *abp1* mutant showed almost the same sensitivity to auxin as WT plants, whereas primary roots of the *abp4* and *abp1/abp4* double mutants were less sensitive than WT to exogenous auxin under RL (Figure 4.3.1C).

4.4 Role of calcium in the development of maize

4.4.1 Effect of exogenous calcium on the growth of maize seedlings *in vitro*

In order to check the sensitivity of *abp* mutant plants to Ca^{2+}, growth of maize seedlings *in vitro* was assessed in dark condition using several concentrations of Ca^{2+}. All genotypes were able to grow in the medium without Ca^{2+} as well as in the medium supplemented with 3 mM (concentration of Ca^{2+} in basal MS medium) and 10 mM Ca^{2+} (Figure 4.4.1).

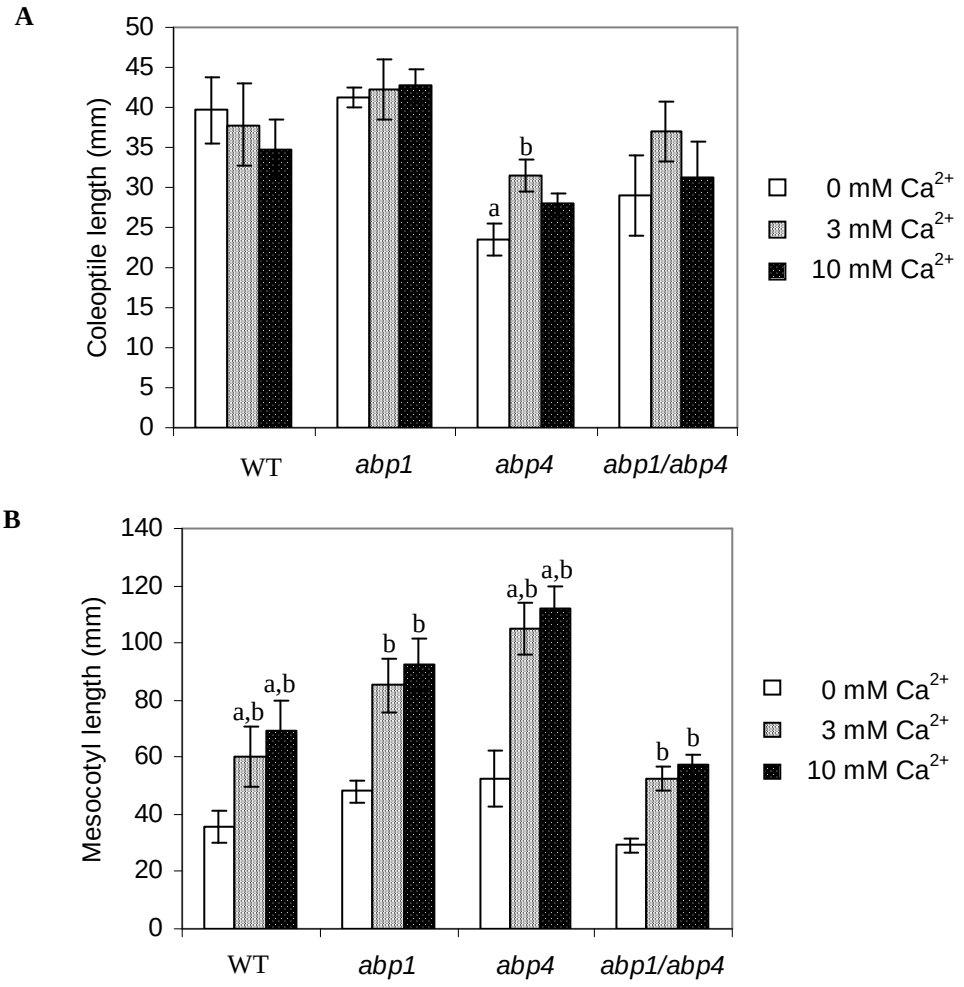

Figure 4.4.1 Effect of exogenous Ca^{2+} on the growth of coleoptile (A) and mesocotyl (B) of single maize *abp1* and *abp4* mutants, *abp1/abp4* double mutant and the corresponding WT grown in the dark.

Maize seedlings grew in conditions *in vitro* for 5 days on the basal MS medium free of $CaCl_2$ or supplemented with $CaCl_2$ in concentrations of 3 or 10 mM. For each genotype, five to ten seedlings were measured in each experiment. Values represent mean ± SE of 4 to 9 experiments. WT and *abp* mutants show significant difference (*t*-test: $p \leq 0.05$): a-significantly different from WT in the same concentration, b-significantly different from the control (0 mM Ca^{2+}) of the same genotype.

Experiments on etiolated seedlings showed that exogenous Ca^{2+} influences growth of coleoptile and mesocotyl in a different way.

In the medium without Ca^{2+} (Figure 4.4.1A), the *abp4* mutant developed significantly shorter coleoptile compare to WT, whereas the mutation in the single *ABP1* gene and in both *ABP1* and *ABP4* genes did not have any significant effect on the coleoptile elongation (Figure 4.4.1A). The data further showed that the coleoptile growth of WT, *abp1* and *abp1/abp4* double mutant was insensitive to exogenous Ca^{2+} (3 mM and 10 mM). Interestingly, elongation of coleoptile in the *abp4* mutant was significantly stimulated by 3 mM Ca^{2+}, but not by 10 mM Ca^{2+}.

In the medium free of Ca^{2+} the mesocotyl length did not differ between WT and *abp* mutants (Figure 4.4.1B). Unlike in the coleoptile, exogenous Ca^{2+} strongly stimulated the mesocotyl elongation in all genotypes with the maximum at 10 mM Ca^{2+}. The greatest growth stimulation at 3 and 10 mM $CaCl_2$ was observed in seedlings with knockout in the *ABP4* gene (Figure 4.4.1B).

4.4.2 Calcium content in maize coleoptile and mesocotyl of etiolated WT and *abp* mutant seedlings

Ca^{2+} content in maize coleoptile and mesocotyl was determined in etiolated seedlings grown in conditions *in vitro* in the medium without Ca^{2+} and in the medium supplemented with 3 mM and 10 mM Ca^{2+} (Figure 4.4.2). Whatever the genotype, the concentration of Ca^{2+} in the aerial parts of the maize etiolated seedlings increased with increasing Ca^{2+}concentration in the medium (Figure 4.4.2). Experiments showed that the mutation in the *ABP1* gene does not affect the accumulation of Ca^{2+} in aerial parts of maize, whereas in the *abp4* mutant the accumulation of Ca^{2+} was three-times higher than in WT both in medium without Ca^{2+} or with 3 mM and 10 mM Ca^{2+}. The mutation in both *ABP1* and *ABP4* genes caused slightly higher accumulation of Ca^{2+} than observed in WT seedlings (Figure 4.4.2).

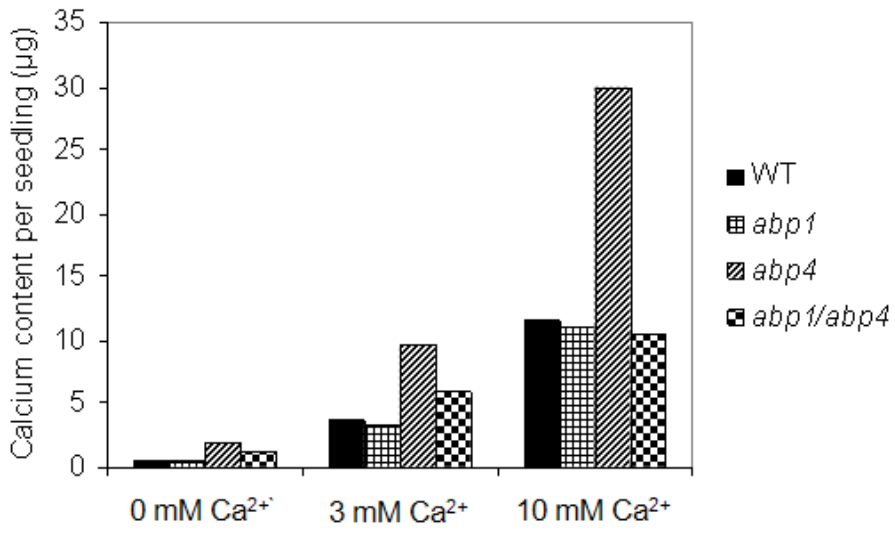

Figure 4.4.2 Accumulation of Ca^{2+} in coleoptile plus mesocotyl of etiolated single maize *abp1* and *abp4* mutants, *abp1/abp4* double mutant and the corresponding WT.

Maize seedlings grew in conditions *in vitro* for 5 days on the basal MS medium free of $CaCl_2$ or supplemented with $CaCl_2$ in concentrations of 3 or 10 mM. Sample consisting of 4 to 11 seedlings was collected from each Ca^{2+} concentration and freeze-dried in lyophilizer. Ca^{2+} was determined by flame atomic absorption spectrometry using acetylene-air flame at wavelength 422.7 nm. Values represent data from one experiment.

4.4.3 Effect of exogenous calcium on the phenotype of WT plants and *abp* mutants developed in the greenhouse

The effect of exogenous Ca^{2+} on the plants developed in the greenhouse was analyzed for the overall growth, leaf blade length and width, and leaf declination.

Treated plants were sprayed every day with a solution of $CaCl_2$ of different concentrations (10 µM, 50 µM, 100 µM, 1 mM and 10 mM) and control group of plants was sprayed in the same time with the same amount of distilled water. No obvious differences were obtained in response to exogenous Ca^{2+} concerning these characteristics neither in the WT nor in the *abp* mutants compare to control (data not shown).

4.5 Isolation and characterization of *Arabidopsis CAX1* homolog in maize. Sequence analyses in silico

In order to isolate and characterize *AtCAX1* homolog in maize, databases NCBI (http://www.ncbi.nlm.nih.gov/) and maize GDB (http://www.maizegdb.org/) were screened using the *AtCAX1* sequence (accession number: AF461691) as a reference. From this analysis three sequences were identified in maize: *ZmHCX1* (accession number: AF256229), *ZmCAX2* (accession number: AB044567) and *ZmPCO087284* (accession number: AY108295).

The 1st sequence, *ZmHCX1*, was assigned to CAX1-like protein sharing 65% identity with AtCAX1. The 2nd sequence, *ZmCAX2*, shares 72.4% of identity with *Arabidopsis AtCAX6*. Finally, the 3rd sequence, *ZmPCO087284*, encodes a protein sharing 71.8% of similarity with *AtCAX3* from *Arabidopsis* and will be further reported as *ZmCAX3*.

Specific primers were designed in order to amplify the full length of *ZmCAX2* and *ZmCAX3* from plant material (WT plants). *ZmCAX2* is 1338 bp long, contains a 1260 bp open reading frame and encodes a protein with 419 residues with a calculated molecular mass of 45.6 kDa. *ZmCAX3* is 1590 bp long, contains a 1389 bp open reading frame and encodes a 462 amino acid long protein with a calculated molecular mass of 48.9 kDa.

An unrooted phylogenetic tree was made using sequences from *Arabidopsis*, *Oryza sativa* and *Zea mays*. The analysis showed that *ZmCAX2* was classified into CAX type IB with other *CAXs*, whereas *ZmCAX3* is clustered into the type IA of CAXs, together with *Arabidopsis AtCAX1* and *AtCAX3* (Shigaki et al, 2006) (Figure 4.5.1). In addition, the analysis showed that on the basis of the amino acid sequences *ZmCAX2* is closely related to *OsCAX3* from the same species, whereas *ZmCAX3* gene is closely related to *OsCAX1a* from *Oryza sativa* (Kamiya et al, 2005).

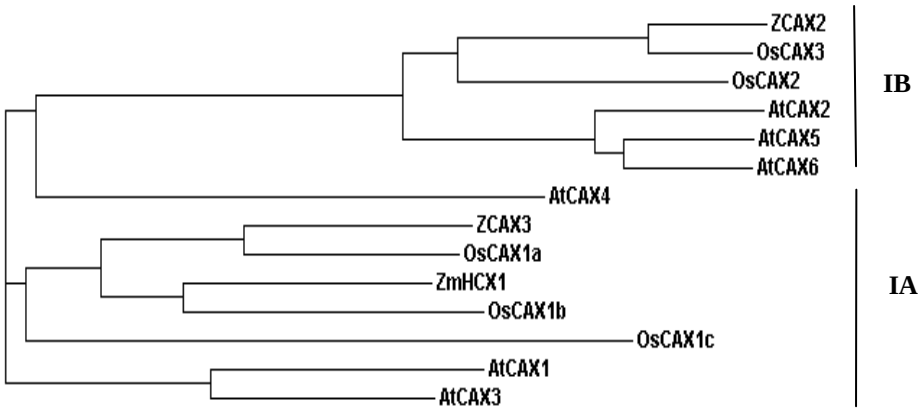

Figure 4.5.1 Phylogenetic relationship of maize (*Z. mays*), Arabidopsis (*A. thaliana*) and rice (*O. sativa*) *CAXs*.

The phylogenetic tree was constructed from alignments of full-length amino acid sequences using the ClustalW2 (Larkin et al, 2007) program. Type IA CAXs predominantly transport Ca^{2+}, whereas type IB CAXs transport cations other than Ca^{2+} such as Mn^{2+}, Mg^{2+} and Cd^{2+}. The accession numbers are as follows: *ZmCAX2* (*Z. mays*, AB044567.1), *ZmCAX3* (*Z. mays*, AY108295.1), *ZmHCX1* (*Z. mays*, AF256229.1), *AtCAX1* (*A. thaliana*, AF461691), *AtCAX2* (*A. thaliana*, AF424628), *AtCAX3* (*A. thaliana*, At3g51860), *AtCAX4* (*A. thaliana*, AF409107), *AtCAX5* (*A. thaliana*, At1g55730), *AtCAX6* (*A. thaliana*, At1g55720), *OsCAX1a* (*O. sativa*, AB112656),*OsCAX1b* (*O. sativa*, AB112770), *OsCAX1c* (*O. sativa*, AB112771), *OsCAX2* (*O. sativa*, AB112772), *OsCAX3* (*O. sativa*, AB112773).

Two programs, TMHMM program (Krogh et al, 2001) and TMpred program (Hofmann and Stoffel, 1993) for prediction of topology of these proteins, were used. They allowed the description of 11 transmembrane domains with a long hydrophilic N-terminal part facing the cytosol (Figure 4.5.2). An acidic amino-acid-rich region was found in the cytosolic loop between the sixth and seventh transmembrane domain of both *CAX* candidates (Figures 4.5.2 and 4.5.3).

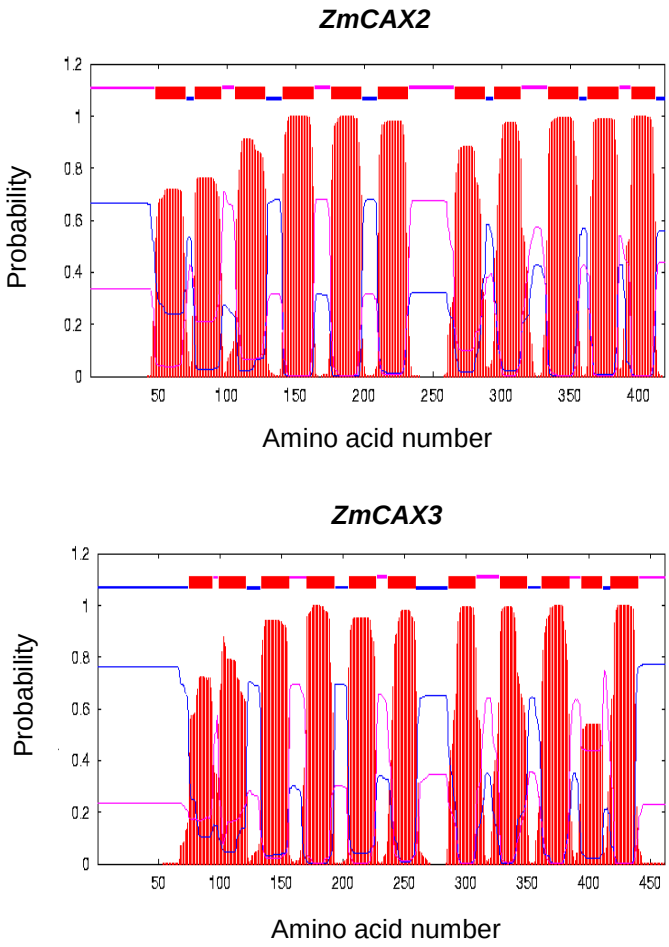

Figure 4.5.2 Membrane topology of *ZmCAX2* (*Z. mays*, AB044567.1) and *ZmCAX3* (*Z. mays*, AY108295.1).

The topologic models were generated by TMHMM program. The red areas indicate predicted TM domains, and the blue and magenta lines indicate the regions that are predicted to be inside or outside of the membrane, respectively.

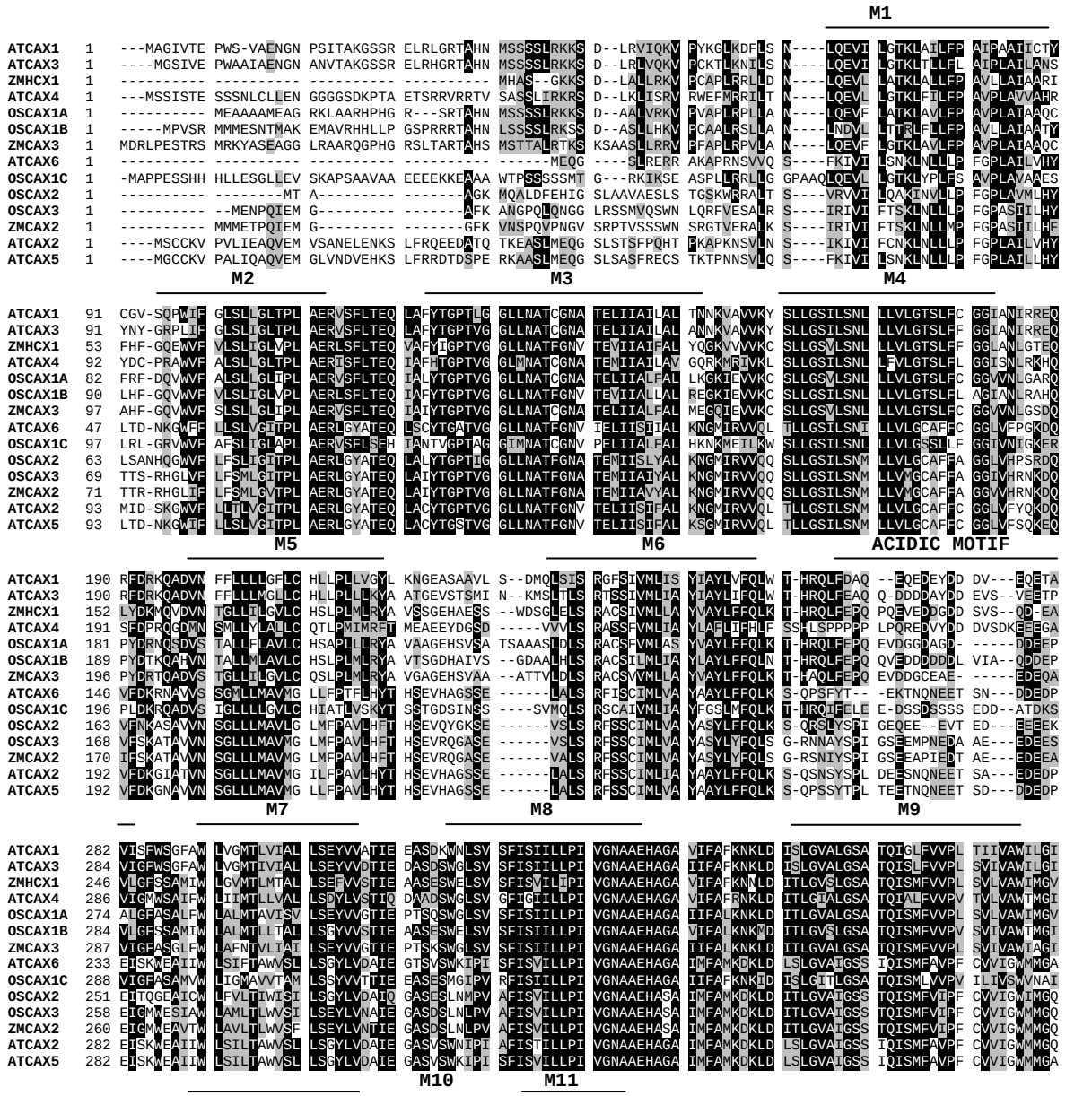

Figure 4.5.3 Multiple sequence alignment of maize (*Z. mays*), Arabidopsis (*A. thaliana*) and rice (*O. sativa*) *CAXs*.

Alignments were performed using ClustalW from the European Bioinformatics Institute Web site. Consensus amino-acid sequences are boxed in black (identical) or gray (similar). Gaps introduced into sequences to increase their similarity are denoted by hyphens. The 11 putative transmembrane spans (M1-M11) predicted for

all transporters and the central hydrophilic motif rich in acidic residues are overlined. The accession numbers are as follows: *ZmCAX3* (*Z. mays*, AY108295.1), *ZmCAX2* (*Z. mays*, AB044567.1), *ZmHCX1* (*Z. mays*, AF256229.1), *AtCAX1* (*A. thaliana*, AF461691), *AtCAX2* (*A. thaliana*, AF424628), *AtCAX3* (*A. thaliana*, At3g51860), *AtCAX4* (*A. thaliana*, AF409107), *AtCAX5* (*A. thaliana*, At1g55730), *AtCAX6* (*A. thaliana*, At1g55720), *OsCAX1a* (*O. sativa*, AB112656), *OsCAX1b* (*O. sativa*, AB112770), *OsCAX1c* (*O. sativa*, AB112771), *OsCAX2* (*O. sativa*, AB112772), *OsCAX3* (*O. sativa*, AB112773).

The alignment of different CAXs showed that these proteins are highly conserved among monocots and dicots, except of the N-terminal domain of the protein. The Ca^{2+} domain (CaD), constituted of 9 amino acids, was localized between the M1 and M2 spanning domains (Figure 4.5.4). CaD is poorly conserved within the CAX family, however the regions flanking CaD region are quite similar to each other.

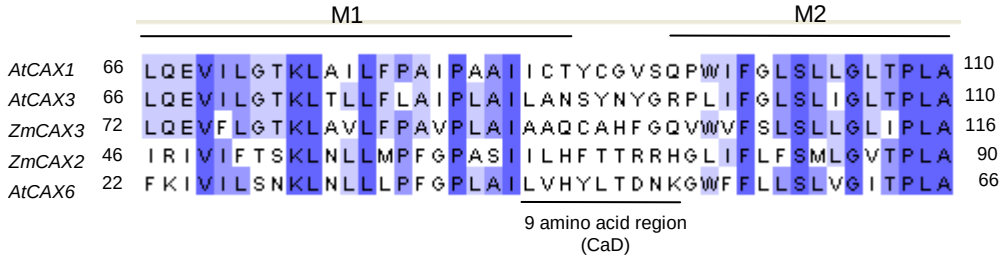

Figure 4.5.4 Ca^{2+} domains in some maize (*Z. mays*) and Arabidopsis (*A. thaliana) CAXs.*

Alignment of deduced amino acid sequences between the deduced first and second membrane-spanning domains (M1 and M2) of polypeptides encoded by *ZmCAX3* (*Z. mays*, AY108295), *ZmCAX2* (*Z. mays*, AB044567), *AtCAX1* (*A. thaliana*, AF461691), *AtCAX3* (*A. thaliana*, At3g51860) and *AtCAX6* (*A. thaliana*, At1g55720). Alignments were performed by using ClustalW2 (Larkin et al, 2007) and Jalview Version2 (Waterhouse et al, 2009) programs.

4.6 Expression analyses of *ZmCAX2* and *ZmCAX3* genes

As one of the aims of this thesis was to study the relationship between CAXs and ABPs during maize development, the expression pattern of the two cloned genes, *ZmCAX2* and *ZmCAX3*, have been investigated in different conditions *in vivo* and *in vitro* by both semiquantitative RT-PCR (*ZmCAX2*) and qRT-PCR (*ZmCAX3*) (due to very low transcript level of *ZmCAX3*). All the results presented here are expressed relative to the gene transcript accumulation in the WT in the control condition.

4.6.1 Expression analyses of *ZmCAX2* and *ZmCAX3* in the leaf base

Finally, as one of the aims of this thesis was to unravel the possible role of CAXs in the leaf development, the expression pattern of *ZmCAX2* and *ZmCAX3* was analysed in the base of the emerging third leaf and fully developed leaf of plants grown in condition *in vivo* since in this leaf the most significant difference in leaf angle between WT and the *abp* mutants was found. The attention was focused on the base of the leaf in order to estimate the expression of these two genes during auricle development. The results are expressed relative to gene transcript accumulation in the base of the emerging leaf of the WT.

The expression of *ZmCAX2* (Figure 4.6.1) in the base of the emerging leaf did not differ between WT and *abp* mutants. *ZmCAX2* expression was not affected in the base of the developed leaf neither in WT nor in *abp1* and *abp4* mutants, whereas it was significantly down regulated in *abp1/abp4* double mutant compared to the emerging leaf of WT.

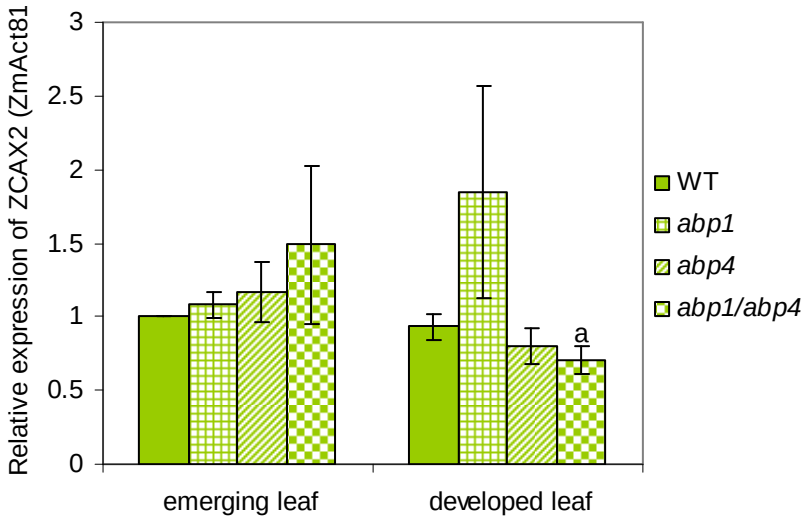

Figure 4.6.1 Relative expression of *ZmCAX2* in the base of the emerging and fully developed third leaf in single *abp1* and *abp4* mutants, *abp1/abp4* double mutant and the corresponding WT.

WT and mutant plants were grown in the greenhouse under long day condition, at temperature of 15 to 27°C and regularly watered. Expression of *ZmCAX2* (*Z. mays, AB044567.1*) was determined in the base of emerging and fully developed third leaf. The expression analysis of *ZmCAX2* was performed by semiqRT-PCR and as a reference gene was used *ZmAct81* (*U60511*). Results are expressed relative to gene transcript level in the emerging leaf of WT. The data were analyzed using the ImageJ program. Results present the data obtained in three independent experiments. a - significantly different (*t*-test: $p \leq 0.05$) from WT control (emerging leaf).

The expression of *ZmCAX3* (Figure 4.6.2) in the base of the emerging leaf did not differ between WT and *abp* mutants. However, in the base of the developed third leaf, the expression of *ZmCAX3* was significantly up regulated in the single *abp1* and double *abp1/abp4* mutant compared to its expression in the base of the emerging leaf of WT.

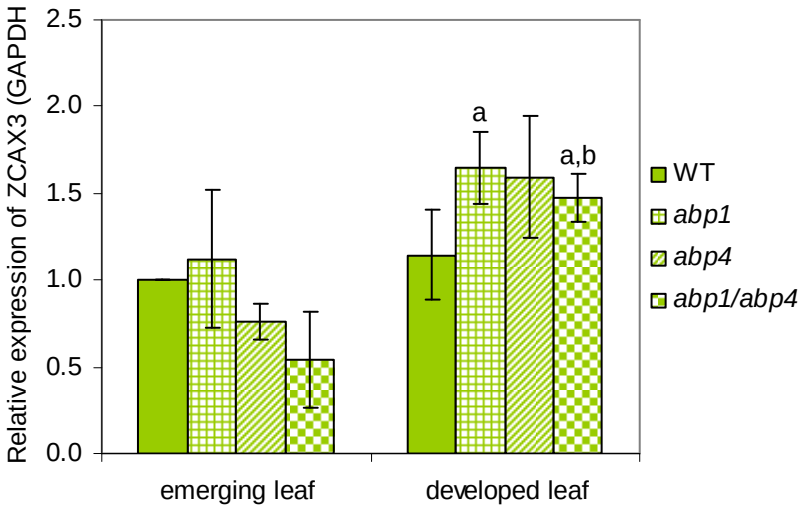

Figure 4.6.2 Relative expression of *ZmCAX3* in the base of the emerging and fully developed third leaf in single *abp1* and *abp4* mutants, *abp1/abp4* double mutant and the corresponding WT.

WT and mutant plants were grown in the greenhouse under long day condition, at temperature of 15 to 27°C and regularly watered. Expression of *ZmCAX3* (*Z. mays*, AY108295.1) was determined in the base of emerging and fully developed third leaf. The expression analysis of *ZmCAX3* was performed by qRT-PCR and as a reference gene *GAPDH* (*Zm.3765*) was used. Results are expressed relative to gene transcript level in the emerging leaf of WT. Results present the data obtained in three independent experiments. a - significantly different (*t*-test: $p \leq 0.05$) from WT control (emerging leaf), *b* - significantly different from the *abp1/abp4* emerging leaf (*t*-test: $p \leq 0.05$)

4.6.2 Expression analyses of *ZmCAX2* and *ZmCAX3* in function of exogenous NAA

Since the *in vitro* phenotype analyses performed in this study showed that WT and *abp* mutants are differently sensitive to exogenous auxin (Figure 4.2.1), the expression pattern of the selected genes was analysed in coleoptiles and mesocotyls of 5-day-old etiolated seedlings in order to unravel the effect of auxin on the expression of *ZmCAX2* and *ZmCAX3*. For this purpose plants were grown in the medium supplemented or not with 50 μM NAA.

The analyses showed that the expression of *ZmCAX2* in the coleoptile and mesocotyl of seedlings grown on BM did not differ (Figure 4.6.3A), whereas *ZmCAX3* was markedly more expressed in the mesocotyls than in the coleoptiles (Figure 4.6.3B).

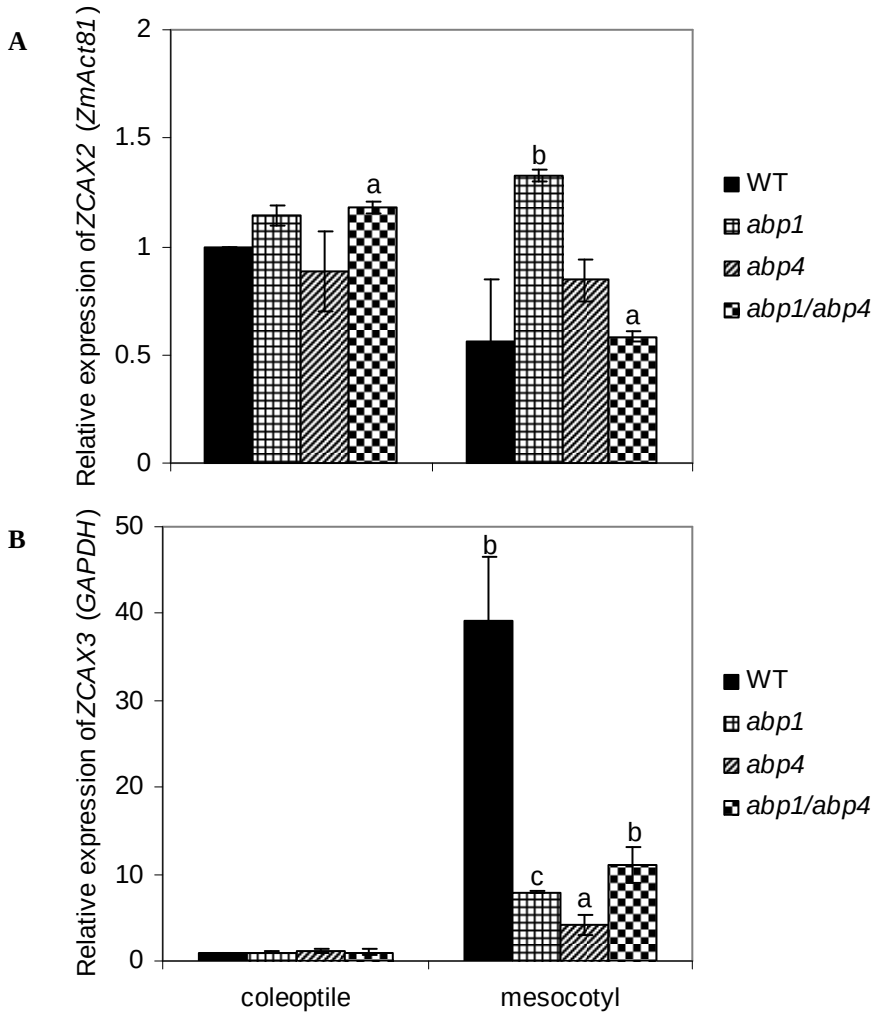

Figure 4.6.3 Expression of *ZmCAX2* and *ZmCAX3* genes in etiolated coleoptiles and mesocotyls in maize single *abp1* and *abp4* mutants, double *abp1/abp4* mutant and the corresponding WT.

WT and mutant seedlings were grown in the dark for 5 days in conditions *in vitro* on the basal MS medium. The expression analysis of *ZmCAX2* (*Z. mays*, AB044567.1) (**A**)was performed by semiqRT-PCR and *ZmCAX3* (*Z. mays*, AY108295.1) (**B**) expression analysis was performed by qRT-PCR. In the case of *ZmCAX2*, *ZmAct81* (U60511) was used as housekeeping gene, and in the case of *ZmCAX3* primers for GAPDH (Zm.3765) were used as a control. Results are expressed relative to the gene transcript accumulation in WT coleoptile. The data for *ZmCAX2* were analyzed using the ImageJ program. Results present the data obtained in two to three independent experiments in each condition and genotype. a (*t*-test: $p \leq 0.05$), b (*t*-test: $p \leq 0.01$), c (*t*-test: $p \leq 0.001$)-significantly different from WT coleoptile.

The expression pattern of *ZmCAX2* gene in the presence of NAA did show any significant difference between *abp* mutants compare to WT neither in the coleoptile nor in the mesocotyl and therefore these data are not presented here. Similarly, the expression of *ZmCAX3* in coleoptile also did not show any difference between maize *abp* mutants and WT grown on BM or BM supplemented with NAA (data not shown).

However, the expression of *ZmCAX3* in the mesocotyl (Figure 4.6.4) of etiolated seedlings grown in BM (containing 3mM $CaCl_2$) was significantly lower in the *abp4* mutant compare to the WT. No significant difference was observed in either the *abp1* mutant or in the *abp1/abp4* double mutant. Treatment of seedlings by 50 μM NAA significantly inhibited the expression of *ZmCAX3* in WT, *abp1* and *abp1/abp4* mutants. However, the expression of *ZmCAX3* gene in the *abp4* mutant did not significantly differ between seedlings grown in auxin-free medium and in the medium supplemented with NAA.

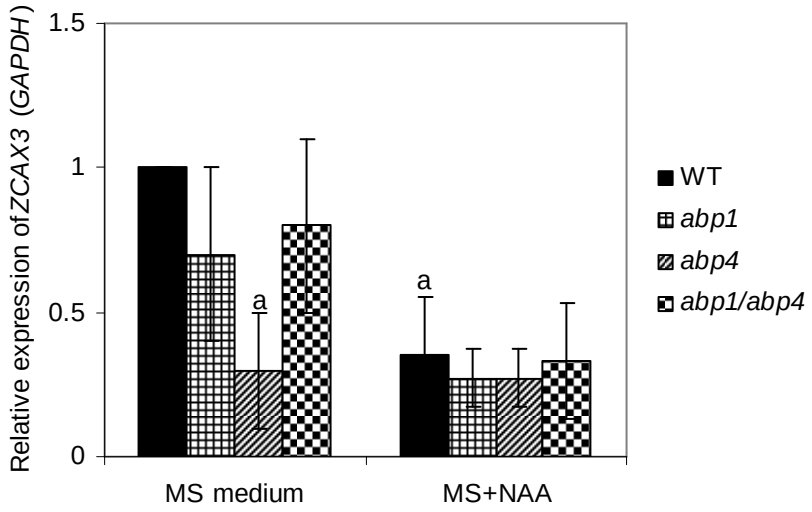

Figure 4.6.4 Auxin-induced expression of *ZmCAX3* gene in mesocotyl of WT and *abp* mutants seedlings grown in the dark.

WT and mutant plants were grown in the dark, *in vitro* and on BM or on BM supplemented with 50 μM NAA. *ZmCAX3* expression analysis was performed by qRT-PCR. Results are expressed relative to the transcript accumulation in WT plants developed in the absence of NAA. *GAPDH* was used as a reference gene. The values represent an average of the data obtained in three independent experiments in each condition and genotype. *a* - significantly different from WT in the absence of NAA (*t*-test: $p \leq 0.05$).

4.6.3 Expression analyses of *ZmCAX2* and *ZmCAX3* in function of exogenous calcium

Since different responses to exogenous Ca^{2+} were observed among genotypes, the expression pattern of *ZmCAX2* and *ZmCAX3* was investigated in coleoptile and mesocotyl of 5-day old etiolated seedlings in relation to Ca^{2+} supply (10 mM). As a control condition plants were grown on BM depleted in Ca^{2+}. In the Ca^{2+}-free medium and in the medium supplemented with 10 mM $CaCl_2$, the expression of *ZmCAX3* was very weak and almost undetectable. In contrast, *ZmCAX2* was expressed in all tested genotypes in both conditions.

Once again, the expression pattern of *ZmCAX2* gene did show any significant difference between *abp* mutants compare to WT neither in coleoptile nor in mesocotyl. Therefore these data are not presented here. Similarly, the expression of *ZmCAX3* in coleoptile did not show any difference between *abp* mutants and the WT grown either in basal Ca^{2+}-free medium or BM supplemented by 10 mM Ca^{2+} (data not shown).

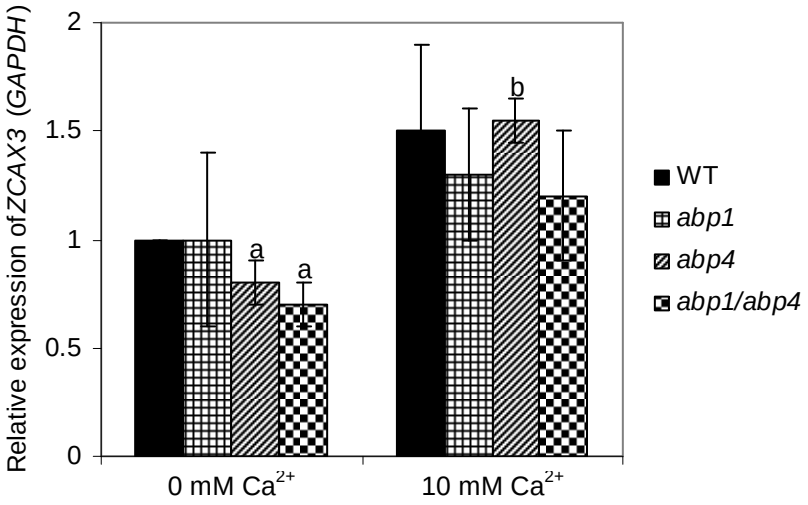

Figure 4.6.5 Calcium-induced expression of *ZmCAX3* gene in mesocotyls of WT and *abp* mutants grown in the dark.

WT and mutant seedlings 771 were developed in darkness, *in vitro*, and on BM free of CaCl2 (control) or supplemented with 10 mM CaCl2. In 5-day-old seedlings, *ZmCAX3* expression analysis was performed by qRT-PCR. Results are expressed relative to the transcript accumulation in WT plants developed with an absence of calcium (0 mM CaCl2). As a reference gene, *GAPDH* was used. The values represent an average ± SE of the data obtained in three independent experiments in each condition and genotype. *a* - significantly different from WT at 0 mM Ca^{2+} (*t*-test: $p \leq 0.05$), *b* - significantly different from the *abp4* at 0 mM Ca^{2+} (*t*-test: $p \leq 0.01$)

The expression of *ZmCAX3* in etiolated mesocotyl (Figure 4.6.5) did not differ between WT and *abp1* mutant, whereas it was significantly lower in both *abp4* and *abp1/abp4* double mutants compare to the WT. Ca^{2+} treatment slightly increased the expression of *ZmCAX3* in the mesocotyl of WT, *abp1* and *abp1/abp4* mutant seedlings, whereas it significantly affected its expression in the mesocotyl of the *abp4* mutant.

4 Discussion

Auxin-Binding Proteins (ABPs) were predicted to be putative auxin receptors. In *Arabidopsis*, the only *ABP* gene (*ABP1*) was identified (Palme et al, 1992). In contrast to *Arabidopsis* the maize ABP family counts at least five ABPs (Schwob et al, 1993). Whereas in *Arabidopsis* knockout of *ABP1* is lethal already at the globular stage of embryo development (Chen et al, 2001), Im et al. (2000) suggested a functional redundancy of ABPs in maize because loss-of-function mutants in *ABP1* and *ABP4* genes did not show significant phenotype. In opposite to the observations of Im et al. (2000), data obtained on the same mutants revealed that these mutants developed more erect and more horizontal leaves, respectively, than corresponding WT plants (Fellner et al, 2006). Therefore, it was proposed that both ABP1 and ABP4 might play an important role in the establishment of maize leaf declination.

The role of ABP1 throughout the plant life has been investigated very thoroughly in several studies, which showed that it controls almost all auxin-dependent responses (reviewed in Tromas et al, 2010). One of the auxin-dependent responses at the cellular level is an increase in cytosolic Ca^{2+} concentration (Felle et al, 1986, 1991; Felle, 1988; Shishova and Lindberg, 1999, 2004). Several mechanisms regulate optimal Ca^{2+} concentration in the cell (reviewed in Spalding and Harper, 2011) including vacuolar CAtion eXchangers (CAXs) (reviewed in Manohar et al, 2011). Recent work of Cho et al. (2012) showed that in *Arabidopsis* guard cells CAX1 and CAX3 are involved in regulation of the apoplastic pH thus also involved in auxin transport. Although a lot of work has been done on the research of CAXs, no maize vacuolar CAX has been cloned so far.

The overall aim of this Ph.D. study was to characterize the phenotype of maize *abp* mutants in more details in order to unravel other possible roles of ABPs during the growth and development of maize plants and to clone and characterize maize vacuolar Ca^{2+}/H^{+} exchanger(s). Using maize mutants with loss-off-function in *ABP1* and/or *ABP4* genes, an

attempt was made in order to unravel the possible relationship between auxin, ABPs, Ca^{2+} and CAXs in growth and development of maize plant. In addition, the research was performed in order to unravel whether defects in *ABP1* and *ABP4* genes may affect light-mediated changes in growth of maize seedlings.

5.1 ABP1 and ABP4 control the architecture of maize leaf.

Phenotypic analyses of *abp* mutant plants grown in the greenhouse showed that *ABP1* and *ABP4* genes are either separately or jointly involved in different aspects of maize plant architecture. The attention was paid on the characterization of maize leaf. A typical maize leaf is divided into three regions: the proximal sheath and the distal blade which are connected by the ligular region, which forms at the blade/sheath boundary (Figure 1.5). Braun et al. (2008) have shown that in *Arabidopsis* the functional inactivation of ABP1 provokes severe leaf growth defects, with reduced lamina width and length and a pronounced downward curling of both cotyledons and leaves. However, the obtained results in this thesis indicate that ABP1 and ABP4, although involved in many aspects of maize leaf growth, do not cause such severe leaf growth effects in maize probably due to the presence of other ABPs. Phenotypic analysis revealed that both ABP1 and ABP4 are involved in the regulation of maize leaf blade elongation as well as lateral blade growth and consequently in the whole blade surface (Figure 5.1.1).

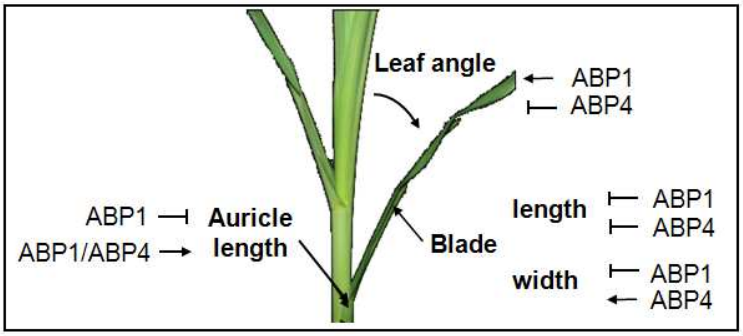

Figure 5.1.1 The proposed roles of ABP1 and ABP4 in the architecture of the maize leaf (i.e. blade length and width, leaf angle and auricle length).

Based on the results obtained, it can be proposed that both ABP1 and ABP4 negatively influence the elongation of the leaf blade. ABP1 negatively contributes to blade width, while ABP4 makes leaves wider. According to the results obtained, ABP1 controls leaf angle declination in positive manner, whereas ABP4 regulates it negatively. In addition, ABPs are involved in auricle length; ABP1 negatively affects auricle elongation, whereas both ABP1 and ABP4 mutually stimulate auricle elongation. Arrows and T-bars represent positive and negative effects, respectively.

The obtained results indicate that ABP1 is negatively involved in the control of the leaf blade elongation early in the plant development, whereas ABP4 affects the leaf blade elongation in the same manner in the later stage of the leaf development (Figure 4.1.2). However, because the double *abp1/abp4* mutant has leaves of length similar to that of the WT, it seems that the negative regulation of the leaf blade growth by ABP1 or ABP4 is indirect, or that the knockout of *ABP1* and *ABP4* triggers the activity of factors that promote the leaf elongation (Figure 4.1.2). ABP1 and ABP4 play also a role in the lateral growth of the leaf blade. The data indicate that the functional ABP1 keeps leaves narrower, whereas ABP4 acts in opposite direction (Figure 4.1.3). But more likely, narrow leaves in the *abp4* mutant result from high level of ABP1 (Im et al, 2000) and it can be hypothesized that the phenotype observed in the *abp4* mutant is a consequence of this accumulation of ABP1 protein. Nevertheless, as the accumulation of ABP1 protein was not measured, this hypothesis remains speculative.

The analysis of the leaf blade declination performed in this study in condition *in vivo* supports the previous data obtained and published by Fellner and co-workers (2006). The results suggest that functional *ABP1* is positively involved in leaf angle declination, whereas the activity of the functional *ABP4* results in reduced leaf angle declination (Figures 4.1.1 and 5.1.1). The fact that leaves in double *abp1/abp4* mutant showed a leaf declination similar to that of the leaves of the *abp4* mutants suggests that functional ABP4 negatively contributes to the development of the leaf angle and/or that simultaneous knockout of *ABP1* and *ABP4* genes triggers substitute pathway(s) involved in the development of the leaf declination. These pathways may include additional members of maize ABP family (Schwob et al, 1993). According to the data obtained in this work it is apparent that both ABP1 and ABP4 play an essential role in leaf development, especially in regards to the establishment of leaf angle as it was supposed by Fellner et al. (2006).

The ligular region of the leaf consists of ligule and auricles (Figure 1.5), specialized triangular structures that allow the blade to bend outwards thus describing leaf declination (Figure 1.6). The differentiation of the auricles is first visible as a thin line of cells that separate the blade and sheath; auricle cells are visible only after the initiation of the ligule (Becraft et al, 1990). The auricle cells enlarge as the ligule differentiates and then divide as the blade and sheath expand (Osmont et al, 2006). While analyzing leaf angle in maize

hybrids, Fellner et al. (2003) suggested that the leaf angle is proportionally associated with the length of the auricle. I observed that mutations in *ABP* genes affect the length of the auricle (Figures 4.1.5 and 5.1.1): whereas *ABP1* gene itself negatively regulated the auricle length, mutation in *ABP4* gene had no impact on the regulation of the auricle elongation. Interestingly, it seemed that *ABP4* together with *ABP1* positively influenced the auricle elongation. However, the assumption of Fellner et al. (2003) could not be confirmed since *abp1* mutant developed a smaller leaf angle than WT, whereas its auricle was significantly longer compare to WT. In addition, *abp4* mutant developed leaf angle greater compare to WT, whereas the *ABP4* mutation did not affect the auricle length. In conclusion, the results showed that in maize *abp* mutants the length of the auricle is not proportionally associated with the leaf declination as it was suggested for maize hybrids (Fellner et al, 2003).

Since phenotypic analysis of WT plants and the *abp* mutants revealed differences in leaf angle and partially in auricle length, the focus of research was moved on microscopic analysis of auricle epidermal cells in order to unravel if differences in this leaf part correlated with differences in leaf angle (Figures 4.1.6. and 4.1.7). The role of ABP1 in the control of cell size was already mentioned. Indeed, in ABP1 overexpressing maize plants, ABP1 is a positive regulator of cell size and the downregulation of ABP1 in leaf tissues reduces the cell size (Jones et al, 1998; Braun et al, 2008). The results of this study showed that the mutation in *ABP1* and/or *ABP4* genes affected the cell length of the auricle epidermis dependently on the stage of the plant development. Whereas functional ABP4 likely positively regulated auricle cell length in the second leaf, i.e. early in the development of the maize plant, functional ABP1 seemed to positively regulate the elongation of the auricle cells in the fourth leaf, i.e. later during the developmental program. Although differences found between WT and *abp* mutants in the structure of the auricle epidermis indicated that *ABP* genes are involved in the auricle cells development, a general conclusion would be speculative since there is no regular correlation between the auricle length and the length of the auricle cells in the examined phenotypes. Interestingly, on the base of the *abp1* mutant phenotype harbouring longer auricle than WT with shorter cells (at least in the later stages of plant development i.e. fourth leaf) it can be speculated that the *abp1* mutant has higher number of cells in the auricle and consequently that the ABP1 could be involved in the cell division of the auricle cells. Unfortunately, this parameter was not investigated here. The role of ABP1

in cell division has already been identified in tobacco (Fellner et al, 1996). Moreover, analyses of *Arabidopsis* loss-of-function mutant in *ABP1* indicated a dual role of the ABP1 protein in cell division and cell expansion during early embryogenesis (Chen et al, 2001).

Because ABPs were described as putative auxin-receptors further investigation was performed in order to see whether exogenously applied auxin could affect the leaf angle declination of the maize *abp* mutants. In this case, the spraying of intact plants in the greenhouse with NAA did not significantly affect the growth of neither WT plants nor *abp* mutants. Several reasons could explain this result:

1) The method used for assigning the effect was inappropriate. Instead of spraying, a drop of lanolin containing NAA could have been deposited directly on the base of the leaf, making the treatment more specific.

2) Concentrations of auxin were not appropriate to observe any significant effect. A larger range of concentrations should have been tested as Hall et al. (1985) reported that auxin is generally less effective when applied to intact whole plants (compare to excised organs or seedlings).

3) NAA simply does not affect the leaf angle development in these maize genotypes and some other forms of synthetic auxin or native auxin IAA should have been tested.

5.2 ABP1 and ABP4 regulate the development of maize seedling differently in the dark and light.

Since phenotypic analysis of maize leaf revealed undoubted involvement of ABPs in the maize growth in condition *in vivo*, further attention was focused on the characterization of maize *abp* mutant seedlings in conditions *in vitro* under different light conditions: dark (D), blue light (BL) and red light (RL). The experiments showed that *ABP1* and *ABP4* genes are also involved in the development of maize seedling and that their roles and functional relations are organ- and light-dependent.

Analysis of etiolated maize *abp* mutants showed that ABP1 was not involved in the coleoptile elongation, whereas it seemed that ABP4 acts positively in its elongation. The phenotype of double *abp1/abp4* mutant supports this idea. Neither BL nor RL affected the

elongation of *abp* mutant's coleoptiles suggesting that ABP1 and ABP4 are not essential for the growth of coleoptile in light.

The obtained results further suggest that both ABP1 and ABP4 are essential for the growth of etiolated mesocotyl. It was particularly visible for the double *abp1/abp4* mutant. The data also indicated that ABP1 and ABP4 could substitute for each other during the etiolated mesocotyl growth. Under BL, the mesocotyl elongation was affected neither in *abp1* nor *abp4* mutants, suggesting that these genes are not involved in BL-mediated growth of this organ (Figure 4.3.1B). Very interestingly, the long mesocotyl of *abp4* mutant suggests that ABP1 stimulated the elongation of mesocotyl in RL. However, the role of ABP4 in this process cannot be excluded. This latest result is in agreement with the observation of Jones et al. (1991) who hypothesized that RL-induced inhibition of the mesocotyl growth could be partially caused by the RL-induced reduction of ABP1 abundance. The fact that the growth of the mesocotyl of the double *abp1/abp4* mutant was not affected under BL and RL indicated that in these conditions some other, alternative pathways, not including ABP1 and ABP4, could be activated and regulate the mesocotyl growth.

The growth of primary root of etiolated seedling is stimulated by both ABP1 and ABP4 although the stimulatory effect of ABP4 was more pronounced (Figures 4.1.9 and 5.2.1). The loss of the ABP1 function resulted in longer primary root under BL and RL, whereas the knockout of *ABP4* resulted in a WT-like phenotype. This suggests that ABP1 itself had no effect on the root elongation in lights, but rather suppressed the promoting effects of ABP4 (Figure 4.3.1C). Taken together, these data suggest the involvement of auxin-binding proteins in light signalling pathways, which controls photomorphogenesis in maize (Figure 5.2.1).

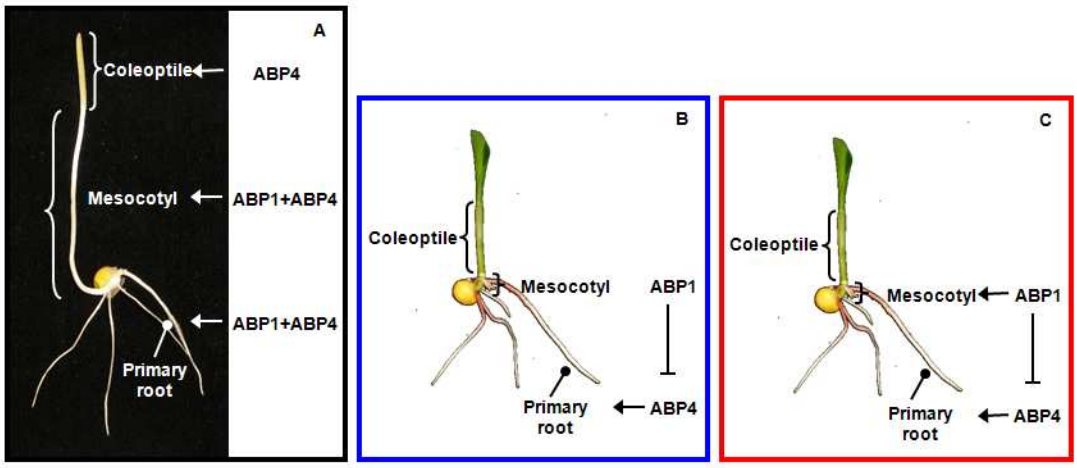

Figure 5.2.1 Scheme showing proposed functions of ABP1 and ABP4 in growth of maize seedlings grown on the BM in dark (D) (A), blue light (BL) (B) and red light (RL) (C).

Based on the results obtained, the model proposes that ABP1 along with ABP4 positively participate on elongation of etiolated mesocotyl and primary root, and ABP4 only is positively involved in elongation growth of coleoptiles (**A**). In BL (**B**), neither ABP1 nor ABP4 affect the growth of either coleoptile or mesocotyl, whereas ABP1 inhibits stimulatory effect of ABP4 on primary root elongation. In RL (**C**), like in BL, neither ABP1 nor ABP4 affect the growth of coleoptile. However, ABP1 stimulates mesocotyl elongation under this light condition. In addition, like in BL, ABP1 inhibits stimulatory effect of ABP4 on primary root elongation. Arrows and T-bars represent positive and negative effects, respectively.

5.3 The loss of ABP1 and/or ABP4 function leads to an altered sensitivity of maize *abp* mutants to exogenous auxin compare to WT both in the dark and in light.

Auxin is a key substance in the control of plant growth; however its physiological functions are question of controversy. Indeed, exogenous auxin reduced the elongation of the etiolated maize coleoptile, mesocotyl and primary roots in intact maize hybrid seedlings (Fellner et al. 2003, 2006) and etiolated seedlings of modern maize hybrids with reduced expression of *ABP4* gene showed reduced auxin-induced responses (Fellner et al, 2006). In opposite, other authors demonstrated that in maize coleoptiles (Baskin et al, 1986; Iino, 1995), pea internodes (Hall et al, 1985; Yang et al, 1993, 1996), and watermelon hypocotyls (Carrington and Esnard, 1988), the growth of intact plants is stimulated by externally supplied IAA. Nevertheless, this stimulation of growth by exogenous IAA was transient even if IAA was supplied continuously (Hall et al, 1985; Carrington and Esnard, 1988). Why exogenous

auxin, in contrast to endogenous auxin, inhibits elongation in many plant species, is still not fully understood. Hasenstein and Evans (1988) proposed the mechanism by which the application of the exogenous auxin results in a supraoptimal concentration of auxin in the tissues causing the inhibition of elongation. In order to better understand the role of *ABP1* and *ABP4* genes in auxin-mediated growth responses the responsiveness (sensitivity) of etiolated intact maize seedling's organs of WT and *abp* mutants to exogenous auxin was analyzed.

The growth capacity of WT and mutant maize seedlings does not simply correspond with the observed changes in levels of IAA in coleoptiles, mesocotyls and primary roots (Jurišić-Knežev et al, 2012). The data showed that etiolated WT plants are more sensitive to exogenous auxin than the *abp* mutants (Figure 4.2.1). Mutation in *ABP1* and/or *ABP4* genes led to a decreased sensitivity of maize seedlings to exogenous auxin suggesting that these *ABP* genes are involved in auxin-regulated growth responses in etiolated intact maize organs. It seemed that the effect of mutation in both genes was additive, at least in coleoptile and mesocotyl. In primary root the loss-of-function in the *ABP4* gene, but not in *ABP1*, led to the decreased sensitivity of primary root to exogenous auxin suggesting that in the dark auxin-induced inhibition of root elongation is controlled through ABP4. Since double *abp1/abp4* mutant showed phenotype similar to WT, I hypothesize that a substitute pathway mediated the response of primary root in dark-grown seedling to exogenous auxin.

The analyses of growth of intact maize seedlings under different light conditions and in the presence of auxin in the medium unravelled the role of light in auxin-regulated growth via ABPs. In BL and RL, compared to dark-grown seedlings, the responsiveness of WT organs to exogenous auxin was decreased, which was visible both in coleoptile and mesocotyl. The results further indicated that both ABP1 and ABP4 contributed to the responses of coleoptile to the inhibitory effects of auxin under BL and RL. Interestingly, the growth of mesocotyl under BL was mediated mostly by ABP4, with no essential influence of ABP1. However, it seemed that both ABP1 and ABP4 were involved in auxin regulated mesocotyl growth under RL. Loss of sensitivity of WT primary roots to exogenous auxin under BL and RL indicated that some other pathways, independently from ABP1- and ABP4-pathways, could be involved in auxin-induced growth responses in primary roots.

5.4 Etiolated coleoptile and mesocotyl are differently sensitive to exogenous calcium and its accumulation in these maize organs is inhibited by ABP4.

Besides the fact that Ca^{2+} is an essential nutrient for plants, it also acts as a second messenger mediating a wide range of cellular responses (Sanders et al, 2002). Because auxin causes an increase of the cytosolic free Ca^{2+} concentrations (Felle et al, 1986, 1991; Felle, 1988; Shishova and Lindberg, 1999, 2004) and considering the fact that ABPs are putative auxin receptors, I hypothesized that the interaction between auxin and Ca^{2+} through ABPs during the growth and development of maize may exists. In a first step the effect of exogenous Ca^{2+} on the growth responses of *abp* mutants was analyzed. The effect of Ca^{2+} on the growth of maize seedlings was assessed in condition *in vitro* in the dark in order to avoid the influence of the light and photoreceptors. The differences were observed both between different maize seedling's organs (coleoptile and mesocotyl) and different genotypes (WT and *abp* mutants) (Figure 4.4.1). Since coleoptile of WT did not show any response to exogenous Ca^{2+}, it can be assumed that Ca^{2+} does not regulate coleoptile elongation. In addition, ABP1 and ABP4 are not involved in this process. In contrast to coleoptile, Ca^{2+} stimulated the growth of mesocotyl in a dose-dependent manner in all genotypes.

Beside the study performed in condition *in vitro*, the effect of Ca^{2+} on the growth of maize WT and *abp* mutants was also analyzed in conditions *in vivo*. Exogenously applied Ca^{2+} in the form of the $CaCl_2$ solution did not show any effect on the leaf growth of neither WT plants nor *abp* mutants. The reason for this result could be:

1) The inappropriately chosen form of the Ca^{2+} for the absorption by the leaves
2) Concentration range tested could be greater or
3) It could be that exogenously applied Ca^{2+} does not affect the leaf growth.

Another step in determination of the relationship between ABPs and Ca^{2+} in maize seedlings was determination of Ca^{2+} content (Figure 4.4.2) in etiolated maize seedling's aerial parts (coleoptile + mesocotyl) in WT plants and *abp* mutants. This approach allowed unravelling the role of ABPs in the regulation of Ca^{2+} accumulation in maize. The fact that *abp4* mutant accumulated more Ca^{2+} in its aerial parts compare to WT plants in all conditions

tested suggests that ABP4 is involved in the inhibition of Ca^{2+} accumulation in shoots of etiolated seedlings. Since *ABP1* gene in *abp4* mutant is still functional, it can be also assumed that ABP1 stimulates accumulation of Ca^{2+} in maize aerial parts.

5.5 ZmCAX2 and ZmCAX3, orthologs of AtCAX1, are putative maize Ca^{2+}/H^{+} exchangers.

As it was mentioned, Ca^{2+} is thought to play an important role in the signalling pathways (Sanders et al, 2002). During the signalling events, the basal cytosolic Ca^{2+} concentration is restored by sequestering the transient increase of free Ca^{2+} into the vacuole (Sanders et al, 2002). One of the effective mechanisms of Ca^{2+} sequestration into the vacuole is the family of antiporters called CAtion eXchangers (CAX) (reviewed in Manohar et al, 2011). In several studies auxin has been shown to cause a transient increase of Ca^{2+} concentration in the cytosol (Felle et al, 1986, 1991; Felle, 1988; Shishova and Lindberg, 1999, 2004). Since ABPs are putative auxin receptors, I assumed that auxin via ABPs could be included in the signalling cascade, which involves Ca^{2+} and CAXs. Therefore the goal was to clone maize Ca^{2+}/H^{+} antiporter(s) and to using maize mutants defective in *ABP1* and *ABP4* genes resolve this assumption.

Up to date several Ca^{2+}/H^{+} antiporters have been characterized at the biochemical and molecular level in different plant species (Schumaker and Sze, 1985; Hirschi et al, 1996; Ueoka-Nakanishi et al, 1999), but no maize Ca^{2+}/H^{+} antiporter has been cloned so far. In *Arabidopsis* and in rice, respectively, six *CAX* genes and five *CAX*-homologs have been isolated (Kamiya et al, 2005; Shigaki et al, 2006). Some of them showed specificity for Ca^{2+} transport and localization on the tonoplast. In order to clone the maize CAX responsible for Ca^{2+} transport, *Arabidopsis AtCAX1* (AF461691) (Hirschi et al, 1996) sequence was used as a reference sequence in database search since it has been shown that this gene encodes the vacuolar Ca^{2+}/H^{+} antiporter.

Two sequences in maize, orthologs of *Arabidopsis AtCAX1*, *ZmCAX3* (AY108295) and *ZmCAX2* (AB044567) were amplified by PCR. *In silico* analyses showed that the sequences isolated from maize encode proteins sharing common features with the already known CAXs of various organisms (Ivey et al, 1993; Hirschi et al, 1996; Ueoka-Nakanishi et

al, 1999; Kamiya and Maeshima, 2004; reviewed in Manohar et al, 2011). They are predicted to have 11 transmembrane (TM) domains with the hydrophilic loop between the 6th and the 7th domain, which bisects the protein into two groups of five and six TM spans (Figures 4.5.2 and 4.5.3). In addition, the analysis of the *ZmCAX3* and *ZmCAX2* sequences showed that corresponding proteins are 462 and 419 amino acids long, respectively.

Phylogenetic analysis showed that *ZmCAX3* belongs to type IA of CAXs, whereas *ZmCAX2* belongs to type IB of CAXs (Figure 4.5.1). This clustering reflected not only the similarity between sequences at the amino acid level (Kamiya et al, 2005) but also probably the different substrate specificity (Shigaki et al, 2006). Evolutional relationships among the characterized and uncharacterized CAXs could lead to a better understanding of their potential roles. Considering the fact that the evolutionary closest relative of maize ZmCAX3 is rice OsCAX1a (Figure 4.5.1), known to be a vacuolar Ca^{2+} transporter (Kamiya et al, 2005), and phylogenetically belongs to the same cluster as AtCAX1 (type IA), it can be assumed that the maize ZmCAX3 could have the same function and localization as this rice transporter. The second CAX, which was identified in this study in maize was ZmCAX2, closely associated to the rice OsCAX3 (Figure 4.5.1), shown to be a vacuolar transporter responsible both for Ca^{2+} and manganese (Mn^{2+}) transport (Kamiya et al, 2005). Considering the fact that ZmCAX2 belongs phylogenetically to the same cluster as rice OsCAX3 and *Arabidopsis* AtCAX2 (type IB), it can be assumed that maize ZmCAX2 might be a vacuolar transporter, which transports both Ca^{2+} and Mn^{2+} in maize plant.

Substrate specificity of transporters is an important determinant of their physiological functions. Substrate range of different CAXs may vary among Ca^{2+}, Mn^{2+} and cadmium (Cd^{2+}). The nine-amino-acid-long region of AtCAX1 has been shown to confer Ca^{2+} transport ability to its close non-Ca^{2+}-transporting homologue AtCAX3 and it has been designated as Ca^{2+} domain (CaD) (Shigaki et al, 2001). However, the inability of AtCAX3 to fully confer CAX1-like phenotype suggests that other regions in AtCAX1 affect some elements of Ca^{2+} transport (Shigaki et al, 2001). The mechanism by which the CaD regulates ion transport is unknown. This domain is one of the most polymorphic regions within the CAX group (Shigaki and Hirschi, 2000) (Figure 1.3). Unfortunately, based only on the sequence analysis the specificity of transport of the protein cannot be predicted, which is the case with these two maize CAXs. Additional complementation tests with the yeast strains

deficient in Ca^{2+} transport must be performed in order to determine the substrate specificity of these two proteins.

In eukaryotic cell, critical factor for the function of the protein is its cellular localization. So far, most of the characterized eukaryotic CAXs, such as VCX1 from yeast (Cunningham and Fink, 1996), VCAX1 from mung bean (Ueoka-Nakanishi et al, 2000), AtCAX1, AtCAX2, AtCAX3, AtCAX4 from *Arabidopsis* (Cheng et al, 2003; Hirschi et al, 2000; Shigaki and Hirschi, 2000; Cheng et al, 2002; Mei et al, 2009), OsCAX1a from rice (Kamiya and Maeshima, 2004) are localized to the vacuole. However, localization of most plant CAXs is still unknown. It is possible that some CAXs are located on membranes other than the vacuolar membrane. For example, biochemical experiments suggest that H^+/Ca^{2+} antiport activity is also present on the plasma membrane and chloroplast thylakoid membrane (Kasai and Muto, 1990; Ettinger et al, 1999). In this study, using the TmPred program (Hofmann and Stoffel, 1993), the preferred model for the N-terminus localization for both maize CAXs, ZmCAX3 and ZmCAX2, was cytosolic. Similarly, the AtCAX1 hydrophobicity plot predicts that the N-terminal regulatory region and the CaD are located on opposite sides of the membrane (Shigaki et al, 2001) suggesting that the N-terminus is cytosolic and that the CaD domain would be found inside the vacuole. Here should be mentioned that beside the computational approach for prediction of protein localization, different constructs of CAX-GFP/YFP fusion were made in order to investigate the localization of maize CAXs by this approach; however, for some unknown/unexplained reasons this approach did not work.

5.6 ABP1 and ABP4 mutually regulate the expression of *ZmCAX2* and *ZmCAX3* in later stages of leaf development.

Since two putative Ca^{2+}/H^+ transporters in maize were cloned and the phenotype of maize *abp* mutants was thoroughly investigated and consequently the role of *ABP1* and *ABP4* genes in maize growth was unravelled, the focus of research was moved on the analyses of possible interaction and relationship between maize CAXs and ABPs. Therefore, the expression pattern of two putative Ca^{2+}/H^+ transporters in different conditions *in vivo* and *in vitro* was analyzed. The expression of *ZmCAX3* was very weak and almost no detectable by semiqRT-

PCR and therefore its expression analysis was determined by the more sensitive method qRT-PCR. In contrast, the second gene, *ZmCAX2*, was very well expressed in all tested genotypes in all conditions.

Considering the fact that the most significant difference in the leaf angle of maize *abp* mutants was found in the third leaf (Figure 4.1.1), the further step was to check out if the genes, *ZmCAX2* and *ZmCAX3*, are differently expressed in different phases of leaf development i.e. in the base of the emerging leaf and in the base of the fully developed leaf and in that way possibly involved in leaf development. Recently, Conn et al. (2011) have shown that in *Arabidopsis thaliana*, AtCAX1, a vacuolar Ca^{2+}/H^{+} transporter, was preferentially expressed in the leaf mesophyll and necessary for significant proportion of mesophyll-specific vacuolar storage of Ca^{2+}.

The expression analyses of *ZmCAX2* and *ZmCAX3* showed that these genes were not developmentally regulated since their expression was not affected by the age of WT plant. However, a significant down-regulation of *ZmCAX2* expression in the base of the developed leaf of double *abp1/abp4* mutant suggests that both ABP1 and ABP4 could be positively involved in its regulation in later stages of leaf development.

Increased expression of *ZmCAX3* in the base of the developed leaf of *abp1* mutant compare to emerging leaf, implicates that functional ABP1 can regulate *ZmCAX3* expression differentially during the leaf development and in the same time suggests that functional ABP1 inhibits the expression of *ZmCAX3* in the developed maize leaf. In *abp4* mutant, the expression of *ZmCAX3* did not significantly change during the leaf development suggesting that functional ABP4 alone is not involved in regulation of this gene expression during the leaf development. However, higher expression of *ZmCAX3* in the base of the developed leaf of double *abp1/abp4* mutant compare to WT suggests that functional ABP4 in cooperation with ABP1 could inhibit the expression of *ZmCAX3* in the fully developed leaf.

5.7 ABP4 is involved in auxin- and Ca^{2+}-regulated expression of *ZmCAX3* in mesocotyl.

Since certain differences between WT and *abp* mutants in responses to auxin and Ca^{2+} in condition *in vitro* were found, gene expression analyses was performed in order to unravel

the putative relationship between CAXs and ABPs in two maize seedling's aerial organs-coleoptile and mesocotyl and the role of auxin and Ca^{2+} in their regulation.

In this study it was shown that maize *abp* mutants were differently sensitive to auxin indicating that ABP1 and ABP4 are involved in auxin-mediated responses in maize. In order to unravel the relationship between auxin, ABPs and CAXs in maize the expression of *ZmCAX3* and *ZmCAX2* was investigated in these mutants in relation to auxin. The obtained data have shown that in the basal conditions, ABP1 and ABP4 were not involved in the regulation of *ZmCAX3* expression in coleoptile, whereas ABP4 stimulated its expression in mesocotyl (Figure 4.6.4). Yamagami et al. (2004) proposed the existence of two signalling pathways participating in auxin-induced internode growth in pea: an ABP1-independent pathway, which depends on exogenous Ca^{2+} and ABP1-dependent pathway independent on extracellular Ca^{2+}. The data collected showed that auxin inhibited expression of *ZmCAX3* in mesocotyl and did this via ABP4. The results also showed that the expression of *ZmCAX2* in coleoptile and mesocotyl was not regulated by ABP1 and ABP4 in basal medium. In addition, auxin did not influence the expression of *ZmCAX2* neither in coleoptile nor in mesocotyl and ABP1 and ABP4 were not involved in this process.

In order to unravel the relationship between Ca^{2+}, ABPs and CAXs in maize, in the next step, the expression of *ZmCAX3* and *ZmCAX2* was investigated in the *abp* mutants in relation to Ca^{2+}. Since the expression of *ZmCAX3* in coleoptile did not differ between control condition and treatment with Ca^{2+}, it could be concluded that the expression of *ZmCAX3* is not regulated by Ca^{2+} in this maize organ. In contrast, in mesocotyl (Figure 4.6.5), *ZmCAX3* was more expressed in the WT organ treated with Ca^{2+} compare to untreated one indicating that in mesocotyl Ca^{2+} stimulates the expression of *ZmCAX3*. These results are consistent with other data obtained in this study, since the *ZmCAX3* expression was higher in mesocotyl compare to coleoptile (Figure 4.6.3 B) and that coleoptile growth was Ca^{2+} independent, whereas mesocotyl growth was stimulated by Ca^{2+}. In addition, the phylogenetic analysis data showed that *ZmCAX3* belongs to the type IA CAXs which are predominantly Ca^{2+} transporters, making the *ZmCAX3* good candidate as a Ca^{2+}/H+ exchanger in maize. Further analysis using yeast strains deficient in Ca^{2+} transport will undoubtedly unravel the ion specificity of this transporter. Since the expression of *ZmCAX3* in the medium without Ca^{2+} in both coleoptile and mesocotyl did not differ between WT and *abp1* mutant (Figure 4.6.5),

the conclusion could be made that ABP1 alone did not play a role in regulation of its expression in the absence of Ca^{2+}. In contrast, lower expression of *ZmCAX3* in mesocotyl of both *abp4* and double *abp1/abp4* mutant (Figure 4.6.5) led to the conclusion that ABP4 alone as well as in cooperation with ABP1 stimulates the expression of *ZmCAX3* in mesocotyl. Increased expression of *ZmCAX3* in mesocotyl of *abp4* mutant treated with Ca^{2+} compare to the same genotype in control condition indicates that Ca^{2+}, via ABP4 as a negative regulator, regulates the expression of *ZmCAX3* in mesocotyl. The fact that Ca^{2+} level was the highest in the aerial part of *abp4* mutant (Figure 4.4.2) contributes to the finding that ABP4 is a negative regulator of *ZmCAX3*, which is putative Ca^{2+} transporter since the lack of ABP4 led to accumulation of Ca^{2+} in this maize part. In addition, in *abp1* mutant that does not lack the ABP4, the level of Ca^{2+} did not change compare to WT, contributing to the finding that ABP4 regulates Ca^{2+} accumulation in maize aerial parts.

The second maize CAX whose expression was investigated in relation to exogenous Ca^{2+} was *ZmCAX2*. The fact that this gene was not differently expressed between WT and *abp* mutants in the medium without Ca^{2+} suggests that ABP1 and ABP4 were not involved in the regulation of its expression neither in coleoptile nor in mesocotyl. Moreover, the fact that *ZmCAX2* was not differently expressed neither in coleoptile nor in mesocotyl of WT in the medium without and with Ca^{2+} suggests that this gene was likely not regulated by Ca^{2+}. This data is consistent with the phylogenetic analysis performed in this study (Figure 4.5.1), which showed that *ZmCAX2* belongs to the group of CAXs more responsible for transport of ions other than Ca^{2+}. As in the case with ZmCAX3, further analyses with yeast strains deficient in Ca^{2+} and/or other ions transport are necessary to be performed in order to determine the ion specificity for this transporter.

6 Conclusions

Maize loss-of-function mutants in *ABP1* and/or *ABP4* genes used in this research have shown to be a powerful tool to study the relationship between auxin, Ca^{2+}, ABPs and Ca^{2+}/H^{+} transporters in maize. In this study, it has been shown that maize loss-of-function mutants in *ABP1* and/or *ABP4* genes show remarkable phenotype. The data indicate that ABP1 and ABP4 are involved in the regulation of the maize plant architecture including the leaf growth and development as well as the elongation of etiolated maize seedlings. Moreover, it has been shown that ABP1 and/or ABP4 are involved in auxin-regulated growth of etiolated maize seedlings. In addition, the experiments revealed that in BL and RL the responsiveness of maize seedlings to exogenous auxin is less than in D and that ABP1 and ABP4 are involved in this process. Determination of the Ca^{2+} content in *abp* mutants gave better insight in the role of ABPs in the regulation of Ca^{2+} homeostasis in maize and recruited ABP4 as a negative regulator of Ca^{2+} accumulation in the aerial parts of maize plant.

In this work two putative CAX transporters in maize designated *ZmCAX2* and *ZmCAX3*, which are homologous to *Arabidopsis AtCAX1*, a vacuolar Ca^{2+}/H^{+} transporter, have been cloned and characterized. Analyses of their expression in maize *abp* mutants allowed unravelling their regulation by ABPs. The obtained results showed that the relationship between ABPs and CAXs in maize occurs at different stages of maize development and it is also organ-dependent. Based on the results obtained in condition *in vitro*, at the level of seedling, a model describing the relationship between auxin, Ca^{2+}, ABP1, ABP4 and *ZmCAX3* in mesocotyl is proposed (Figure 6.1). According to this model, both auxin and Ca^{2+} stimulate ABP4, which is a negative regulator of ABP1. In that way, both auxin and Ca^{2+} via ABP4 inhibit the expression of *ZmCAX3* in mesocotyl thus regulating Ca^{2+} accumulation in this maize organ and consequently its growth. In condition *in vivo*, at the level of developed plant, the obtained data showed that ABP1 and ABP4 are

mutually involved in the regulation of the expression of both *ZmCAX2* and *ZmCAX3* in later stages of leaf development.

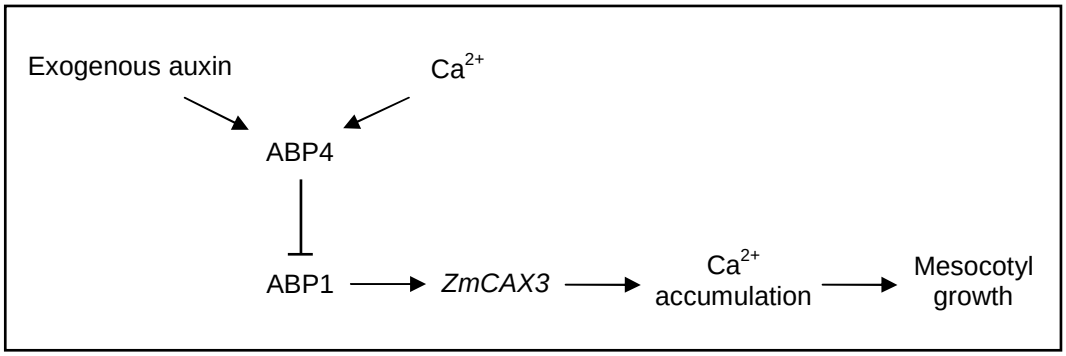

Figure 6.1 A proposed model of the relationship between auxin, Ca^{2+}, ABP1, ABP4 and *ZmCAX3* in maize mesocotyl.

According to the model proposed auxin and Ca^{2+} regulate the expression of *ZmCAX3* via ABP4 and ABP1. ABP4 is a negative regulator of ABP1, which stimulates the expression of *ZmCAX3* in mesocotyl. Consequently, accumulation of Ca^{2+} in mesocotyl and its growth are affected. Arrows and T-bars represent positive and negative effects, respectively.

The complex interplay of auxin, Ca^{2+}, ABPs and CAXs in maize is still at the beginning of its story. Nevertheless, I believe that this work contributed to the understanding of their interesting interaction and triggered a lot of questions for some future research.

7 Závěr

Mutanti kukuřice s nefunkčními geny *ABP1* a/nebo *ABP4*, použití v disertační práci, jsou velice vhodní pro studium interakce mezi auxinem, Ca^{2+}, ABP a Ca^{2+}/H^{+} transportéry. V předkládané práci bylo zjištěno, že mutanti s nefunkčními geny *ABP1* a *ABP4* ukazují výrazný fenotyp. Získané výsledky naznačují, že proteiny ABP1 a ABP4 jsou zapojeny v regulaci vývoje a růstu listů a rovněž v prodlužování etiolizovaných rostlin kukuřice. Dále bylo v předkládané práci ukázáno, že ABP1 a ABP4 jsou zapojeny v auxinem-regulovaném růstu etiolizovaných rostlin kukuřice. Experimenty vedle toho rovněž odhalily, že na modrém a červeném světle je růstová reakce rostlin k exogennímu auxinu slabší než ve tmě a že ABP1 a ABP4 jsou do těchto procesů zapojeny. Stanovení obsahu Ca^{2+} v *abp* mutantech pak poskytuje lepší pohled na úlohu proteinů ABP v regulaci homeostáze vápníku v kukuřici a ukazuje, že ABP4 by mohl fungovat jako negativní regulátor akumulace vápníku v nadzemních částech rostlin kukuřice.

Během disertační práce byly rovněž klonovány a charakterizovány dva geny kódující domnělé kukuřičné transportéry skupiny CAX, pojmenované *ZmCAX2* a *ZmCAX3*, které jsou homologní k vakuolárnímu Ca^{2+}/H^{+} transportéru *AtCAX1*, nalezenému u *Arabidopsis*. Analýzy jejich exprese v mutantech *abp* umožnily poodhalení jejich regulace prostřednictvím proteinů ABP. Získané výsledky ukazují, že funkční vztah mezi proteiny ABP a CAX u kukuřice je pozorován v různých stádiích vývoje rostlin kukuřice a je rovněž závislý na orgánu. Na základě výsledků získaných v podmínkách *in vitro* u mladých rostlin byl navržen model, který popisuje funkční vztah mezi auxinem, Ca^{2+}, ABP1, ABP4 a *ZmCAX3* v mezokotylu kukuřice (Obr. 6.1). Podle tohoto modelu auxin a Ca^{2+} stimulují ABP4, který funguje jako negativní regulátor ABP1. Tímto způsobem, auxin i vápník inhibují expresi genu *ZmCAX3* v mezokotylu prostřednictvím ABP4 a tím regulují akumulaci Ca^{2+} v této části rostliny a následně tak její růst. V podmínkách *in vivo* na úrovni vyvinutých rostlin získaná

data ukazují, že v regulaci exprese obou genů *ZmCAX2* a *ZmCAX3* v pozdějším stádiu vývoje listu jsou ABP1 a ABP4 funkčně vzájemně propojeny.

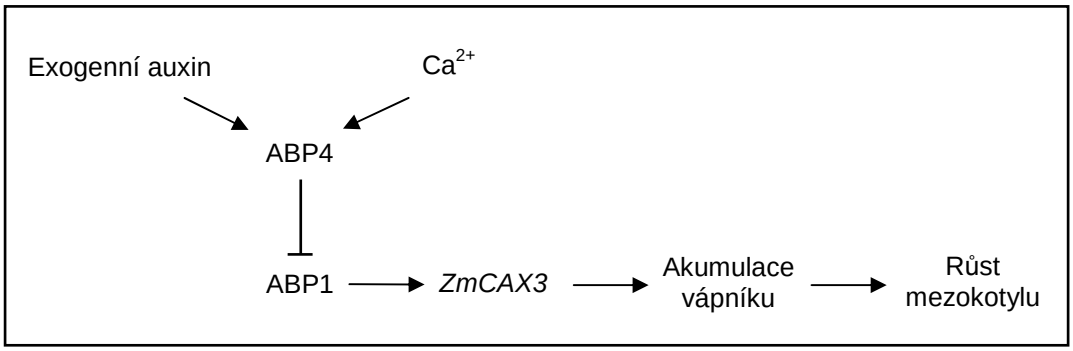

Obr. 6.1 Model možné interakce mezi auxinem, Ca^{2+}, ABP1, ABP4 a *ZmCAX3* v mezokotylu kukuřice.

Podle tohoto modelu auxin a Ca^{2+} regulují expresi genu *ZmCAX3* prostřednictvím ABP4 a ABP1. ABP4 funguje jako negativní regulátor ABP1, který stimuluje expresi *ZmCAX3* v mezokotylu. Tím byla ovlivněna akumulace Ca^{2+} v mezokotylu a jeho růst. Šipky označují stimulaci, kdežto značky ve tvaru T reprezentují inhibici.

Složitá souhra auxinu, Ca^{2+} a proteinů ABP a CAX u kukuřice je dosud na počátku odhalení. Nicméně věřím, že tato práce přispěla k porozumění jejich vzájemné interakce a vyvolala další otázky pro budoucí výzkum.

8 List of Abbreviations

2,4-D	Dichlorophenoxyacetic acid
ABP	Auxin-Binding Protein
ABP	Auxin-Binding Protein gene
abp	Auxin-Binding Protein loss-off-function mutant
ARF	Auxin Response Factor
At	*Arabidopsis thaliana*
ATP	Adenosine Triphosphate
Aux/IAA	Auxin/indole-3-acetic acid protein
BL	Blue Light
BLAST	Basic Local Alignment Search Tool
BM	Basal Medium
Ca^{2+}	Calcium
CaD	Calcium Domain
CaM	Calmodulin
CAX	CAtion eXchanger
cDNA	Complementary Deoxyribonucleic Acid
CDPKs	Ca^{2+}-dependent protein kinases
D	Dark
DNA	Deoxyribonucleic Acid
DNase	Deoxyribonuclease
dNTP	Deoxyribonucleotide Triphosphate
DTT	Dithiothreitol
ER	Endoplasmic reticulum
F	Forward primer
G_1/S	Transition between growth 1 (G_1) and synthetic (S) phase of cell cycle

G_2/M	Transition between growth 2 (G_2) and meta-phase (M) of cell cycle
GAPDH	Glyceraldehyde 3-phosphate Dehydrogenase
H^+-ATPase	Proton pump
H^+-PPase	H^+-pyrophosphatase
IAA	Indole-3-acetic Acid
IBA	Indole-3-butyric acid
KDEL	Retention signal for endoplasmatic reticulum
LB	Luria-Bertani broth
Mes	2-(N-morpholino)-ethanesulfonic acid
Mg^{2+}	Magnesium
Mn^{2+}	Manganese
MS	Murashige and Skoog medium
NAA	1-Naphtaleneacetic Acid
NCBI	National Center for Biotechnology Information
Ni^{2+}	Nickel
NPA	N-1-naphthylphthalamic Acid
Os	*Oryza sativa*
PAT	Polar Auxin Transport
PCR	Polymerase Chain Reaction
qRT-PCR	quantitative Real Time-PCR
R	Reverse primer
RL	Red Light
RNA	Ribonucleic Acid
SE	Standard Error
TIR1	Transport Inhibitor Response 1
WT	Wild Type
Xgal	5-bromo-4-chloro-3-indolyl- -D-galactopyranoside
Zm	*Zea mays*
Zn^{2+}	Zink

9 List of Figures

10 List of Tables

11 References

Abramoff M, Magelhaes P, Ram S (2004) Image processing with ImageJ. *Biophotonics International* **11**: 36-42.

Arvidsson S, Kwasniewski M, Riaño-Pachón DM, Mueller-Roeber B (2008) QuantPrime-a flexible tool for reliable high-throughput primer design for quantitative PCR. *BMC Bioinformatics* **9**: 465.

Bandurski RS, Schulze A, Cohen JD (1977) Photo-regulation of the ratio of ester to free indole-3-acetic acid. *Biochemical and Biophysical Research Communications* **79**: 1219-1223.

Barbier-Brygoo H, Ephritikhine G, Klämbt D, Ghislain M, Guern J (1989) Functional evidence for an auxin receptor at the plasmalemma of tobacco mesophyll protoplasts. *Proceedings of the National Academy of Sciences of the United States of America* **86**: 891-895.

Barbier-Brygoo H, Ephritikhine G, Klämbt D, Maurel C, Palme K, Schell J, Guern J (1991) Perception of the auxin signal at the plasma membrane of tobacco mesophyll protoplasts. *Plant Journal* **1**: 83-93.

Barker-Bridgers M, Ribnicky DM, Cohen JD, Jones AM (1998) Red-light-regulated growth. Changes in the abundance of indoleacetic acid in the maize (Zea mays L.) mesocotyl. *Planta* **204**: 207-211.

Barkla B.J, Hirschi KD, Pittman JK (2008) Exchangers man the pumps: Functional interplay between proton pumps and proton-coupled Ca^{2+} exchangers. *Plant Signalling and Behavior* **3(5)**: 354-356.

Baskin TI, Briggs WR, Iino M (1986) Can lateral redistribution of auxin account for phototropism of maize coleoptile? *Plant Physiology* **81**: 306-309.

Becraft PW, Bongard-Pierce DK, Sylvester AW, Poethig RS, Freeling M (1990) The liguleless-1 gene acts tissue specifically in maize leaf development. *Developmental Biology* **141**: 220-232.

Bennetzen JL (1996) The contributions of retroelements to plant genome organization, function and evolution. *Trends in Microbiology* **4**: 347-353.

Bennetzen JL and Hake SC (TM Foster and MCP Timmermans) (2009), Handbook of Maize: Its Biology, Chapter: Axial Patterning of the Maize Leaf, *Springer New York*: 161-162.

Blackford S, Rea PA and Sanders D (1990) Voltage sensitivity of H^+/Ca^{2+} antiport in higher plant tonoplast suggests a role in vacuolar calcium accumulation. *Journal of Biological Chemistry* **65**: 9617-9620.

Blatt MR (2000) Ca^{2+} signalling and control of guard-cell volume in stomatal movements. *Current Opinion in Plant Biology* **3**: 196-204.

Bořucká J, Fellner M (2012) Auxin binding proteins ABP1 and ABP4 are involved in the light- and auxin-induced down-regulation of phytochrome gene *PHYB* in maize (*Zea mays* L.) mesocotyl. *Plant Growth Regulation* **68**: 503-509.

Braun N, Wyrzykowska J, Muller P, David K, Couch D, Perrot-Rechenmann C, Fleming AJ (2008) Conditional repression of AUXIN BINDING PROTEIN1 reveals that it coordinates cell division and cell expansion during postembryonic shoot development in Arabidopsis and tobacco. *Plant Cell* **20(10)**: 2746-27062.

Briggs WR (1963) Red light, auxin relationships, and the phototropic responses of corn and oat coleoptiles. *American Journal of Botany* **50**: 196-207.

Bush DS (1995) Calcium regulation in plant cells and its role in signalling. *Annual Review of Plant Physiology and Plant Molecular Biology* **46**: 95-122.

Carrington CMS, Esnard J (1988) The elongation response of watermelon hypocotyls to indole-3-acetic acid: a comparative study of excised segments and intact plants. *Journal of Experimental Botany* **39**: 441-450.

Casal JJ, Luccioni LG, Oliverio KA and Boccalandro HE (2003) Light, phytochrome signalling and photomorphogenesis in *Arabidopsis*. *Photochemical & Photobiological Sciences* **2**: 625-636.

Catala R, Santos E, Alonso JM, Ecker JR, Martinez-Zapater JM, Salinas J (2003) Mutations in the Ca^{2+}/H^+ transporter CAX1 increase *CBF/DREB1* expression and the cold-acclimation response in Arabidopsis. *Plant Cell* **15(12)**: 2940-2951.

Chen J-G (2001) Dual Auxin Signalling Pathways Control Cell Elongation and Division. *Journal of Plant Growth Regulation* **20**: 255-264.

Chen JG, Ullah H, Young JC, Sussman MR, Jones AM (2001) ABP1 is required for organized cell elongation and division in Arabidopsis embryogenesis. *Genes & Development* **15(7)**: 902-911.

Cheng NH, Pittman JK, Barkla BJ, Shigaki T, Hirschi KD (2003) The *Arabidopsis cax1* mutant exhibits impaired ion homeostasis, development, and hormonal responses and reveals interplay among vacuolar transporters. *The Plant Cell* **15**: 347-364.

Cheng NH, Pittman JK, Shigaki T, Hirschi KD (2002) Characterization of CAX4, an *Arabidopsis* H^+/cation antiporter. *Plant Physiology* **128**: 1245-1254.

Cheng N-H, Pittman JK, Shigaki T, Lachmansingh J, LeClere S, Lahner B, Salt DE, and Hirschi KD (2005) Functional Association of *Arabidopsis CAX1* and *CAX3* Is Required for Normal Growth and Ion Homeostasis. *Plant Physiology* **138**: 2048-2060.

Cho D, Villiers F, Kroniewicz L, Lee S, Seo YJ, Hirschi KD, Leonhardt N, Kwak JM (2012) Vacuolar CAX1 and CAX3 influence auxin transport in guard cells via regulation of apoplastic pH. *Plant Physiology* **160**: 1293-1302.

Chung WS, Lee SH, Kim JC, Heo WD, Kim MC, Park CY, Park HC, Lim CO, Kim WB, Harper JF (2000) Identification of a calmodulin-regulated soybean Ca^{2+}-ATPase (SCA1) that is located in the plasma membrane. *Plant Cell* **12**: 1393-1407.

Clapham DE (1995) Calcium signalling. *Cell* **80(2)**: 259-268.

Clarkson DT and Hanson JB (1980) The mineral nutrition of plants. *Annual Review of Plant Physiology* **31**: 239-298.

Cleland RE, Buckley G, Nowbar S, Lew NM, Stinemetz C, Evans ML, Rayle DL (1991) The pH profile for acid-induced elongation of coleoptile and epicotyl sections is consistent with the acid-growth theory. *Planta* **186**: 70-74.

Cleland RE, Virk SS, Taylor D and Bjorkman T (1990) Calcium, cell walls and growth. In Calcium in Plant Growth and Development (ed. Hepler P. K. and Leonard R. T). *American Society of Plant Physiology Symposium series* **4**: 9-16.

Conn SJ, Gilliham M, Athman A, Schreiber AW, Baumann U, Moller I, Cheng NH, Stancombe MA, Hirschi KD, Webb AA, Burton R, Kaiser BN, Tyerman SD, Leigh RA (2011) Cell-specific vacuolar calcium storage mediated by CAX1 regulates apoplastic calcium concentration, gas exchange, and plant productivity in *Arabidopsis*. *Plant Cell* **23(1)**: 240-257.

Cosgrove DJ (1994) Photomodulation of growth. In: Kendrick RE, Kronenberg GHM, Kendrick RE, Kronenberg GHM, editors. Photomorphogenesis in plants, 2nd edition. Dordrecht: *Kluwer Academic Publishers*: 631-658.

Cosgrove DJ (2000) Loosening of plant cell walls by expansins. *Nature* **407(6802)**: 321-326.

Cross JW (1991) Cycling of auxin-binding protein through the plant cell: pathways in auxin signal transduction. *New Biologist* **3(8)**: 813-819.

Cunningham KW, Fink GR (1996) Calcineurin inhibits VCX1-dependent H^+/Ca^{2+} exchange and induces Ca^{2+}-ATPases in *Saccharomyces cerevisiae*. *Molecular Cell Biology* **16**: 2226-2237.

Curran AC, Hwang I, Corbin J, Martinez S, Rayle D, Sze H, Harper JF (2000) Autoinhibition of a calmodulin-dependent calcium pump involves a structure in

the stalk that connects the transmembrane domain to the ATPase catalytic domain. *Journal of Biological Chemistry* **275**: 30301-30308.

Dale JE (1988*)* Light-stimulated cell expansion in bean...The control of leaf expansion. *Annual Review of Plant Physiology and Plant Molecular Biology* **39**: 267-295.

David KM, Couch D, Braun N, Brown S, Grosclaude J, Perrot-Rechenmann C (2007) The auxin-binding protein 1 is essential for the control of cell cycle. *Plant Journal* **50(2)**: 197-206.

Dengler N, Kang J (2001) Vascular patterning and leaf shape. *Current Opinion in Plant Biology* **4**: 50-56.

Dharmasiri N, Dharmasiri S, Estelle M (2005) The F-box protein TIR1 is an auxin receptor. *Nature* **435(7041)**: 441-445.

Diekman, W, Venis, MA and Robinson DG (1995) Auxins induce clustering of auxin-binding protein at the surface of maize coleoptile protoplasts. *Proceedings of the National Academy of Sciences of the United States of America* **92**: 3425-3429.

Downs RJ (1955) Photoreversibility of Leaf and Hypocotyl Elongation of Dark Grown Red Kidney Bean Seedlings. *Plant Physiology* **30**: 468-473.

Duvick DN (2001) Biotechnology in the 1930s: the development of hybrid maize. *Nature Reviews Genetics* **2**: 69-74.

Edmond C, Shigaki T, Ewert S, Nelson M, Connorton J, Chalova V, Noordally Z, Pittman JK (2008) Comparative analysis of CAX2-like cation transporters indicates functional and regulatory diversity *Biochemical Journal Immediate Publication*. Manuscript BJ20081814.

Effendi Y, Rietz S, Fischer U, Scherer GF (2011) The heterozygous *abp1/ABP1* insertional mutant has defects in functions requiring polar auxin transport and in regulation of early auxin-regulated genes. *Plant Journal* **65(2)**: 282-294.

Elzenga JTM (1997) Kinetic properties of blue light pulse induced acidification by leaf epidermal cells of pea. *Plant Physiology* **144**: 1474.

Ephritikhine G, Barbier-Brygoo H, Muller J.F, Guern J (1987) Auxin Effect on the Transmembrane Potential Difference of Wild-Type and Mutant Tobacco Protoplasts Exhibiting a Differential Sensitiity to Auxin. *Plant Physiology* **83**: 801-804.

Ettinger WF, Clear AM, Fanning KJ, Peck ML (1999) Identification of a Ca^{2+}/H^{+} antiport in the plant chloroplast thylakoid membrane. *Plant Physiology* **119**: 1379-1386.

Evans DE, Williams LE (1998) P-type calcium ATPase in higher plants-biochemical, molecular and functional properties. *Biochimica et Biophysica Acta* **1376**: 1-25.

Feckler C, Muster G, Feser W, Römer A, Palme K (2001) Mass spectrometric analysis reveals a cysteine bridge between residues 2 and 61 of the auxin-binding protein 1 from *Zea mays* L. *FEBS Letters* **509(3)**: 446-450.

Felle H (1988) Auxin causes oscillations of cytosolic free calcium and pH in *Zea mays* coleoptiles. *Planta* **174**: 495-499.

Felle H, Brummer B, Bertl A, Parish RW (1986) Indole-3-acetic acid and fusicoccin cause cytosolic acidification of corn coleoptile cells. *Proceedings of the National Academy of Sciences of the United States of America* **83**: 8992-8995.

Felle H, Peters W, Palme K (1991) The electrical response of maize to auxins. *Biochimica et Biophysica Acta* **1064**: 199-204.

Fellner M, Ford E.D, Van Volkenburgh E (2006) Development of erect leaves in a modern maize hybrid is associated with reduced responsiveness to auxin and light of young seedlings *in vitro. Plant Signalling and Behavior* **1**: 201-211.

Fellner M, Horton LA, Cocke AE, Stephens NR, Ford ED, Van Volkenburgh E (2003) Light interacts with auxin during leaf elongation and leaf angle development in young corn seedlings. *Planta* **216**: 366-376.

Fellner M, Ephritikhine G, Barbier-Brygoo H, Guern J (1996) An antibody raised to a maize auxin-binding protein has inhibitory effects on cell division of tobacco mesophyll protoplasts. *Plant Physiology and Biochemistry* **34***:* 133-138.

Fricker MD, White NS, Thiel G, Millner P, Blatt MR (1994) Peptides derived from the auxin binding protein elevate Ca^{2+} and pH in stomatal guard cells of *Vicia faba*: a confocal fluorescence ratio imaging study. *Symposia of the Society of Experimental Biology* **48**: 215-228.

Friml J, Benková E, Blilou I, Wisniewska J, Hamann T, Ljung K, Woody S, Sandberg G, Scheres B, Jürgens G, Palme K (2002) AtPIN4 mediates sink-driven auxin gradients and root patterning in *Arabidopsis*. *Cell* **108(5)**: 661-673.

Galston AW and Baker RS (1953) Studies on the physiology of light action. V. Photoinductive alteration of auxin metabolism in etiolated peas. *American Journal of Botany* **40**: 512-516.

Gehring CA, McConchie RM, Venis MA, Parish RW (1998) Auxin-binding-protein antibodies and peptides influence stomatal opening and alter cytoplasmic pH. *Planta* **205(4)**: 581-586.

Goldsmith MH (1993) Cellular signalling: new insights into the action of the plant growth hormone auxin. *Proceedings of the National Academy of Sciences of the United States of America* **90(24)**: 11442-11445.

Hall JL, Brummell DA, Gillespie J (1985) Does auxin stimulate the elongation of intact plant stems? *New Phytologist* **100**: 341-345.

Hall TA (1999) BioEdit: a user-friendly biological sequence alignment editor and analysis program for Windows 95/98/NT. *Nucleic Acids Symposium Series* **41**: 95-98.

Halliday KJ, Martínez-García, JF, Josse E-M (2010) Integration of light and auxin signalling. Cold Spring Harbor Perspectives in Biology 00:a001586. Review.

Hasenstein KH and Evans ML (1988) Effects of cations on hormone transport in primary roots of *Zea mays*. *Plant Physiology* **86(3)**: 890-894.

Henderson J, Bauly JM, Ashford DA, Oliver SC, Hawes CR, Lazarus CM, Venis MA, Napier RM (1997) Retention of maize auxin-binding protein in the endoplasmic reticulum: quantifying escape and the role of auxin. *Planta* **202(3)**: 313-323.

Hertel R, Thomson KS and Rusoo VEA (1972) *In vitro* auxin binding to particulate cell fractions from corn coleoptiles. *Planta* **107**: 325-340.

Hesse T, Feldwisch J, Balshüsemann D, Bauw G, Puype M, Vandekerckhove J, Löbler M, Klämbt D, Schell J, Palme K (1989) Molecular cloning and structural analysis of a gene from *Zea mays* (L.) coding for a putative receptor for the plant hormone auxin. *The European Molecular Biology Organization Journal* **8(9)**: 2453-2461.

Hesse T, Garbers C, Brzobohaty B, Kreimer G, Söll D, Melkonian M, Schell J, Palme K (1993) Two members of the ERabp gene family are expressed differentially in reproductive organs but to similar levels in the coleoptile of maize. *Plant Molecular Biology* **23(1)**: 57-66.

Hirschi K (2001) Vacuolar H^+/Ca^{2+} transport: who's directing the traffic? *Trends in Plant Science* **6**: 100-104.

Hirschi KD, Korenkov VD, Wilganowski NL, Wagner GJ (2000) Expression of *Arabidopsis* CAX2 in tobacco. Altered metal accumulation and increased manganese tolerance. *Plant Physiology* **124**: 125-133.

Hirschi KD, Zhen RG, Cunningham KW, Rea PA, Fink GR (1996) CAX1, a H^+/Ca^{2+} antiporter from *Arabidopsis*. *Proceedings of the National Academy of Sciences of the United States of America* **93**: 8782-8786.

Hirschi KD (1999) Expression of Arabidopsis *CAX1* in tobacco: altered calcium homeostasis and increased stress sensitivity. *Plant Cell* **11(11)**: 2113-2122.

Hoecker U, Toledo-Ortiz G, Bender J, Quail PH (2004) The photomorphogenesis-related mutant red1 is defective in CYP83B1, a red light-induced gene encoding a cytochrome P450 required for normal auxin homeostasis. *Planta* **219**: 195-200.

Hofmann K, Stoffel W (1993) TMbase - A database of membrane spanning proteins segments. *Biological Chemistry* Hoppe-Seyler **374**: 166.

Huisinga B (1964) Influence of light on growth, geotropism and guthation of Avena seedlings grown in total darkness. *Acta Botanica Neerlandica* **13**: 445-487.

Huisinga B (1967) Influence of irradiation on the distribution of growth in dark-grown *Avena* seedlings. *Acta Botanica Neerlandica* **16**: 197-201.

Iino M (1982a) Action of red light on indole-3-acetic-acid status and growth in coleoptiles of etiolated maize seedlings. *Planta* **156**: 21-32.

Iino M (1982b) Inhibitory action of red light on the growth of the maize mesocotyl: Evaluation of the auxin hypothesis. *Planta* **156**: 388-395.

Iino M (1995) Gravitropism and phototropism of maize coleoptiles: evaluation of the Cholodny-Went theory through effects of auxin application and decapitation. *Plant Cell Physiology* **36**: 361-367.

Im KH, Chen JG, Meeley RB, Jones AM (2000) Auxin-Binding Protein Mutants in Maize. *Maydica* **45**: 319-325.

Ivey DM, Guffanti AA, Zemsky J, Pinner E, Karpel R, Padan E, Schuldiner S. and Krulwich TA (1993) Cloning and characterization of a putative Ca^{2+}/H^{+} antiporter gene from *Escherichia coli* upon functional complementation of Na^{+}/H^{+} antiporter-deficient strains by the overexpressed gene. *Journal of Biological Chemistry* **268**: 11296-11303.

Jensen PJ, Hangarter RP, Estelle M (1998) Auxin transport is required for hypocotyls elongation in light-grown but not dark-grown Arabidopsis. *Plant Physiology* **116**: 455-462.

Jones AM (1990) Do we have the auxin receptor yet? *Physiologia Plantarum* **80**: 154-158.

Jones AM (1994) Auxin-Binding Proteins. *Annual Review of Plant Physiology and Plant Molecular Biology* **45**: 393-420.

Jones AM, Cochran DS, Lamerson PM, Evans ML, Cohen JD (1991) Red light-regulated growth. I. Changes in the abundance of indoleacetic acid and a 22-kilodalton auxin-binding protein in the maize mesocotyl. *Plant Physiology* **97**: 352-358.

Jones AM, Im KH, Savka MA, Wu MJ, DeWitt G, Shillito R, Binns AN (1998) Auxin-dependent cell expansion mediated by overexpressed auxin-binding protein 1. *Science* **282**: 1114-1117.

Jones AM, Lamerson PM, Venis MA (1989) Comparison of site I auxin binding and a 22-kilodalton auxin-binding protein in maize. *Planta* **179**: 409-413.

Jones AM, Venis MA (1989) Photoaffinity labeling of indole-3-acetic acid-binding proteins in maize. *Proceedings of the National Academy of Sciences of the United States of America* **86**: 6153-6156.

Jurišić-Knežev D, Čudejková M, Zalabák D, Hlobilová M, Rolčík J, Pěnčík A, Bergougnoux V, Fellner M (2012) Maize AUXIN-BINDING PROTEIN 1 and AUXIN-BINDING PROTEIN 4 impact on leaf growth, elongation, and seedling responsiveness to auxin and light. *Botany/Botanique* **90(10)**: 990-1006.

Kamiya T, Akahori T, Maeshima M (2005) Expression profile of the genes for rice cation/H^+ exchanger family and functional analysis in yeast. *Plant Cell Physiology* **46**: 1735-1740.

Kamiya T, Maeshima M (2004) Residues in internal repeats of the rice cation/H^+ exchanger are involved in the transport and selection of cations. *Journal of Biological Chemistry* **279**: 812-819.

Kasai M, Muto S (1990) Ca^{2+} pump and Ca^{2+}/H^+ antiporter in plasma membrane vesicles isolated by aqueous two-phase partitioning from corn leaves. *Journal of Membrane Biology* **114**: 133-142.

Kepinski S, Leyser O (2005a) Plant development: auxin in loops. *Current Biology* **15(6)**: R208-210.

Kepinski S, Leyser O (2005b) The *Arabidopsis* F-box protein TIR1 is an auxin receptor. *Nature* **435(7041)**: 446-451.

Klämbt D (1990) A view about the function of auxin-binding proteins at plasma membranes. *Plant Molecular Biology* **14(6)**: 1045-1050.

Kondo N, Fujii T, Yamaki T (1969) Effect of light on auxin transport and elongation of *Avena* mesocotyl. *Development, Growth and Differentiation* **11(1)**: 46-61.

Krogh A, Larsson B, von Heijne G, Sonnhammer ELL (2001) Predicting transmembrane protein topology with a hidden Markov model: Application to complete genomes. *Journal of Molecular Biology* **305**: 567-580.

Larkin MA, Blackshields G, Brown NP, Chenna R, McGettigan PA, McWilliam H, Valentin F, Wallace IM, Wilm A, Lopez R, Thompson JD, Gibson TJ and Higgins DG (2007) ClustalW and ClustalX version 2. *Bioinformatics* **23**: 2947-2948.

Leblanc N, David K, Grosclaude J, Pradier JM, Barbier-Brygoo H, Labiau S, Perrot-Rechenmann C (1999) A novel immunological approach establishes that the auxin-binding protein, Nt-abp1, is an element involved in auxin signalling at the plasma membrane. *Journal of Biological Chemistry* **274(40)**: 28314-28320.

Levine A, Pennell RI, Alvarez ME, Palmer R, Lamb C (1996) Calcium-mediated apoptosis in a plant hypersensitive disease resistance response. *Current Biology* **6(4)**: 427-437.

Lin J, Zhang W, Shi M, Wang X, Sun X, Tang K (2008) Isolation and molecular characterization of a cax gene from *Capsella bursa-pastoris*. *Biocell* **32(3)**: 229-235.

Löbler M, Klämbt D (1985) *Auxin-binding protein from coleoptile membranes of corn (Zea mays* L.). I. Purification by immunological methods and characterization. *Journal of Biological Chemistry* **260(17)**: 9848-9853.

Malhó R, Moutinho A, Van der Luit A, Trewavas AJ (1998) Spatial characteristics of Ca^{2+} signalling; the calcium wave as a basic unit in plant cell calcium signalling. *Philosophical Transactions of the Royal Society of London Series B* **353**: 1463-1473.

Manohar M, Shigaki T, Hirschi KD (2011) Plant cation/H^+ exchangers (CAXs): biological functions and genetic manipulations. *Plant Biology (Stuttg).* **13**: 561-569. Review.

Marty F (1999) Plant Vacuoles. *The Plant Cell* **11**: 587-599.

Mäser P, Thomine S, Schroeder JI, Ward JM, Hirschi K, Sze H, Talke IN, Amtmann A, Maathuis FJ, Sanders D, Harper JF, Tchieu J, Gribskov M, Persans MW, Salt DE, Kim SA, Guerinot ML (2001) Phylogenetic relationships within cation transporter families of *Arabidopsis*. *Plant Physiology* **126**: 1646-1667.

Mei H, Cheng NH, Zhao J, Park S, Escareno RA, Pittman JK and Hirschi KD (2009) Root development under metal stress in *Arabidopsis thaliana* requires the H^+/cation antiporter CAX4. *New Phytologist* **183**: 95-105.

Murashige T, Skoog A (1962) A Revised Medium for Rapid Growth and Bio Assays with Tobacco Tissue Cultures. *Physiologia Plantarum* **15**: 473-497.

Nagashima A, Suzuji G, Uehara Y, Saji K, Furukawa T, Koshiba T, Sekmoto M, Fujioka S, Kuroha T, Kojima M, et al. (2008) Phytochromes and cryptochromes regulate the differential growth of *Arabidopsis* hypocotyls in both a PGP10-dependent and a PGP19-independent manner. *Plant Journal* **53**: 516-529.

Napier RM, David KM, Perrot-Rechenmann C (2002) A short history of auxin-binding proteins. *Plant Molecular Biology* **49(3-4)**: 339-348.

Napier RM, Fowke LC, Hawes C, Lewis M, Pelham HR (1992) Immunological evidence that plants use both HDEL and KDEL for targeting proteins to the endoplasmic reticulum. *Journal of Cell Science* **102**: 261-271.

Napier RM, Venis MA, Bolton MA, Richardson LI, Butcher GW (1988) Preparation and characterization of monoclonal antibodies to maize membrane auxin-binding protein. *Planta* **176**: 519-526.

Naqvi SM (1975) Kinetics of auxin transport in light and in dark grown *Zea mays* L. coleoptile segments. *Zeitschrift Pflanzenphysiol* **76**: 379-383.

Nelson JM, Lane B, Freeling M (2002) Expression of a mutant maize gene in the ventral leaf epidermis is sufficient to signal a switch of the leaf's dorsoventral axis. *Development* **129**: 4581-4589.

Nishimura T, Mori Y, Furukawa T, Kadota A, Koshiba T (2006) Red light causes a reduction in IAA levels at the apical tip by inhibiting de novo biosynthesis from tryptophan in maize coleoptiles. *Planta* **224**: 1427-1435.

Osmont KS, Sadeghian N, Freeling M (2006) Mosaic analysis of extended auricle1 (eta1) suggests that a two-way signalling pathway is involved in positioning the blade/sheath boundary in *Zea mays*. *Developmental Biology* **295:** 1-12.

Palme K, Hesse T, Campos N, Garbers C, Yanofsky MF, Schell J (1992) Molecular analysis of an auxin binding protein gene located on chromosome 4 of Arabidopsis. *Plant Cell* **4(2)**: 193-201.

Pelham HR (1990) The retention signal for soluble proteins of the endoplasmic reticulum. *Trends in Biochemical Sciences* **15**: 483-486. Review.

Philippar K, Fuchs I, Luthen H, Hoth S, Bauer CS, Haga K, Thiel G, Ljung K, Sandberg G, Bottger M, Becker D, Hedrich R (1999) Auxin-induced K^+-channel expression represents an essential step in coleoptile growth and gravitropism. *Proceedings of the National Academy of Sciences of the United States of America* **96(21)**: 12186-12191.

Philippar K, Ivashikina N, Ache P, Christian M, Lüthen H, Palme K, Hedrich R (2004) Auxin activates KAT1 and KAT2, two K^+-channel genes expressed in seedlings of Arabidopsis thaliana. *Plant Journal* **37(6)**: 815-827.

Pittman JK, Hirschi KD (2001) Regulation of CAX1, an *Arabidopsis* Ca^{2+}/H^+ antiporter. Identification of an N-terminal autoinhibitory domain. *Plant Physiology* **127**: 1020-1029.

Pittman JK, Hirschi KD (2003) Don't shoot the (second) messenger: endomembrane transporters and binding proteins modulate cytosolic Ca^{2+} levels. *Current Opinion in Plant Biology* **6**: 257-262.

Pittman JK, Shigaki T, Hirschi KD (2005) Evidence of differential pH regulation of the *Arabidopsis* vacuolar Ca^{2+}/H^+ antiporters CAX1 and CAX2. *FEBS Letters* **579**: 2648-2656.

Pittman JK, Shigaki T, Marshall JL, Morris JL, Cheng NH, Hirschi KD (2004) Functional and regulatory analysis of the *Arabidopsis thaliana* CAX2 cation transporter. *Plant Molecular Biology* **56(6)**: 959-971.

Pittman JK, Sreevidya CS, Shigaki T, Ueoka-Nakanishi H, Hirschi KD (2002) Distinct N-terminal regulatory domains of Ca^{2+}/H^+ antiporters. *Plant Physiology* **130(2)**: 1054-1062.

Rayle DL, Cleland RE (1980) Evidence that Auxin-induced Growth of Soybean Hypocotyls Involves Proton Excretion. *Plant Physiology* **66**: 433-437.

Ritchie SM, Swanson SJ, Gilroy S (2002) From common signalling components to cell specific responses: insights from the cereal aleurone. *Physiologia Plantarum* **115(3)**: 342-351.

Robert S, Kleine-Vehn J, Barbez E, Sauer M, Paciorek T, Baster P, Vanneste S, Zhang J, Simon S, Čovanová M, Hayashi K, Dhonukshe P, Yang Z, Bednarek SY, Jones AM, Luschnig C, Aniento F, Zažímalová E, Friml J (2010) ABP1 mediates auxin inhibition of clathrin-dependent endocytosis in *Arabidopsis. Cell* **143(1)**: 111-121.

Rück A, Palme K, Venis MA, Napier RM, Felle HH (1993) Patch-clamp analysis establishes a role for an auxin binding protein in the auxin stimulation of plasma membrane current in *Zea mays* protoplasts. *The Plant Journal* **4(1)**: 41–46.

Sanders D, Brownlee C, Harper JF (1999) Communicating with calcium. *The Plant Cell* **11**: 691-706.

Sanders D, Pelloux J, Brownlee C, Harper JF (2002) Calcium at the crossroads of signalling. *The Plant Cell* **14**: S401-S417.

Sauer M, Kleine-Vehn J (2011) AUXIN BINDING PROTEIN1: the outsider. *Plant Cell* **23(6)**: 2033-2043. Review.

Scherer GF (2011) AUXIN-BINDING-PROTEIN1, the second auxin receptor: what is the significance of a two-receptor concept in plant signal transduction? *Journal of Experimental Botany* **62(10)**: 3339-3357. Review.

Schumaker KS, Sze H (1985) A Ca^{2+}/H^{+} Antiport System Driven by the Proton Electrochemical Gradient of a Tonoplast H-ATPase from Oat Roots. *Plant Physiology* **79**: 1111-1117.

Schwob E, Choi S.Y, Simmons C, Migliaccio F, Ilag L, Hesse T, Palme K, Söll D (1993) Molecular analysis of three maize 22 kDa auxin-binding protein genes--transient promoter expression and regulatory regions. *Plant Journal* **4**: 423-432.

Shi JH, Yang ZB (2011) Is ABP1 an auxin receptor yet? *Molecular Plant* **4(4):** 635-640. Review.

Shigaki T, Cheng NH, Pittman JK and Hirschi K (2001) Structural determinants of Ca^{2+} transport in the *Arabidopsis* H^{+}/Ca^{2+} antiporter CAX1. *The Journal of Biological Chemistry* **276**: 43152-43159.

Shigaki T, Hirschi K (2000) Characterization of CAX-like genes in plants: implications for functional diversity. *Gene* **257**: 291-298.

Shigaki T, Rees I, Nakhleh L, Hirschi KD (2006) Identification of Three Distinct Phylogenetic Groups of CAX Cation/Proton Antiporters. *Journal of Molecular*

Evolution **63**: 815-825.**Shigaki T, Sreevidya C, Hirschi KD** (2002) Analysis of the Ca^{2+} domain in Arabidopsis H^{+}/Ca^{2+} antiporters CAX1 and CAX3. *Plant Molecular Biology* **50(3)**: 475-483.

Shimomura S (2006) Identification of a glycosylphosphatidylinositol-anchored plasma membrane protein interacting with the C-terminus of auxin-binding protein 1: a photoaffinity crosslinking study. *Plant Molecular Biology* **60(5)**: 663-677.

Shimomura S, Watanabe S, Ichikawa H (1999) Characterization of auxin-binding protein 1 from tobacco: content, localization and auxin-binding activity. *Planta* **209(1)**: 118-125.

Shishova M, Lindberg S (1999) Auxin-induced cytosol acidification in wheat leaf protoplasts depends on external concentration of Ca^{2+}. *Journal of Plant Physiology* **155**: 190-196.

Shishova M, Lindberg S (2004) Auxin induces rapid increase of Ca^{2+} concentration in the cytosol of wheat leaf protoplasts. *Journal of Plant Physiology* **161**: 937-945.

Shishova M, Lindberg S (2010) A new perspective on auxin perception. *Journal of Plant Physiology* **167**: 417-422.

Sidler M, Hassa P, Hasan S, Ringli C, Dudler R (1998) Involvement of an ABC transporter in a developmental pathway regulating hypocotyl elongation in the light. *Plant Cell* **10**: 1623-1636.

Spalding EP, Harper JF (2011) The ins and outs of cellular Ca^{2+} transport. *Current Opinion in Plant Biology* **14(6)**: 715-720. Review.

Staal M, Elzenga JTM, Van Elk AG, Prins HBA, Van Volkenburgh E (1994) Red and blue light-stimulated proton efflux by epidermal leaf cells of the Argentum mutant of *Pisum sativum*. *Journal of Experimental Botany* **45**: 278-278, 1213-1218.

Steffens B, Feckler C, Palme K, Christian M, Böttger M, Lüthen H (2001) The auxin signal for protoplast swelling is perceived by extracellular ABP1. *Plant Journal* **27(6)**: 591-599.

Tanaka S, Mochizuki N, Nagatani A (2002) Expression of the *AtGH3a* gene, an Arabidopsis homologue of the soybean *GH3* gene, is regulated by phytochrome B. *Plant Cell Physiology* **43**: 281-289.

Tian Q, Reed JW (2001) Molecular links between light and auxin signalling pathways. *Journal of Plant Growth Regulators* **20**: 274-280.

Tillmann U, Viola G, Kayser B, Siemeister G, Hesse T, Palme K, Löbler M, Klämbt D (1989) cDNA clones of the auxin-binding protein from corn coleoptiles (*Zea mays* L.): isolation and characterization by immunological methods. *The European Molecular Biology Organization Journal* **8(9)**: 2463-2467.

Timpte C (2001) Auxin binding protein: curiouser and curiouser. *Trends in Plant Science* **6**: 586-590.

Trewavas A (1999) Le calcium, C'est la vie: calcium makes waves. *Plant Physiology* **120(1)**: 1-6.

Tromas A, Paponov I, Perrot-Rechenmann C (2010) AUXIN BINDING PROTEIN 1: functional and evolutionary aspects. *Trends in Plant Science* **15(8):** 436-446. Review.

Tromas A, Perrot-Rechenmann C (2010) Recent progress in auxin biology. Comptes Rendus Biologie **333**: 297-306. Review.

Ueoka-Nakanishi H, Nakanishi Y, Tanaka Y, Maeshima M (1999) Properties and molecular cloning of Ca^{2+}/H^{+} antiporter in the vacuolar membrane of mung bean. *European Journal of Biochemistry* **262**: 417-425.

Ueoka-Nakanishi H, Tsuchiya T, Sasaki M, Nakanishi Y, Cunningham KW, Maeshima M (2000) Functional expression of mung bean Ca^{2+}/H^{+} antiporter in yeast and its intracellular localization in the hypocotyl and tobacco cells. *European Journal of Biochemistry* **267**: 3090-3098.

Van Overbeek (1936) Growth hormone and mesocotyl growth. *Rec Trav Bot Neerl.* **33**: 333-340.

Van Volkenburgh E (1999) Leaf expansion-an integrating plant behavior. *Plant Cell Environment* **22**: 1463-1473.

Van Volkenburgh E, Cleland RE (1990) Light-stimulated cell expansion in bean (*Phaseolus vulgaris* L.) leaves. I. Growth can occur without photosynthesis. *Planta* **182**: 72-76.

Van Volkenburgh E, Cleland RE, Watanabe M (1990) Light-stimulated cell expansion in bean (*Phaseolus vulgaris L.*) leaves. II. Quantity and quality of light required. *Planta* **182**: 77-80.

Vanderhoef LN, Briggs WR (1978) Red light-inhibited mesocotyl elongation in maize seedlings. *Plant Physiology* **61**: 534-537.

Venis, MA, Napier RM, Barbier-Brygoo H, Maurel C, Perrot-Rechenmann C and Guern J (1992) Antibodies to a peptide from the maize auxin-binding protein have auxin agonist activity. *Proceedings of the National Academy of Sciences of the United States of America* **89(15)**: 7208-7212.

Walton JD, Ray PM (1981) Evidence for receptor function of auxin binding sites in maize. Red light inhibition of mesocotyl elongation and auxin binding. *Plant Physiology* **68**: 1334-1338.

Waterhouse AM, Procter JB, Martin DM, Clamp M, Barton GJ (2009) Jalview Version 2--a multiple sequence alignment editor and analysis workbench. *Bioinformatics* **25(9)**: 1189-1191.

White PJ, Broadley MR (2003) Calcium in plants. *Annals of Botany* **92(4)**: 487-511. Review.

Wu Z, Liang F, Hong B, Young JC, Sussman MR, Harper JF, Sze H (2002) An endoplasmic reticulum-bound Ca^{2+}/Mn^{2+} pump, ECA1, supports plant growth and confers tolerance to Mn^{2+} stress. *Plant Physiology* **130(1)**: 128-137.

Xu T, Wen M, Nagawa S, Fu Y, Chen JG, Wu MJ, Perrot-Rechenmann C, Friml J, Jones AM, Yang Z (2010) Cell surface- and rho GTPase-based auxin signalling controls cellular interdigitation in *Arabidopsis*. *Cell* **143**: 99–110.

Yamagami M, Haga K, **Napier RM**, **Iino M** (2004) Two distinct signalling pathways participate in auxin-induced swelling of pea epidermal protoplasts. *Plant Physiology* **134**: 735-747.

Yang T, Davies PJ, Reid JB (1996) Genetic dissection of the relative roles of auxin and gibberellin in the regulation of stem elongation in intact light-grown peas. *Plant Physiology* **110**: 1029-1034.

Yang T, Law DM, Davies PJ (1993) Magnitude and kinetics of stem elongation induced by exogenous indole-3-acetic acid in intact light-grown pea seedlings. *Plant Physiology* **102**: 717-724.

Zhao J, Barkla BJ, Marshall J, Pittman JK, Hirschi KD (2008) The *Arabidopsis cax3* mutants display altered salt tolerance, pH sensitivity and reduced plasma membrane H^+-ATPase activity. *Planta* **3**: 659-669.

12 Appendix

Dejana Jurišić-Knežev, Mária Čudejková, David Zalabák, Marta Hlobilová, Jakub Rolčík, Aleš Pěnčík, Véronique Bergougnoux, Martin Fellner (2012) Maize AUXIN-BINDING PROTEIN 1 and AUXIN-BINDING PROTEIN 4 impact on leaf growth, elongation, and seedling responsiveness to auxin and light. *Botany/Botanique* **90(10)**: 990-1006.

Maize *AUXIN-BINDING PROTEIN 1* and *AUXIN-BINDING PROTEIN 4* impact on leaf growth, elongation, and seedling responsiveness to auxin and light

Dejana Jurišić-Knežev, Mária Čudejková, David Zalabák, Marta Hlobilová, Jakub Rolčík, Aleš Pěnčík, Véronique Bergougnoux, and Martin Fellner

Abstract: In maize, at least five auxin-binding proteins (ABPs) have been identified, yet their functions remain unclear. The present study reports the use of maize *abp1*, *abp4*, and *abp1abp4* mutants to investigate the role of ABPs during maize growth and development. Single and double *abp* mutant plants grown in a greenhouse differ from the wild type (WT) in their leaf declination and leaf blade growth. The effect of the dark (D), blue light (BL), red light (RL), and exogenous auxin on the development of mutant seedlings was also studied. Relative to WT, etiolated mutant seedlings were shorter and showed a reduced responsiveness to exogenous auxin. In BL or RL, the responsiveness of maize seedlings to auxin was distinctly less than in D. The reducing effect of light on seedling responsiveness to auxin is mediated at least by phytochromes. The suppression of *ABP1* and (or) *ABP4* led to a distinct accumulation of free indole-3-acetic acid (IAA) in etiolated and light-grown seedling organs. We concluded that ABP1 and ABP4 participate in the growth of maize seedlings, mediate seedling responses to auxin, and interact with light signaling pathway(s). We also deduce a functional interaction between ABP1 and ABP4, which is that the relationship between them is light-, organ- and response-dependent.

Key words: auxin, auxin-binding protein, growth, light, maize.

Résumé : Les auteurs ont identifié cinq protéines liant l'auxines « auxin-binding proteins » (ABPs), chez le maïs, sans pouvoir établir clairement leurs fonctions. Ils ont utilisé trois mutants de maïs (*abp1*, *abp4* et *abp1abp4*) pour comprendre le rôle des ABPs dans la croissance et le développement du maïs. En serre, les mutants diffèrent du témoin par la croissance de la feuille et son angle d'insertion sur la tige. Ils ont également étudié la croissance des mutants cultivés in vitro, dans le noir, exposés à la lumière bleue (BL) ou rouge (RL), en présence d'auxine exogène. Les plantules étiolées des mutants s'avèrent plus courtes et moins sensibles à l'auxine que les témoins de type sauvage. Les BL et RL atténuent la sensibilité des plantules à l'auxine, cette réaction étant partiellement contrôlée par les phytochromes. La suppression de *ABP1* et (ou) *ABP4* se caractérise par une accumulation différente d'auxine dans les organes des plantules étiolées ou cultivées à la lumière. En conclusion, ABP1 et ABP4 jouent un rôle dans la croissance des plantules de maïs et leur réponse à l'auxine, et interagissent avec la(es) voie(s) de signalisation de la lumière. Nous suggérons une interaction entre ABP1 et ABP4, toutefois dépendante de la lumière, de l'organe et de la réaction étudiés.

Mots-clés : auxine, protéine liant l'auxine, croissance, lumière, maïs.

Introduction

Auxins play a central role in plant growth and development, as they are involved in broad spectrum processes, including embryogenesis, stem elongation, apical dominance, photo- and gravitropism, and lateral root formation (reviewed in Davies 2004 and Vanneste and Friml 2009). At the cellular level, auxin acts to regulate these processes through changes in cell division, cell expansion, and differentiation (reviewed in Teale et al. 2006 and Perrot-Rechenmann 2010). At the plant level, it has been demonstrated that endogenous, as well as externally supplied, indole-3-acetic acid (IAA) stimulates the growth of intact maize coleoptiles (Baskin et al.1986; Iino 1995; Haga and Iino 1998). Epstein et al. (1980) reported that maize kernels supply the coleoptile tip with auxin in a conjugate form, from which free IAA is released by specific enzymes and moved from the coleoptile tip to the elongation zone via polar transport (Goldsmith

Received 7 November 2011. Accepted 17 June 2012. Published at www.nrcresearchpress.com/cjb on 14 September 2012.

D. Jurišić-Knežev, M. Čudejková,* D. Zalabák,* M. Hlobilová, V. Bergougnoux,* and M. Fellner. Palacky University in Olomouc and Institute of Experimental Botany, Academy of Science of the Czech Republic, v.v.i, Laboratory of Growth Regulators, Group of Molecular Physiology, Šlechtitelů 11, 783 71 Olomouc, Czech Republic.
J. Rolčík and A. Pěnčík. Palacky University in Olomouc and Institute of Experimental Botany, Academy of Science of the Czech Republic, v.v.i, Laboratory of Growth Regulators, Šlechtitelů 11, 783 71 Olomouc, Czech Republic.

Corresponding author: Martin Fellner (e-mail: martin.fellner@upol.cz).

*Present address: Department of Molecular Biology, Centre of the Region Haná for Biotechnological and Agricultural Research, Palacký University in Olomouc, Šlechtitelů 11, 783 71 Olomouc, Czech Republic.

1977; Lomax et al. 1995). The underlying mechanisms of cell elongation still remain the subject of debate, although distinct interpretations of auxin-induced growth have been proposed (Hager et al. 1971; Rayle and Cleland 1972, 1992; Hoth et al. 1997; Claussen et al. 1998; Philippar et al. 1999; Bauer et al. 2000; Becker and Hedrich 2002). On a longer time scale (days), the elongation of various plant organs in intact plants was shown to be inhibited by exogenous auxin (Marten et al. 1991; Zimmermann et al. 1994; Boerjan et al. 1995; King et al. 1995; Keller and Van Volkenburgh 1996; Thomine et al. 1997; Ephritikhine et al. 1999; Fellner et al. 2003, 2006).

The primary step of auxin signaling is the binding of an auxin to an auxin receptor. In addition to the described function of auxin receptors from the TRANSPORT INHIBITOR RESPONSE 1/AUXIN-BINDING F-BOX PROTEIN (TIR1/AFB) family, putative auxin receptor, the AUXIN-BINDING PROTEIN 1 (ABP1) has been identified (reviewed in Tromas and Perrot-Rechenmann 2010, Shi and Yang 2011, Sauer and Kleine-Vehn 2011, and Scherer 2011). ABP1 is a protein with a high-affinity to auxin that was identified in maize coleoptiles over 30 years ago by its capacity to bind to radiolabelled auxin (Hertel et al. 1972; Löbler and Klämbt 1985). Several studies demonstrated that ABP1 acts at the plasma membrane (Barbier-Brygoo et al. 1989; Leblanc et al. 1999), conversely the predominant localization of ABP1 was found to be in the endoplasmic reticulum lumen (Jones and Herman 1993). It was demonstrated that ABP1 mediates very early auxin responses including modifications of ion fluxes across the plasma membrane through the activation or deactivation of ion channels (K^+ cations) or transporters (H^+) (Rayle and Cleland 1980; Cleland et al. 1991; Ephritikhine et al. 1987; Barbier-Brygoo et al. 1989, 1991; Leblanc et al. 1999; Napier et al. 2002). ABP1 specifically binds auxin and the level of ABPs roughly correlates with the extent of cell responses to auxin (Ray et al. 1977; Shimomura et al. 1988; Jones et al. 1989). In addition, constitutive over-expression of *ABP1* in maize or tobacco cells resulted in larger cells; this effect was auxin dependent. These facts are consistent with ABP1 having an auxin receptor function (Jones et al. 1998; Chen et al. 2001). The results of Chen et al. (2001) suggest that in tobacco leaf cells, ABP1 acts with a relatively low level of auxin to mediate cell expansion, whereas high auxin levels stimulate cell division potentially via an unidentified receptor TIR1. However, the involvement of ABP1 in cell division has also been identified in tobacco (Fellner et al. 1996), and the characterization of the *Arabidopsis* loss-of-function mutant in *ABP1* indicates a dual role for the protein in cell expansion and cell division during early embryogenesis (Chen et al. 2001). Previously, it was shown that ABP1 acts on the control of the cell cycle (David et al. 2007). The authors demonstrated that cell cycle arrest provoked by ABP1 inactivation could not be bypassed by exogenous auxin, suggesting the role of ABP1 in an auxin-mediated control of the cell cycle. Until 2008, no evidence had been provided that the ABP1 was involved in auxin-regulated gene expression. However, recently Braun et al. (2008) demonstrated that ABP1 coordinates cell division and cell expansion during postembryonic shoot development in *Arabidopsis* and tobacco. The down-regulation of ABP1 activity in *Arabidopsis* results in a decrease of the expression of a large spectrum of *Aux/IAA* genes during shoot development (Braun et al. 2008), and ABP1 is required for the auxin-induced expression of a subset of *Aux/IAA* genes in roots (Tromas et al. 2009). The authors present a model in which ABP1 is the major regulator of auxin action on the cell cycle and regulates auxin-mediated gene expression and cell elongation along with the TIR1-mediated ubiquitination pathway. Recently, evidences were provided that ABP1 is involved in the regulation of polar auxin transport (PAT), thus affecting local auxin concentration, cell expansion, and early auxin gene regulation (Braun et al. 2008; Robert et al. 2010; Xu et al. 2010; Effendi et al. 2011). In addition to ABP1, at least four other closely related ABPs have been identified in maize so far (Hesse et al. 1989; Schwob et al. 1993), but their roles in growth and development have yet to be elucidated. Moreover, as far as we know the existence of maize mutant knockout in genes other than *ABP1* or *ABP4* (Im et al. 2000) have not been reported.

Light is an external factor that essentially regulates plant growth in a complex interaction with internal factors including auxins (reviewed in Tian and Reed 2001 and Halliday et al. 2009). How auxins can be involved in light-induced growth inhibition is not yet fully understood. Various studies have shown a correlation between light responses and auxin accumulation or PAT (reviewed in Tian and Reed 2001; Liu et al. 2011). In fact, light reduces the intensity of PAT in the etiolated coleoptile segments (Huisinga 1964, 1967; Naqvi 1975; Fellner et al. 2003) and reduces the content of free IAA in etiolated maize seedlings (Briggs 1963; Bandurski et al. 1977; Iino 1982*a*). Similarly, light was shown to decrease auxin transport in maize mesocotyls, revealing the important role of light and PAT in the mesocotyl photomorphogenesis (Van Overbeek 1936; Vanderhoef and Briggs 1978; Iino 1982*b*; Jones 1990; Barker-Bridgers et al. 1998). Recent research efforts led to the revelation that light pathways can modify auxin distribution by controlling the abundance of P-glycoproteins and PIN-FORMED proteins (Sidler et al. 1998; Friml et al. 2002; Nagashima et al. 2008; Zazimalova et al. 2010). A number of reports demonstrated the existence of signaling elements shared by light and auxin during elongation. Several links between light and auxins have been defined using primary auxin-response genes as genetic and molecular tools (Abel et al. 1995; Abel and Theologis 1996; Sitbon and Perrot-Rechenmann 1997; Tepperman et al. 2001; Devlin et al. 2003). Other hypotheses on the mechanism of light-regulated growth have included ABP1 (Walton and Ray 1981; Napier et al. 1988; Jones et al. 1989; Jones and Venis 1989). This idea was supported by the observation that a reduced abundance of ABP1 and a reduced level of free IAA in red light (RL)-grown seedlings were associated with a decrease in the mesocotyl growth (Jones et al. 1991). It was also reported that the expression of the *ABP1* gene in leaf tissues of 2-week-old green maize seedlings and in mature green leaves is much less than in etiolated seedlings (Im et al. 2000). By contrast, the expression of another member of the ABP family, *ABP4*, in maize mesocotyls was up-regulated in RL- and far-red light (FR)-grown seedlings (Fellner et al. 2006).

We previously reported that in comparison to old maize hybrids, cells of modern maize varieties developing upright leaves were insensitive to auxin- and light-induced hyperpolarization of the plasma membrane. The expression analysis

revealed an up-regulation of the *ABP4* gene by auxin and light in old hybrids but not in the modern ones (Fellner et al. 2003, 2006). Although Im et al. (2000) reported no phenotypic changes in loss-of-function mutants in *ABP1* and *ABP4* genes in maize, they found that a knockout of the *ABP4* gene resulted in a strong elevation (four to seven times) of the ABP1 protein in etiolated seedlings. In contrast to their observations, we previously found and reported distinct differences between the maize *abp* mutants and the wild type (WT) in leaf declination (Fellner et al. 2006). To uncover more information about the role of ABP1 and ABP4 in the growth and development of maize seedlings and their cross-talk with light signaling pathways, we investigated in more detail the phenotypes and growth responses in the loss-of-function mutants in *ABP1* and *ABP4* genes.

Material and methods

Plant material, growth conditions, and measurement of seedling growth

The loss-of-function mutants in *ABP1* and *ABP4* genes in maize (*Zea mays* L.) were used for all experiments (Im et al. 2000). The *abp* mutants contained the Robertson's *Mutator* transposable elements (Bennetzen 1996) in *ABP1* and (or) *ABP4* genes. Seeds of single mutants *abp1* (*B2* allele) and *abp4* (*B2/K1* allele), double mutant *abp1abp4* (*B2/K1* allele), and a near isogenic line (inbred line A619, here called WT) were a gift from Alan M. Jones (The University of North Carolina, Chapel Hill, N.C.). All mutants were tested for the lack of *ABP1* and (or) *ABP4* gene expression (see Supplemental Fig. S1)[1]; they all showed stable phenotypes. The fytochromobilin-deficient mutant *elm1* (*elongated mesocotyl 1*) was initially identified in the W22 background (Sawers et al. 2002), and it was also introgressed into the B73 background (inbred maize line) by backcrossing five times (Dubois et al. 2010). Kernels of *elm1* and B73 were kindly provided by Thomas P. Brutnell (Boyce Thompson Institute for Plant Research, Ithaca, N.Y.).

For experiments in Magenta plant culture boxes, seeds were first washed with 70% ethanol for 3 min, rinsed with distilled sterile water, and then soaked in Savo original solution (~5% sodium hypochlorite; Bochemie, s.r.o, Czech Republic) that was supplemented with a drop of Tween20 (Calbiochem, USA). Finally, the solution was shaken on a stirrer for 30 min and then rinsed extensively with sterile distilled water. These seeds were germinated on a 0.7% (*w*/*v*) agar medium in Magenta GA-7 boxes (77 mm × 77 mm × 196 mm; Sigma-Aldrich, Prague, Czech Republic) (six to nine seeds per box). The basal medium (BM) contained Murashige and Skoog salts (MS medium; Sigma-Aldrich, Prague, Czech Republic) (Murashige and Skoog 1962), 1% (*w*/*v*) sucrose, and 1 mmol·L^{-1} MES (2-(*N*-morpholino)-ethanesulfonic acid); pH was adjusted to 6.1 before autoclaving. In experiments with auxin, the BM was supplemented with 1-naphthalene acetic acid (NAA) in various concentrations. Seeds in the Magenta boxes were placed in a growth chamber (Microclima MC1000E, Snijders Scientific, the Netherlands) and incubated at a temperature of 23 °C. For the development of etiolated seedlings, the boxes were wrapped in aluminum foil. Maize seeds were also incubated under continuous blue light (BL) with a maximum irradiance at 460 nm or in continuous red light (RL) with a maximum irradiance at 660 nm and both at 23 °C. BL and RL were provided by blue (Philips TLD-36W/18-Blue, Phillips, USA) and red (Philips TLD-36W/15-Red, Phillips, USA) fluorescent tubes. The total photon fluence rates of BL and RL were 10 μmol·m^{-2}·s^{-1}. The fluence rate was measured with a portable spectroradiometer (model LI-1800; LI-COR; Lincoln, Nebr.) calibrated by the Department of Biophysics at Palacky University in Olomouc. In all conditions, 5-day-old seedlings were measured. For experiments in the greenhouse, plants were grown in soil (Potgrond H, Klasmann Deilmann GmBH, Germany) in small pots (190 mm × 190 mm; one seed per pot; 1 cm deep) and regularly watered. In summer, the plants grew in natural light conditions with temperatures of 15 °C and higher. In winter, the plants grew under high-pressure sodium lamps using PlantaStar E40/ES 400 W (Osram GmbH, Germany) to maintain a 16-h photoperiod. The temperature was adjusted from 15 to 27 °C.

The size of various organs was measured with a ruler on 5-day-old intact seedlings developed in Magenta boxes on BM. The mesocotyl length was measured from the scutellar to the coleoptilar node, and the coleoptile length was measured from the coleoptilar node to the tip of the coleoptile. The primary root length was measured from the scutelar node to the root tip. For genotype, six to nine seedlings per treatment that germinated on the same day were measured in each experiment. When necessary, changes in growth (i.e., inhibition or stimulation) caused by an effector (light, exogenous auxin) in the individual genotype were expressed in percents based on the following formula: $X = 100 \times (A - B) / A$, where X is the change in growth (in %) and A and B stand for growth (in mm) in the absence and presence, respectively, of the effector.

For the study of the leaf characteristics, plants were grown in soil in a greenhouse as described above and watered regularly. Leaf angle (declination from vertical) was measured with a protractor held at the leaf base, as described by Fellner et al. (2003), in 5–10 intact plants of each genotype from 2 to 4 weeks after seed germination. Blade length was measured with a ruler to the nearest millimetre. Leaf blades were scanned with a scanner and the width and blade surface were determined using ImageJ software (Abramoff et al. 2004).

Mesocotyl cross-section light microscopy and cell diameter

Cross-sections (~0.5 mm) of etiolated maize mesocotyls were performed using a razor blade. The sections were stained ~5 min in methylene blue dye, subsequently washed with distilled water, and then placed on a microscopy slide into a drop of distilled water and overlapped with a cover glass. Samples were examined using a light microscope model OLYMPUS BX-60 and microphotographs were taken using a CCD camera OLYMPUS DP71 (Olympus Czech Group, Prague, Czech Republic). The diameter of cortical cells was measured on microphotographs using ImageJ soft-

[1]Supplementary data are available with the article through the journal Web site (http://nrcresearchpress.com/doi/suppl/10.1139/b2012-071).

ware (Abramoff et al. 2004). In each genotype tested, the diameter of the cells in five cross-sections was measured, and in each microphotograph, the diameter of ~70 randomly selected cells was measured.

Extraction and quantification of endogenous auxin

For analysis of endogenous free IAA in coleoptiles, mesocotyls, and primary roots, 5-day-old maize seedlings grown in Magenta boxes in dark (D), RL, or BL conditions as described above were used. Organs were each separately excised from the seedling, placed individually into prechilled aluminum foil envelopes, immediately frozen in liquid nitrogen, and then stored at –80 °C. Samples of ~10 mg of fresh mass were extracted and purified by solid-phase extraction on C8 column as described by Pěnčík et al. (2009). The eluates were evaporated until dry in vacuo and analyzed for free IAA content by UPLC (Acquity UPLC System, Waters) coupled to triple quadrupole mass detection (Quatro micro, Waters).

Analysis of *ABP* transcripts

The presence or absence of *ABP1* and (or) *ABP4* transcripts in the loss-of-function mutants in *ABP1* and *ABP4* genes in maize was confirmed by reverse transcription PCR (RT–PCR) as described in Fellner et al. (2006) with a slight modification. PCR of 25 cycles for *ABP1* and of 28 cycles for *ABP4* were performed by denaturing the template cDNAs at 94 °C for 3 min followed by cycles of 94 °C for 30 s, 60 °C for 30 s, 72 °C for 45 s, and 72 °C for 5 min. An *ABP1* fragment (maize *ABP1* gene accession No. L08425) was amplified using oligonucleotides 5′-CCGCAAAGCAGCTATGGGATT-3′ from exon 2 and 5′-CGAAGGGGAATTTCAGTACCGCG-3′ from exon 5. An *ABP4* fragment (maize *ABP4* gene accession No. L08426) was amplified using oligonucleotides 5′-CAGCAGCGCAACTACGGGAGG-3′ from exon 2 and 5′-AGTAGGGGAATTTCAGCTTTGCA-3′ from exon 5. The primer pairs were previously described in Fellner et al. (2006). PCR products (*ABP1* as well as *ABP4*, each 403 bp in size) were size fractionated by electrophoresis in a 1% (*w*/*v*) agarose gel stained with ethidium bromide.

Statistical analysis

When needed, the statistical significance of the treatment differences was assessed using Student's *t* test.

Results

Contrary to Im et al. (2000) who reported no phenotypic differences between *abp* mutants and the corresponding WT, we previously observed distinct differences between the genotypes in leaf angle development when plants were grown in growth chambers (Fellner et al. 2006). Similarly, we observed a number of other phenotypes in the *abp* mutants developed in the greenhouse in WL conditions and in the Magenta boxes on the BM when grown in D, BL, or RL conditions. Im and co-authors observed that the level of the ABP1 protein in the *abp4* mutant was four to seven times higher than in WT, indicating that the elimination of the *ABP4* gene activates *ABP1* expression post-transcriptionally because the *ABP1* transcript levels did not differ among WT and *abp4* mutants (Im et al. 2000). Based on this, and on our previous observations of differential leaf angles in WT and *abp* mutants, we expected some phenotype patterns in single or double *abp* mutants. First, we expect that the single mutants *abp1* and *abp4* will show opposite phenotypes. The opposite phenotypes were observed for example in leaf angle and width or length of the etiolated coleoptile (see below). Second, if the increased ABP1 protein is partly responsible for the *abp4* single mutant phenotype, we expect that the *abp1abp4* double mutant will show a less extreme phenotype than *abp4*, possibly similar to WT. This was found for example in leaf blade length, diameter of etiolated mesocotyl, mesocotyl length in RL, and the sensitivity of the etiolated primary root to NAA (see below). Third, we also expect a phenotype more extreme than single mutants or WT in the case that the two genes are acting together, rather than in opposition. This would be for example, in the case of the length of the etiolated mesocotyl and the primary responsiveness of the etiolated coleoptile and mesocotyl to NAA, or the level of endogenous IAA in the etiolated coleoptile and primary root (see below).

Fig. 1. Leaf angle of single maize mutants *abp1* and *abp4*, double mutant *abp1abp4*, and corresponding wild type (WT) grown in the greenhouse. The leaf angle, measured as a declination from vertical in 25-day-old plants (2nd leaf), 32-day-old plants (3rd leaf), and 35-day-old plants (4th leaf), was determined with a protractor to the nearest degree. For each genotype, 4 to 10 seedlings were measured in every experiment. The values show the leaf angle (mean ± SE) obtained in 12 independent experiments. * and ** indicate significant differences (*t*-test; $P \leq 0.05$ and $P \leq 0.01$, respectively) from the corresponding WT leaf.

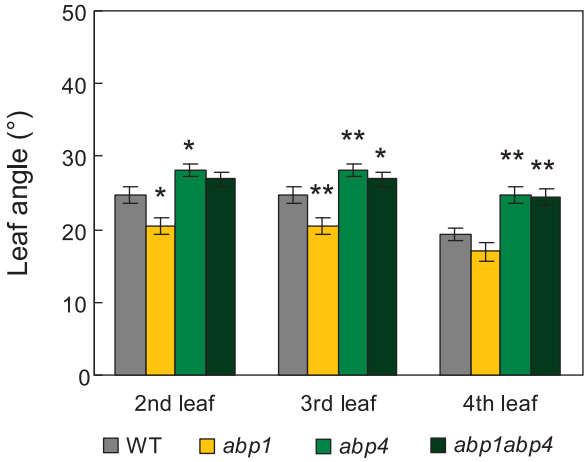

Loss-of-function mutants in *ABP1* and *ABP4* genes show differential leaf growth

In this study, we investigated leaf development in 4-week-old plants that were grown in a greenhouse. In WT, declination of the 2nd and 3rd leaf reached ~25° (Fig. 1). The mutation in *ABP1* led to the development of a significantly smaller leaf declination (~20°), whereas the defect in the *ABP4* gene resulted in the development of leaves with a larger angle (~28°). Interestingly, the loss of function in both genes resulted in leaves with a declination similar to that observed in the *abp4* mutant. A comparable situation was observed in the fully developed 4th leaf (Fig. 1). Leaf declination in the double mutant and WT was not significantly different for the 2nd leaf.

Fig. 2. Length of leaf blade, leaf width, and leaf surface of single maize mutants *abp1* and *abp4*, double mutant *abp1abp4*, and corresponding wild type (WT) grown in the greenhouse. (*a*) The blade length and (*b*) leaf width in 25-day-old plants (2nd leaf), 32-day-old plants (3rd leaf), and 35-day-old plants (4th leaf) were measured with a ruler to the nearest millimetre. (*c*) Examples of the widths of the bases in the 2nd, 3rd, and 4th leaf in 1-month-old WT and *abp* mutant plants are shown. Scale bar = 5 mm. (*d*) The blade surface in 2nd, 3rd, and 4th leaf plants was measured by scanning the leaf blades and afterwards determined using ImageJ software. For each genotype, 4 to 10 seedlings were measured in every experiment. The values show the measured parameters (mean ± SE) obtained in 12 independent experiments. * and ** indicate significant differences (*t*-test; $P \leq 0.05$ and $P \leq 0.01$, respectively) from the corresponding WT leaf.

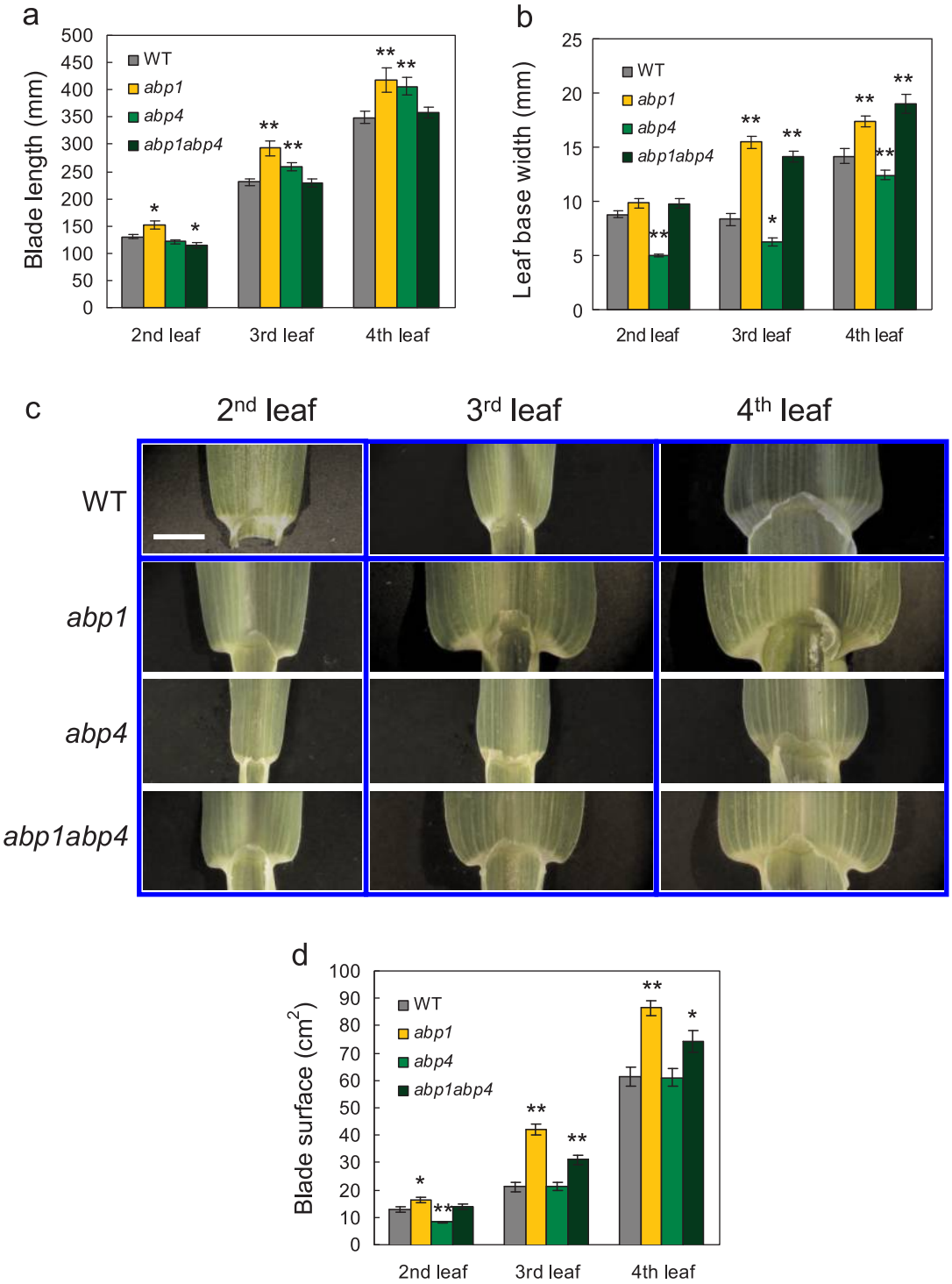

Mutations in *ABP1* or *ABP4* affected the overall features of the leaves. In the single mutant *abp1*, leaf blades of the 2nd, 3rd, and 4th leaf were longer than in WT plants. In *abp4* mutants, the 2nd leaves were the same size as in WT, and blades of the 3rd and 4th leaves were significantly longer than those in WT (by ~17%) (Fig. 2*a*). The 2nd leaf of the double mutant *abp1abp4* was shorter than in WT plants, and the 3rd and 4th leaves reached lengths similar to those observed in

WT plants (Fig. 2*a*). Leaf width was also affected by the mutations (Figs. 2*b*, 2*c*). The base of the leaf in *abp1* and the double mutant was wider than in WT plants, especially in the 3rd and 4th leaf. The narrowest leaf base was found in the *abp4* mutant (Fig. 2*b*). The examples of the base width in the 2nd, 3rd, and 4th leaves in WT and the mutants are shown on Fig. 2*c*. We also estimated the blade surface in the 2nd, 3rd, and 4th leaves using ImageJ software. Figure 2*d* shows that the greatest blade surface was measured in plants where *ABP1* or both *ABP1* and *ABP4* were knocked out. The single mutant *abp4* showed a blade surface similar to that observed in WT plants with the exception of the 2nd leaf, where the mutant blade surface was distinctly smaller than that measured in the WT plants (Fig. 2*d*).

Defects in *ABP1* and (or) *ABP4* cause changes in the development of young maize seedlings in darkness or light

The effect of light on plant growth is extremely evident in seedlings in the early stages of development. Based on the differential phenotypes of *abp* mutants and WT in the greenhouse, we determined the phenotypes of WT and mutant seedlings developed in Magenta boxes on the BM 5 days after kernel germination (Fig. 3). The single mutant *abp1* grown in D developed a coleoptile similar to that of the WT seedlings, whereas in *abp4* and the double mutant the coleoptile was about 20%–30% shorter than the WT plant (Fig. 3*a*). Different from the etiolated plants, mutations in *ABP1* and *ABP4* only slightly affected elongation of coleoptiles in seedlings developed under BL and had no effect on the coleoptile elongation in plants grown in RL (Fig. 3*a*).

Whereas the etiolated seedlings of single mutants *abp1* and *abp4* did not show distinct differences in the mesocotyl length compared with WT, the double mutant developed mesocotyls significantly shorter than that observed in WT (Fig. 3*b*). Whatever the genotype, mesocotyls grown in BL were much shorter in comparison with the etiolated organs, and the lengths of BL-grown mesocotyls were comparable to WT and mutant seedlings. RL also strongly inhibited the mesocotyl elongation in all genotypes. However, the knockout of the *ABP4* gene led to the development of a significantly longer mesocotyl than in WT, *abp1*, and the double mutant (Fig. 3*b*).

Defects in *ABP1* and (or) *ABP4* also had an impact on the length of the primary root (Fig. 3*c*). In etiolated seedlings, loss of function in *ABP1* or *ABP4* resulted in a significant reduction in the primary root growth. Notably, the double mutation caused development of a primary root almost half the length of the one observed in WT. The growth of the primary root in WT was reduced in BL by ~35%, whereas in single mutants BL did not have an inhibitory effect on root elongation. Compared with WT, the *abp1* root in BL was even longer. The length of the primary roots in BL-grown *abp4* seedlings was similar to those developed in WT plants, whereas the lack of both genes led to the development of significantly shorter primary roots than observed in WT plants. Primary roots of WT seedlings developed under RL were about 30% shorter than in etiolated plants. RL did not inhibit the root growth in single or double mutants but roots in *abp1* had a tendency to be longer (no significant difference was observed) than the primary roots in WT. In *abp4* and the

Fig. 3. Comparison of seedling growth in single maize mutants *abp1* and *abp4*, double mutant *abp1abp4*, and corresponding wild type (WT) in response to darkness and light. Elongation of the (*a*) coleoptile, (*b*) mesocotyl, and (*c*) primary root was measured with a ruler to the nearest millimetre in 5-day-old seedlings grown in Magenta boxes on the BM in dark (D), blue light (BL), or red light (RL) conditions. The results are the mean length ± SE obtained from 5 to 12 independent experiments. In each genotype, six to nine seedlings were measured in every experiment. * and ** indicate significant differences (*t*-test; $P \leq 0.05$ and $P \leq 0.01$, respectively) from WT in D; letters a, b indicate significant differences (*t*-test; $P \leq 0.01$ and $P \leq 0.05$, respectively) from dark-grown seedlings of the same genotype; c indicates a significant difference (*t*-test; $P \leq 0.05$) from WT in BL; d indicates a significant difference (*t*-test; $P \leq 0.05$) from WT in RL.

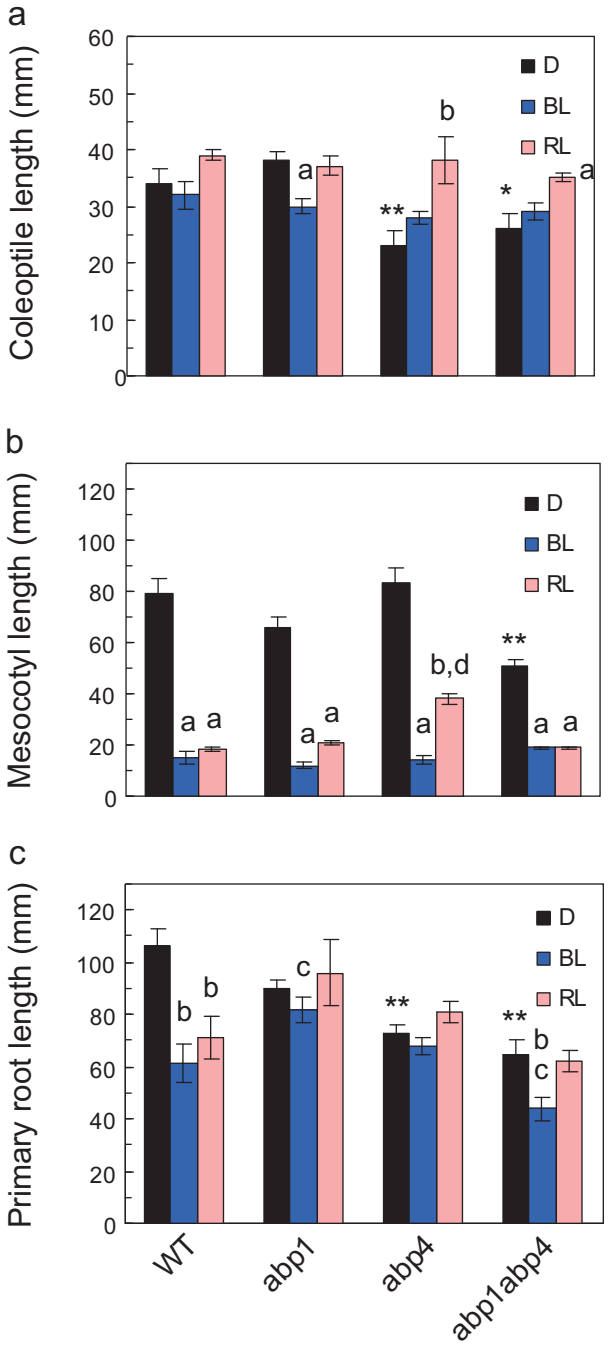

Fig. 4. Comparison of mesocotyl diameter in single maize mutants *abp1* and *abp4*, double mutant *abp1abp4*, and corresponding wild type (WT) seedlings grown in Magenta boxes in darkness. (*a*) Mesocotyl cross-section microphotograps (Scale bar = 200 μm). (*b*) Diameter of cortical cells in etiolated mesocotyls of the WT and *abp* mutants. The values represent the mean ± SE obtained by measurement of cells in five cross-section microphotographs for each genotype tested. In each cross-section, the diameter of ~70 randomly selected cortical cells was measured. Values with different letters are significantly different (*t*-test; $P \leq 0.05$) from each other.

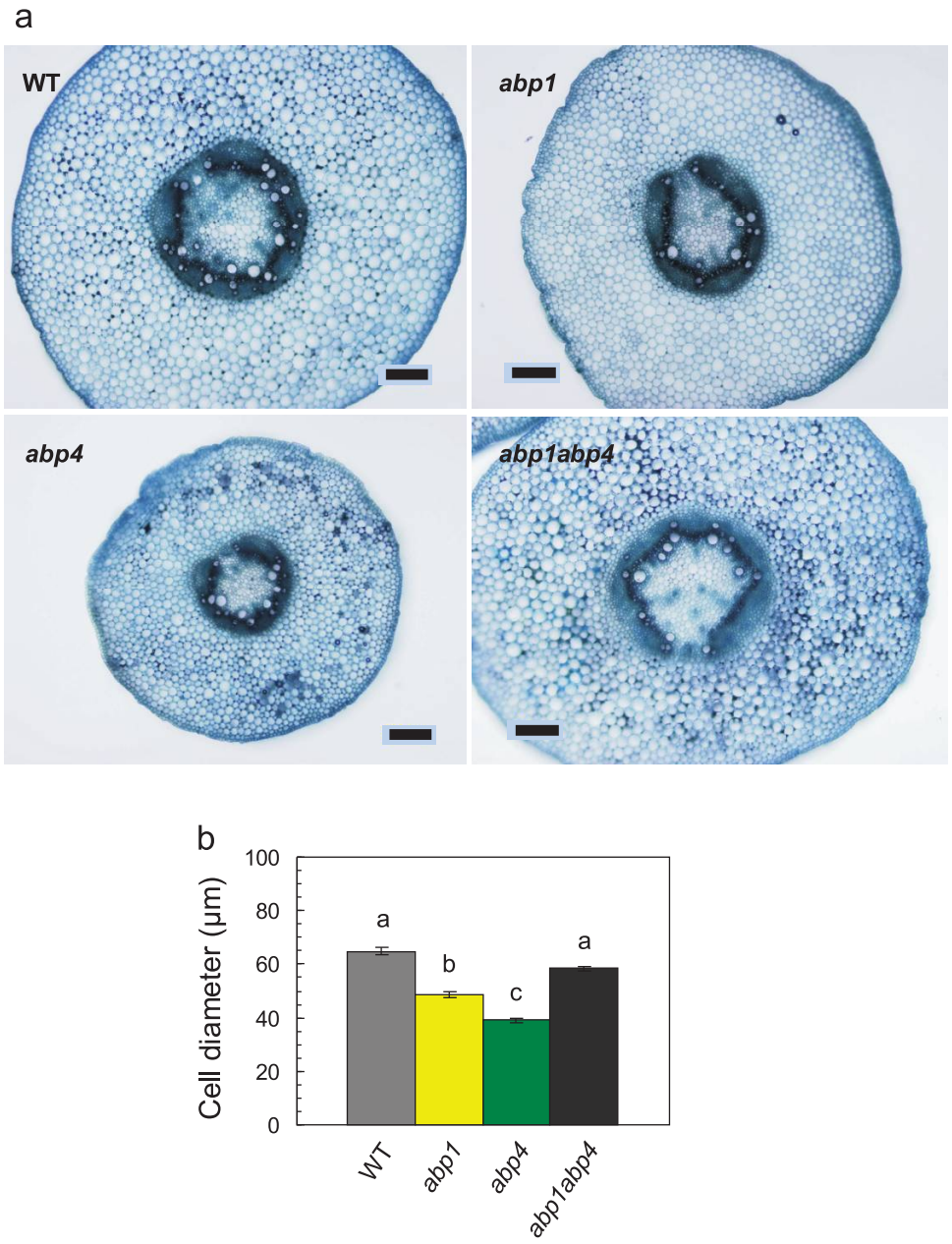

double mutant *abp1abp4*, primary roots were of a length similar to those observed in WT plants (Fig. 3*c*).

In etiolated mesocotyls, the mutation in *ABP1* or *ABP4* affected the cell size. Figure 4*a* shows the microphotography of the mesocotyl cross-sections stained with methylene blue dye. It is manifested that in single mutants, the cells in all rows are essentially smaller in radial direction than the cells of WT plants. Interestingly, cell expansion was not significantly affected in the double mutant. As shown in Fig. 4*b*, a reduced mesocotyl diameter in single mutants *abp1* and *abp4* corresponded with the reduced diameter of cortical cells. It is also evident that the loss of function in *ABP1* or *ABP4* does not affect cell division, as the number of cells was the same in WT and mutant plants (Fig. 4*a*).

Elimination of the *ABP1* and (or) *ABP4* gene alters seedling growth responses to NAA

We previously reported that exogenous auxin reduces the elongation of the etiolated maize coleoptile, mesocotyl, and primary roots in intact maize hybrid seedlings (Fellner et al. 2003, 2006). We also revealed that the etiolated seedlings of modern maize hybrids with reduced expression of the *ABP4* gene showed reduced auxin-induced responses (Fellner et al. 2006). To determine the role of ABP1 and ABP4 in seedling

Fig. 5. Elongation of the coleoptile, mesocotyl, and primary root in 5-day-old wild type (WT) and *abp* mutants in maize grown in vitro on the BM in the absence or presence of auxin 1-naphthalene acetic acid (NAA; 10^{-6} to 10^{-4} mol·L^{-1}), in dark (D), blue light (BL), or red light (RL) conditions. Dose-response curves of the (*a*) etiolated coleoptile growth, (*c*) etiolated mesocotyl growth, and (*e*) primary root growth. For each genotype and condition, the organ length in six to nine seedlings was measured in every experiment. The values represent the mean organ length ± SE obtained from 5 to 12 independent experiments. NAA-induced growth inhibition of the (*b*) coleoptile, (*d*) mesocotyl, and (*f*) primary root in seedlings developed in D, BL, or RL at an auxin concentration of 5×10^{-5} mol·L^{-1}. The values are the mean growth inhibition ± SE calculated from the mean values in 5 to 12 independent experiments. $^{+}$, *, and ** indicate significant differences (*t* - test; $P \leq 0.1$, $P \leq 0.05$ and $P \leq 0.01$, respectively) from WT in D; letters a, b indicate significant differences (*t*-test; $P \leq 0.01$ and $P \leq 0.05$, respectively) from dark-grown seedlings of the same genotype; c indicates a significant difference (*t*-test; $P \leq 0.01$ or 0.05) from WT in BL; d indicates a significant difference (*t*-test; $P \leq 0.05$) from WT in RL; e indicates a significant difference (*t*-test; $P \leq 0.1$) from *abp1abp4* in RL.

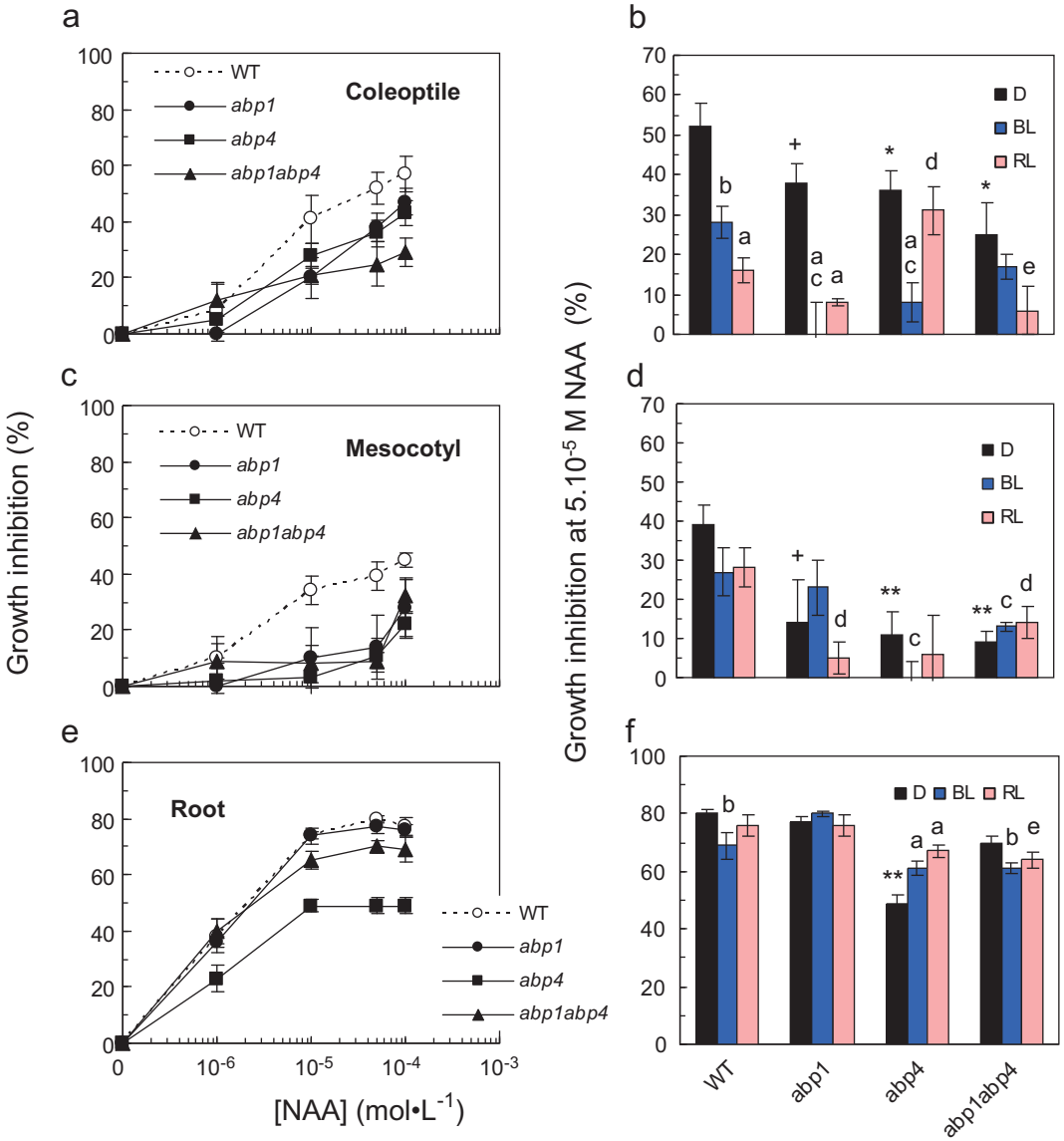

responses to auxin, we studied the effect of the auxin NAA on the growth of *abp* mutants in D. The elongation of the coleoptile in etiolated seedlings of all genotypes was gradually inhibited by auxin in a concentration-dependent manner. However, as shown in Fig. 5*a*, the inhibition of the coleoptile growth was essentially greater in WT plants than in all *abp* mutants. Except for the lowest auxin concentration tested, the double mutant showed half of the reduction of the coleoptile growth by NAA compared with the inhibition observed in WT plants. For example, the coleoptile growth in WT at the concentration 5×10^{-5} mol·L^{-1} NAA was inhibited by ~50%, whereas in the double mutant the inhibition reached ~25% (Fig. 5*b*).

Earlier we revealed that the modern hybrids respond less than the old hybrids to light (Fellner et al. 2003, 2006). To determine the role of ABP1 and ABP4 in possible auxin-light cross-talk we further characterized the growth response of the *abp* mutants in the presence of auxin in BL or RL conditions. WT coleoptiles developed under BL or RL were essentially less inhibited by NAA than the coleopiles grown in D. For a clearer demonstration of the light effects on the coleoptile responsiveness to auxin, the data obtained for the growth

of seedlings in BL and RL are shown in percentage of inhibition by NAA at the concentration 5×10^{-5} mol·L^{-1} (Figs. 5*b*, 5*d*, 5*f*), and similar results were obtained for the other auxin concentrations tested (data not shown). The figure shows that in BL, NAA inhibited the coleoptile growth in WT by ~28% and in RL by ~16%, i.e., two and three times less, respectively, than in D (50%). The figures further show that in BL, the coleoptile responsiveness to NAA of the single mutants *abp1* and *abp4* was significantly less than in WT, whereas BL-grown seedlings of the double mutant responded to NAA similar to WT plants. Under RL, *abp1* and the double mutant showed very low responsiveness to auxin similar to that in WT. Interestingly, the knockout of the *ABP4* gene resulted in a high sensitivity to the auxin of the coleoptile developed in RL (Fig. 5*b*), i.e., similar to that observed for coleoptiles in etiolated mutant plants.

Exogenous auxin inhibited the elongation of etiolated WT and *abp* mesocotyls in a concentration-dependent manner, and again, a stronger response to exogenous auxin was observed for the WT seedlings (Fig. 5*c*). Auxin-induced inhibition of the WT mesocotyl growth was only slightly reduced by BL or RL. Except for *abp1*, the percentage of growth inhibition by NAA in *abp4* and double mutant mesocotyls in BL was distinctly less than in WT. In addition, the RL-grown mesocotyls of all the mutants were markedly less responsive to auxin than in WT plants (Fig. 5*d*).

The strongest inhibition of growth by exogenous auxin was observed in the primary roots (Fig. 5*e*). Etiolated WT, *abp1*, and double mutants showed similar responsiveness to NAA (70%–80% at concentrations from 10^{-5} to 10^{-4} mol·L^{-1}), whereas etiolated roots in *abp4* mutants were distinctly less inhibited by auxin in all the concentrations tested. BL and RL slightly decreased (in WT and double mutant), increased (in *abp4*), or did not essentially influence (in *abp1*) the primary root responsiveness to NAA (Fig. 5*f*). A similar trend was observed at all higher auxin concentrations tested (data not shown).

Knockout of *ABP1* and (or) *ABP4* has a strong impact on the levels of endogenous auxin

Differential responsiveness of WT and *abp* mutants to exogenous auxin could reflect a differential level of endogenous auxin. This led us to examine the amounts of free endogenous IAA in all experimental genotypes. Free IAA was analyzed in 5-day-old coleoptiles, mesocotyls, and primary roots of seedlings grown in D, BL, or RL conditions.

In etiolated coleoptiles, mutation in the *ABP1* or *ABP4* gene did not result in any essential change in the accumulation of free IAA. However, a twofold augmentation of free IAA was observed in etiolated coleoptiles of the double mutant (Fig. 6*a*). In WT, *abp1*, and double mutants, the amount of IAA in the coleoptiles was markedly reduced in seedlings grown in BL compared with those grown in D. Of note was that the reduction was not significant in seedlings with the *ABP4* gene knocked out. In these cases the auxin level was similar to that observed in the etiolated coleoptiles. RL distinctly reduced the accumulation of free IAA in the coleoptile and the amount of auxin was similar in WT and *abp* mutants (Fig. 6*a*).

In etiolated seedlings, mesocotyls of WT and *abp* mutants accumulated a similar amount of free IAA and no matter the

Fig. 6. Level of free indole-3-acetic acid (IAA) in (*a*) coleoptiles, (*b*) mesocotyls, and (*c*) primary roots of 5-day-old seedlings of wild type (WT) and *abp* mutants developed in Magenta boxes on the BM in dark (D), blue light (BL), or red light (RL) conditions. Auxin analysis was performed using an immunoaffinity column with an immobilized polyspecific rabbit polyclonal antibody against IAA. The final analysis was performed by HPLC coupled to MS/MS detection with the use of a triple quadrupole mass spectrometer. The data represent mean ± SE obtained from three independent replicates. $^{+}$ and ** indicate significant differences (*t*-test; $P \leq 0.1$ and $P \leq 0.01$, respectively) from WT in D; letters a, b indicate significant differences (*t*-test; $P \leq 0.01$ and $P \leq 0.05$, respectively) from dark-grown seedlings of the same genotype; c, d indicate significant differences (*t*-test; $P \leq 0.01$ and $P \leq 0.05$) from WT in BL; e indicates a significant difference (*t*-test; $P \leq 0.05$) from WT in RL.

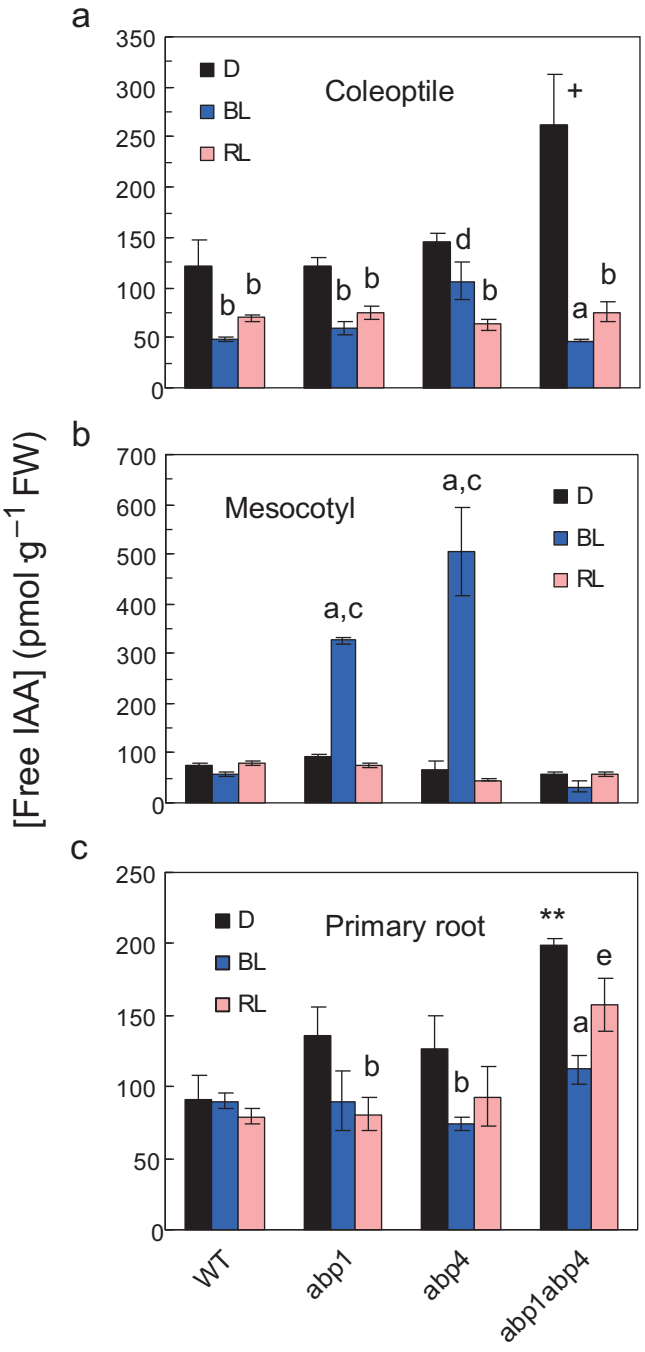

Fig. 7. Growth responses of the maize *elm1* mutant and corresponding wild type (WT; B73) cultured in dark (D), blue light (BL), and red light (RL) conditions on the BM, some of which were supplemented with 1-naphthalene acetic acid (NAA; 5×10^{-5} mol·L^{-1}). The effect of BL or RL on the elongation of etiolated (*a*) coleoptiles and (*c*) mesocotyls are shown. The values are the mean length ± SE from six independent experiments, with six to nine plants measured in every experiment in each of the light conditions. The growth inhibition of the (*b*) coleoptile and (*d*) mesocotyl in seedlings was developed in D, BL, or RL conditions on the BM, supplemented with NAA (5×10^{-5} mol·L^{-1}). The values are the mean growth inhibition ± SE calculated from the mean values in six independent experiments. The letter a represents a significant difference (*t*-test; $P \leq 0.05$) from B73 in D.

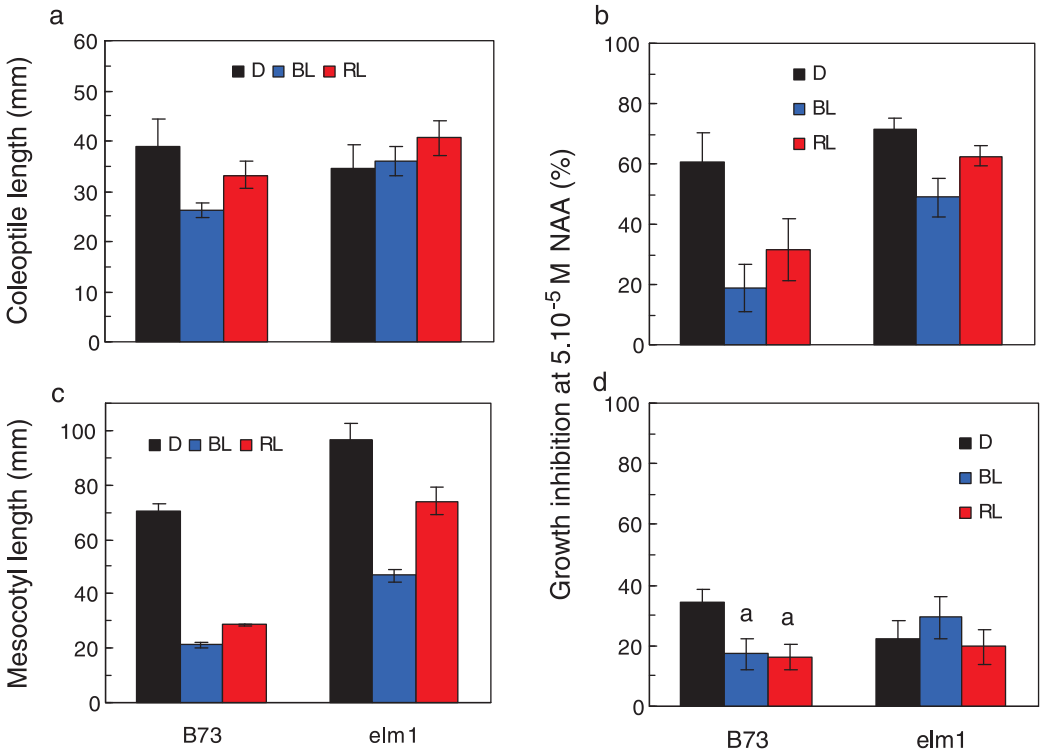

genotype, RL had a negligible effect on the auxin content. Interestingly, the loss of function in the *ABP1* or *ABP4* gene led to a dramatic increase of IAA amounts in mesocotyls of seedlings developed under BL. Even though the single mutants exhibited changes in IAA amounts, the double mutant grown in BL accumulated a similar amount of IAA to the WT in their mesocotyls (Fig. 6*b*).

Knockout of the *ABP1* or *ABP4* gene led to a slight (not significant) increase of IAA content in the primary roots of etiolated seedlings. However, when both genes were switched off the IAA amount was two times higher than in WT roots (Fig. 6*c*). In the primary roots of WT seedlings grown under BL or RL, the amount of free IAA was found to be similar to that in etiolated roots. In comparison to WT roots, the mutation in both genes led to a minor (not significant) augmentation of IAA in BL-grown roots and to a distinct increase of auxin amounts in primary roots of seedlings developed in RL (Fig. 6*c*).

The phytochrome-deficient mutant *elm1* shows light-dependent super-sensitivity to exogenous auxin

We showed that in WT seedlings BL and RL reduced the inhibitory effect of exogenous auxin on the coleoptile elongation (Fig. 5*b*). We also revealed that coleoptiles of *abp4* mutants developed in RL were super-sensitive to the inhibitory effect of exogenous auxin (Fig. 5*b*). The data indicated that functional ABP4 could be an element or a target of the RL signaling pathway, leading to the loss or reduction of the sensitivity to exogenous auxin of the coleoptile. To test the hypothesis if phytochromes are involved in this response, we investigated the phytochrome-deficient mutant *elm1* in maize for its sensitivity to exogenous auxin. On the BM, etiolated seedlings of WT and *elm1* mutants developed coleoptiles of similar length, and BL- or RL-induced de-etiolation of coleoptiles was less evident in *elm1* than in WT plants (Fig. 7*a*). In D, NAA inhibited the coleoptile elongation in a concentration-dependent manner in both genotypes. The inhibition of the coleoptile growth is shown in Fig. 7*b* for the concentration 5×10^{-5} mol·L^{-1}. In BL and RL, auxin inhibited the coleoptile growth in B73 significantly less than in D. However, the responsiveness of the *elm1* coleoptile to auxin in BL and RL was comparable to that observed in the etiolated coleoptile (Fig. 7*b*). In the absence of NAA, BL and RL inhibited the mesocotyl growth in *elm1* essentially less than in B73 (Fig. 7*c*). When seedlings grew in the presence of NAA, the inhibition of mesocotyl elongation in B73 was much less in BL and RL compared with the etiolated plants. In contrast, auxin inhibited mesocotyl growth in *elm1* in the same manner as in D, BL, or RL conditions (Fig. 7*d*).

Discussion

In *Arabidopsis*, the sole *ABP* gene, *ABP1*, was identified (Palme et al. 1992), and its knockout resulted in an arrest of seedling development at the globular stage of the embryo

(Chen et al. 2001). Different from *Arabidopsis*, the maize ABP family contains at least five closely related members (Hesse et al. 1989; Schwob et al. 1993). It was reported that two available loss-of-function mutants in *ABP1* and *ABP4* genes do not show a distinct phenotype (Im et al. 2000), suggesting a functional redundancy in maize. We previously reported that the *abp1* and *abp4* mutants develop more erect and more horizontal leaves, respectively, than corresponding WT plants (Fellner et al. 2006). Our results therefore suggest that ABP1 and ABP4 play an important role in the development of maize leaf declination. The aim of this study was to characterize the phenotype of maize *abp* mutants with more detail to indicate other possible roles of ABPs in the growth and development of maize plants. In addition, based on our previous work (Fellner et al. 2003, 2006), we investigated whether defects in *ABP1* and *ABP4* genes may affect light- and auxin-mediated changes in the growth of maize seedlings.

ABPs control different aspects of the maize plant architecture

Our experiments on leaf declination in plants grown in the greenhouse support our previous data obtained in growth chamber conditions (Fellner et al. 2006), i.e., *abp1* mutants develop more erect, whereas *abp4* less erect, leaves than WT plants. Im et al. (2000) previously reported that knockout of *ABP4* results in a dramatic increase of ABP1 level. We did not analyze the accumulation of ABP1. However, in agreement with the results of Im and co-authors, our data suggest that functional *ABP4* may negatively regulate ABP1, which would positively mediate leaf angle development. Thus, the *abp4* phenotype reflects the overproduction of the ABP1 protein. The absence of ABP1 and ABP4 transcripts in the double mutant resulted in expectation of a leaf angle similar to *abp1* or even smaller. However, the opposite occurred with leaves in the double mutant showing a big declination similar to that in the *abp4* mutants, and thus suggesting that the simultaneous knockout of *ABP1* and *ABP4* triggers substitute pathway(s) for maintaining development of leaf declination. These pathways may include the involvement of other members of the ABP family (Schwob et al. 1993) or, of course, other signaling elements.

Phenotypic analyses of *abp* mutants further revealed that ABP1 and (or) ABP4 control the elongation and the lateral growth of the leaf blade and therefore the final blade surface. Based on our results, it seems that later in the plant development, ABP1 or ABP4 positively influences blade elongation, but simultaneously they reduce the activity of each other in this growth response. The WT phenotype of the double mutant knockout of *ABP1* and *ABP4* thus confirms the phenotype expectation above (see Results). The phenotypes of single mutants further indicate that the functional ABP1 keeps leaf blades narrower, while a positive role of ABP4 in the blades lateral growth cannot be excluded. The phenotype of the double mutant then indicate that when both genes are knocked out, an alternative and even stronger pathway may assure blade growth. Altogether, the model in Fig. 8 proposes that the functional ABP1 is positively involved in leaf declination and blade elongation but negatively regulates lateral blade growth. We further suggest that ABP4 reduces the activity of ABP1 in all these growth processes, and that for blade elongation ABP1 may suppress the activity of ABP4.

Fig. 8. A working model showing the effect of ABP1 and ABP4 on the development of the leaf angle and the growth of the leaf blade. We propose that ABP1 is positively involved in the leaf angle development and blade elongation, and it negatively contributes to lateral blade growth. ABP4 then seems to play a negative role in leaf declination, whereas it contributes positively to blade elongation and likely in lateral blade growth. Simultaneously, it seems that in all the growth responses tested, ABP4 (or *ABP4*) suppress the activity of ABP1, whereas for blade elongation, ABP1 (or *ABP1*) suppress the activity of ABP4. The arrows and T-bars represent positive and negative effects, respectively.

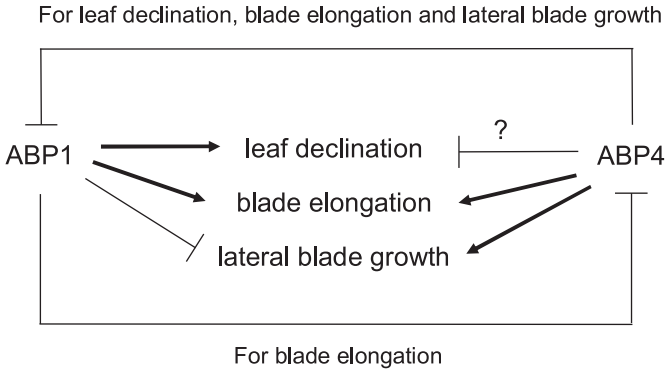

ABPs regulate development of maize seedlings differentially in darkness and light

Our experiments on adult mutants suggested that ABP1 and ABP4 are involved in maize leaf growth. We therefore investigated whether the ABPs control the development of seedlings. Our results indicate that ABP1 and (or) ABP4 are involved in the growth of maize seedlings, and that their effects and functional relationship are organ- and light-dependent (Table 1). First, our analysis of mutant seedlings suggests that ABP4, but not ABP1, is required for the growth of the etiolated coleoptile. The short coleoptile in the double mutant *abp1abp4* supports this idea. Since the loss of function of *ABP1* and (or) *ABP4* genes had no significant effect on the coleoptile growth in BL or RL, we conclude that for growth of the coleoptile in light conditions, functional ABP1 and ABP4 are not essential.

The development of a markedly shorter etiolated mesocotyl in double but not in single mutants indicates the requirement of both ABP1 and ABP4 during the elongation of the etiolated mesocotyl and suggests that ABP1 and ABP4 may substitute for each other. Our results further indicate that these genes are not essential for the BL-induced mesocotyl de-etiolation. In RL, the defect in *ABP1* does not influence the mesocotyl growth, whereas the mesocotyl of *ABP4* knockout plants was twice as long as in the WT. Considering that the *abp4* mutant contains high levels of the ABP1 protein (Im et al. 2000) even in RL, our data indicate that ABP1 has a positive effect on the mesocotyl elongation, whereas the direct effect of ABP4 remains obscure. Our results may support the hypothesis of Jones et al. (1991) that the RL-induced inhibition of the mesocotyl growth could be partially caused by the RL-induced reduction of ABP1 abundance. The normal mesocotyl elongation in the double mutant *abp1abp4* grown in BL or RL leads to the conclusion that in the light

Table 1. Proposed functions of ABP1 and ABP4 during growth of maize seedlings cultured for 5 days in sterile conditions in the Magenta boxes in dark (D), blue light (BL), or red light (RL) conditions.

Measured response	Light condition	Effect of ABP1 and (or) ABP4
Coleoptile		
Elongation	D	ABP4(+)
	BL	x
	RL	x
IAA accumulation	D	ABP1(–), ABP4 (–)*
	BL	ABP1(+), ABP4 (?)
	RL	x
Mesocotyl		
Elongation	D	ABP1(+), ABP4 (+)*
	BL	x
	RL	ABP1(+), ABP4 (?)
IAA accumulation	D	x
	BL	ABP1(+), ABP4 (+)■
	RL	x
Cell size	D	ABP1(–), ABP4 (–)
Primary root		
Elongation	D	ABP4(+)
	BL	ABP4(+)■
	RL	ABP4(+)■
IAA accumulation	D	ABP1(–), ABP4 (–)*
	BL	x
	RL	ABP1(–), ABP4 (–)*

Note: x, indicates no involvement of ABP1 or ABP4; +, a positive effect; –, a negative effect; *, a substitution for each other; ■, where ABP1 (*ABP1*) affects negativey ABP4. Based on Im et al. (2000) post-transcriptional activation of ABP1 by *ABP4* is assumed in all the responses measured.

Table 2. Proposed involvement of ABP1 and ABP4 in NAA-induced inhibition of maize seedlings cultured for 5 days in sterile conditions in the Magenta boxes in dark (D), blue light (BL), or red light (RL) conditions.

Measured response	Light condition	Effect of ABP1 and (or) ABP4
Coleoptile		
Growth inhibition	D	ABP1(?), ABP4 (+)
	BL	ABP1(+), ABP4 (+)
	RL	ABP1(+)
Mesocotyl		
Growth inhibition	D	ABP1(?), ABP4 (+)
	BL	ABP4(+)
	RL	ABP1(+), ABP4 (+)
Primary root		
Growth inhibition	D	ABP4(+)
	BL	x
	RL	x

Note: x, indicates no involvement of ABP1 or ABP4; +, a positive effect; –, a negative effect. Based on Im et al. (2000) post-transcriptional activation of ABP1 by the *ABP4* is assumed in all the responses measured.

the elimination of both *ABP1* and *ABP4* triggers an alternative pathway regulating the mesocotyl growth.

The knockout of the *ABP4* gene causes the reduction of the primary root length in etiolated single mutants and even more in the double mutant, whereas the knockout of ABP1 only weakly affect the root growth. The data suggest that ABP4 is preferentially involved in the stimulation of the elongation of the etiolated primary root. Contrary to *Arabidopsis*, in maize seedlings BL or RL inhibits primary root elongation. Our results show that the knockout of *ABP1* enables roots to grow significantly more in BL (and RL, but insignificantly), whereas the knockout of *ABP4* results in normal (WT-like) root growth. It therefore seems that especially in BL, ABP1 itself has no effect on the root elongation but it suppresses the promoting effect of ABP4 on this growth response. The fact that in BL and RL the primary root of the double mutant grew more or less similar to WT just confirms this conclusion (expected phenotype, see Results).

The knockout of *ABP1*, but especially the lack of the *ABP4* gene, causes a reduction of the radial expansion of cells of all types in the etiolated mesocotyl (Fig. 4). This indicates that ABP1 and ABP4 are negatively involved in the mesocotyl cell enlargement but also that both proteins may belong to a regulatory loop, affecting their mutual activity. Therefore, as expected (see Results), the double mutant *abp1abp4* shows WT phenotype.

Knockout of *ABP1* and (or) *ABP4* affects the accumulation of endogenous auxin in maize seedlings

Analysis of the endogenous auxin revealed that functional ABP1 and ABP4 are, depending on the organ and light conditions, involved in the accumulation of free endogenous IAA (Table 1). Based on our measurements, we suggest that in the etiolated coleoptile, functional ABP1 and ABP4 reduce the level of endogenous IAA and that they likely substitute for each other in the maintenance of the normal (WT-like) level of IAA. We further deduce that in BL conditions, the level of endogenous IAA in the coleoptile is positively controlled by ABP1, whereas the role of ABP4 remains unclear. Finally, the level of IAA in RL-developed coleoptile does not seem to be controlled by ABP1 nor ABP4. It further seems that in the mesocotyl, the level of IAA is positively regulated mainly via ABP1 (or possibly via ABP4) only in seedlings developed in BL conditions, while ABP1 and ABP4 suppress each other's activity (Fig. 6*b*). This is supported by the expected WT level of IAA in the mesocotyl of the double mutant developed in BL. Levels of IAA in the primary roots in D and RL conditions seem to be regulated similarly as observed in etiolated coleoptiles. It does not appear likely that ABPs regulate the IAA levels in roots developed in BL.

Growth responses of loss-of-function mutants indicate that ABP1 and ABP4 are involved in maize seedling responses to exogenous auxin

The concentration of and sensitivity to hormones is the controlling aspect of hormone action (Davies 1995). To better understand the role of ABP1 and ABP4 in the auxin- and light-regulated growth of maize seedlings, we analyzed, in addition to the amounts of endogenous free IAA, the sensitivity (responsiveness) of maize seedlings to auxin NAA in various organs of the seedlings reacting to light conditions. The study of intact seedling responses to exogenous auxin (often roots) became one of the methods for the selection of various mutants affected in auxin physiology (e.g., Maher and Bell 1990; de Souza and King 1991; reviewed in Fellner 1999). Therefore, the testing of plant responses to exogenous auxin is one of the appropriate methods for the investigation of auxin-regulated growth and development. It is not still fully understood why exogenous auxin, in contrast to endogenous auxin, inhibits elongation growth in various plant species. It is expected that the mechanism of this auxin effect is quite complex and may involve for example, cross-talk between various hormones (Ephritikhine et al. 1999). However, one of the proposed mechanisms is that the application of exogenous auxin results in a supraoptimal concentration of auxin in the tissues that results in the inhibition of elongation (Hasenstein and Evans 1988). In agreement with this, we clearly have shown that the etiolated WT coleoptile, with a high level of free IAA, is sensitive to the inhibitory effect of NAA much more than light-developed coleoptiles, which contain significantly less free IAA when compared with coleoptiles of etiolated seedlings (Fig. 5*a*). In the mesocotyl and primary root, the levels of endogenous IAA was not significantly altered by BL or RL. In agreement with that, the sensitivity of the organs did not change much in BL or RL (Figs. 5*b*, 5*c*).

Our experiments further showed that etiolated coleoptiles and mesocotyls of the single mutants partially lost their responsiveness to exogenous auxin, and the responsiveness to NAA in the double mutant was the lowest. The data indicate that the ABP1 and ABP4 act together in responsiveness to exogenous auxin. The results suggest that rather than ABP1, ABP4 mediates the growth inhibition of the etiolated maize coleoptile and mesocotyl induced by exogenous auxin (Table 2).

In comparison to the responsiveness in D, the responsiveness of the coleoptile and mesocotyl in light-developed WT seedlings to the inhibitory effect of exogenous auxin was reduced. Using the phytochrome mutant *elm1* in maize, we demonstrated that the effect of BL and RL on the coleoptile and mesocotyl responsiveness to exogenous auxin is mediated at least partially by phytochromes. Our results further suggest that under BL and especially in RL conditions, ABP1 and ABP4 contribute to the responses of coleoptiles to the inhibitory effect of exogenous auxin. Again, this is supported by the expected WT-like responsiveness to NAA of the double mutant. Our results further indicate that in BL the inhibition of the mesocotyl elongation by exogenous auxin is mediated by ABP4 without the essential participation of ABP1, whereas both ABP4 and ABP1 seem to be involved in the mesocotyl responses to exogenous auxin in RL conditions.

A loss of function in the *ABP4* gene, but not in *ABP1*, resulted in decreased sensitivity of the etiolated primary roots to exogenous auxin. The data suggest that auxin-induced inhibition of elongation in the etiolated primary roots is controlled via ABP4. The high responsiveness of the double mutant roots to exogenous auxin indicates that the simultaneous knockout of *ABP1* and *ABP4* results in a substitute pathway that enables the primary root to respond almost fully to exogenous auxin. BL and RL did not essentially affect WT root growth responses to the inhibitory effect of auxin. It indicates that the responsiveness of light-grown roots to exogenous auxin is controlled via ABP1- and ABP4-independent pathways.

In conclusion, we have shown that the loss-of-function mutants in *ABP1* and (or) *ABP4* genes in maize show striking phenotypes. Our results indicate that functional maize ABP1 and ABP4 are involved in the leaf development and growth, and in the elongation of etiolated seedlings. Furthermore, we have shown that ABP1 and (or) ABP4 mediate the responses of etiolated seedlings to exogenous auxin. Results of the analyses of endogenous auxin suggest that in darkness or light the growth capacity of WT and mutant seedlings does not simply correspond with the observed changes in levels of free IAA in coleoptiles, mesocotyls, and primary roots (Table 1). Differentially, the changes in the levels of endogenous IAA in etiolated and light-grown WT seedlings likely influences their responsiveness to exogenous auxin. This confirms that the auxin-regulated growth of maize seedlings

is a complex process and certainly involves the activity of the putative receptors ABPs and endogenous IAA. Here, we further showed that in BL or RL the responsiveness of maize seedlings to exogenous auxin is less than in D, and our data led to the conclusion that the light-induced reduction of the responsiveness to exogenous auxin is mediated at least by phytochromes. Based on our results, we propose that ABP1 and ABP4 cross the phytochrome pathway, and thus they can function as common elements of the light and auxin signaling pathways involved in the development of maize seedlings. However, because our data also showed that the functional relationship between ABP1 and ABP4 is organ- and response-dependent, additional research is required to elucidate the molecular mechanisms of the interaction between light and ABPs in the growth and development of maize plants.

Acknowledgements

We thank Renáta Plotzová, Marie Karlická, Věra Chytilová, and Jan Humplík for their excellent technical assistance. We especially thank Alan M. Jones (University of North Carolina) and Thomas Brutnell (Boyce Thompson Institute for Plant Research) for providing kernels of the maize mutants. We also thank Pamela Lewis for her help in revising the English text. The work was supported by the Ministry of Education of the Czech Republic (grant no. 1P05ME792 to M.F.) and by EU (grant no. MRTN-CT-2006-035833).

References

Abel, S., and Theologis, A. 1996. Early genes and auxin action. Plant Physiol. **111**(1): 9–17. doi:10.1104/pp.111.1.9. PMID:8685277.

Abel, S., Nguyen, M.D., and Theologis, A. 1995. The *PS-IAA4/5*-like family of early auxin-inducible mRNAs in *Arabidopsis thaliana*. J. Mol. Biol. **251**(4): 533–549. doi:10.1006/jmbi.1995.0454. PMID:7658471.

Abramoff, M., Magelhaes, P., and Ram, S. 2004. Image processing with ImageJ. Biophotonics Int. **11**(7): 36–42.

Bandurski, R.S., Schulze, A., and Cohen, J.D. 1977. Photo-regulation of the ratio of ester to free indole-3-acetic acid. Biochem. Biophys. Res. Commun. **79**(4): 1219–1223. doi:10.1016/0006-291X(77)91136-6. PMID:603655.

Barbier-Brygoo, H., Ephritikhine, G., Klämbt, D., Ghislain, M., and Guern, J. 1989. Functional evidence for an auxin receptor at the plasmalemma of tobacco mesophyll protoplasts. Proc. Natl. Acad. Sci. U.S.A. **86**(3): 891–895. doi:10.1073/pnas.86.3.891. PMID:16594015.

Barbier-Brygoo, H., Ephritikhine, G., Klämbt, D., Maurel, C., Palme, K., Schell, J., and Guern, J. 1991. Perception of the auxin signal at the plasma membrane of tobacco mesophyll protoplasts. Plant J. **1**(1): 83–93. doi:10.1111/j.1365-313X.1991.00083.x.

Barker-Bridgers, M., Ribnicky, D.M., Cohen, J.D., and Jones, A.M. 1998. Red-light-regulated growth. Changes in the abundance of indoleacetic acid in the maize (*Zea mays* L.) mesocotyl. Planta, **204**(2): 207–211. doi:10.1007/s004250050248.

Baskin, T.I., Briggs, W.R., and Iino, M. 1986. Can lateral redistribution of auxin account for phototropism of maize coleoptile? Plant Physiol. **81**(1): 306–309. doi:10.1104/pp.81.1.306. PMID:16664796.

Bauer, C.S., Hoth, S., Haga, K., Philippar, K., Aoki, N., and Hedrich, R. 2000. Differential expression and regulation of K^+ channels in the maize coleoptile: molecular and biophysical analysis of cells isolated from cortex and vasculature. Plant J. **24**(2): 139–145. doi:10.1046/j.1365-313X.2000.00844.x. PMID:11069689.

Becker, D., and Hedrich, R. 2002. Channelling auxin action: modulation of ion transport by indole-3-acetic acid. Plant Mol. Biol. **49**(3–4): 349–356. doi:10.1023/A:1015211231864. PMID:12036259.

Bennetzen, J.L. 1996. The contributions of retroelements to plant genome organization, function and evolution. Trends Microbiol. **4**(9): 347–353. doi:10.1016/0966-842X(96)10042-1. PMID:8885169.

Boerjan, W., Cervera, M.T., Delarue, M., Beeckman, T., Dewitte, W., Bellini, C., Caboche, M., Van Onckelen, H., Van Montagu, M., and Inzé, D. 1995. *superroot*, a recessive mutation in Arabidopsis, confers auxin overproduction. Plant Cell, **7**(9): 1405–1419. doi:10.1105/tpc.7.9.1405. PMID:8589625.

Braun, N., Wyrzykowska, J., Muller, P., David, K., Couch, D., Perrot-Rechenmann, C., and Fleming, A.J. 2008. Conditional repression of AUXIN BINDING PROTEIN1 reveals that it coordinates cell division and cell expansion during postembryonic shoot development in *Arabidopsis* and tobacco. Plant Cell, **20**(10): 2746–2762. doi:10.1105/tpc.108.059048. PMID:18952781.

Briggs, W.R. 1963. Red light, auxin relationships, and the phototropic responses of corn and oat coleoptiles. Am. J. Bot. **50**(2): 196–207. doi:10.2307/2439853.

Chen, J.G., Ullah, H., Young, J.C., Sussman, M.R., and Jones, A.M. 2001. ABP1 is required for organized cell elongation and division in *Arabidopsis* embryogenesis. Genes Dev. **15**(7): 902–911. doi:10.1101/gad.866201. PMID:11297513.

Claussen, M., Lüthe, H., Blatt, M., and Böttger, M. 1998. Auxin-induced growth and its linkage to potassium channels. Planta, **201**(2): 227–234. doi:10.1007/BF01007708.

Cleland, R.E., Buckley, G., Nowbar, S., Lew, N.M., Stinemetz, C., Evans, M.L., and Rayle, D.L. 1991. The pH profile for acid-induced elongation of coleoptile and epicotyl sections is consistent with the acid-growth theory. Planta, **186**(1): 70–74. doi:10.1007/BF00201499. PMID:11538124.

David, K.M., Couch, D., Braun, N., Brown, S., Grosclaude, J., and Perrot-Rechenmann, C. 2007. The auxin-binding protein 1 is essential for the control of cell cycle. Plant J. **50**(2): 197–206. doi:10.1111/j.1365-313X.2007.03038.x. PMID:17376160.

Davies, P.J. 1995. The plant hormone concept: concentration, sensitivity and transport. *In* Plant hormones: biosynthesis, signal transduction and action! *Edited by* P.J. Davies. Kluwer Academic Publisher, Dordrecht, the Netherlands. pp. 13–38. [ISBN: 978-0792329855.]

Davies, P.J. 2004. Plant hormones: physiology, biochemistry and molecular biology. Kluwer Academic Publishers, Dordrecht, the Netherlands.

de Souza, L., and King, P.J. 1991. Mutants of *Nicotiana plumbaginifolia* with increased sensitivity to auxin. Mol. Gen. Genet. **231**(1): 65–75. doi:10.1007/BF00293823. PMID:1836527.

Devlin, P.F., Yanovsky, M.J., and Kay, S.A. 2003. A genomic analysis of the shade avoidance response in *Arabidopsis*. Plant Physiol. **133**(4): 1617–1629. doi:10.1104/pp.103.034397. PMID:14645734.

Dubois, P.G., Olsefski, G.T., Flint-Garcia, S., Setter, T.L., Hoekenga, O.A., and Brutnell, T.P. 2010. Physiological and genetic characterization of end-of-day far-red light response in maize seedlings. Plant Physiol. **154**(1): 173–186. doi:10.1104/pp.110.159830. PMID:20668057.

Effendi, Y., Rietz, S., Fischer, U., and Scherer, G.F.E. 2011. The heterozygous *abp1/ABP1* insertional mutant has defects in functions requiring polar auxin transport and in regulation of

early auxin-regulated genes. Plant J. **65**(2): 282–294. doi:10.1111/j.1365-313X.2010.04420.x. PMID:21223392.

Ephritikhine, G., Barbier-Brygoo, H., Muller, J.-F., and Guern, J. 1987. Auxin effect on the transmembrane potential difference of wild-type and mutant tobacco protoplasts exhibiting a differential sensitiity to auxin. Plant Physiol. **83**(4): 801–804. doi:10.1104/pp.83.4.801. PMID:16665342.

Ephritikhine, G., Fellner, M., Vannini, C., Lapous, D., and Barbier-Brygoo, H. 1999. The *sax1* dwarf mutant of *Arabidopsis thaliana* shows altered sensitivity of growth responses to abscisic acid, auxin, gibberellins and ethylene and is partially rescued by exogenous brassinosteroid. Plant J. **18**(3): 303–314. doi:10.1046/j.1365-313X.1999.00454.x. PMID:10377995.

Epstein, E., Cohen, J.D., and Bandurski, R.S. 1980. Concentration and metabolic turnover of indoles in germinating kernels of *Zea mays* L. Plant Physiol. **65**(3): 415–421. doi:10.1104/pp.65.3.415. PMID:16661204.

Fellner, M. 1999. Research on mechanisms of auxin action: isolation and characterization of auxin-related mutants. *In* Advances in regulation of plant growth and development. *Edited by* M. Strnad, P. Peč, and E. Beck. Peres Publishers, Prague. pp. 139–156. [ISBN: 80-86360-06-7.]

Fellner, M., Ephritikhine, G., Barbier-Brygoo, H., and Guern, J. 1996. An antibody raised to a maize auxin-binding protein has inhibitory effects on cell division of tobacco mesophyll protoplasts. Plant Physiol. Biochem. **34**(1): 133–138.

Fellner, M., Horton, L.A., Cocke, A.E., Stephens, N.R., Ford, E.D., and Van Volkenburgh, E. 2003. Light interacts with auxin during leaf elongation and leaf angle development in young corn seedlings. Planta, **216**(3): 366–376. PMID:12520327.

Fellner, M., Ford, E.D., and Van Volkenburgh, E. 2006. Development of erect leaves in a modern maize hybrid is associated with reduced responsiveness to auxin and light of young seedlings in vitro. Plant Signal. Behav. **1**(4): 201–211. doi:10.4161/psb.1.4.3106. PMID:19521486.

Friml, J., Wisniewska, J., Benkova, E., Mendgen, K., and Palme, K. 2002. Lateral relocation of auxin efflux regulator PIN3 mediates tropism in *Arabidopsis*. Nature, **415**(6873): 806–809. doi:10.1038/415806a. PMID:11845211.

Goldsmith, M.H.M. 1977. The polar transport of auxin. Annu. Rev. Plant Physiol. **28**(1): 439–478. doi:10.1146/annurev.pp.28.060177.002255.

Haga, K., and Iino, M. 1998. Auxin-growth relationships in maize coleoptiles and pea internodes and control by auxin of the tissue sensitivity to auxin. Plant Physiol. **117**(4): 1473–1486. doi:10.1104/pp.117.4.1473. PMID:9701602.

Hager, A., Menzel, H., and Krauss, A. 1971. Versuche und Hypothese zur Primärwirkung des Auxins beim Streckungswachstum. Planta, **100**(1): 47–75. doi:10.1007/BF00386886.

Halliday, K.J., Martínez-García, J.F., and Josse, E.-M. 2009. Integration of light and auxin signaling. Cold Spring Harb. Perspect. Biol. **1**(6): a001586. doi:10.1101/cshperspect.a001586. PMID:20457562.

Hasenstein, K.H., and Evans, M.L. 1988. Effects of cations on hormone transport in primary roots of *Zea mays*. Plant Physiol. **86**(3): 890–894. doi:10.1104/pp.86.3.890. PMID:11538240.

Hertel, R., Thomson, K.-S., and Russo, V.E.A. 1972. In vitro auxin binding to particulate cell fractions from corn coleoptiles. Planta, **107**(4): 325–340. doi:10.1007/BF00386394.

Hesse, T., Feldwisch, J., Balshüsemann, D., Bauw, G., Puype, M., Vandekerckhove, J., Löbler, M., Klämbt, D., Schell, J., and Palme, K. 1989. Molecular cloning and structural analysis of a gene from *Zea mays* (L.) coding for a putative receptor for the plant hormone auxin. EMBO J. **8**(9): 2453–2461. PMID:2555179.

Hoth, S., Dreyer, I., Dietrich, P., Becker, D., Müller-Röber, B., and Hedrich, R. 1997. Molecular basis of plant-specific acid activation of K^+ uptake channels. Proc. Natl. Acad. Sci. U.S.A. **94**(9): 4806–4810. doi:10.1073/pnas.94.9.4806. PMID:9114073.

Huisinga, B. 1964. Influence of light on growth, geotropism and guthation of *Avena* seedlings grown in total darkness. Acta Bot. Neerl. **13**: 445–487.

Huisinga, B. 1967. Influence of irradiation on the distribution of growth in dark-grown *Avena* seedlings. Acta Bot. Neerl. **16**: 197–201.

Iino, M. 1982*a*. Action of red light on indole-3-acetic-acid status and growth in coleoptiles of etiolated maize seedlings. Planta, **156**(1): 21–32. doi:10.1007/BF00393439.

Iino, M. 1982*b*. Inhibitory action of red light on the growth of the maize mesocotyl: evaluation of the auxin hypothesis. Planta, **156**(5): 388–395. doi:10.1007/BF00393308.

Iino, M. 1995. Gravitropism and phototropism of maize coleoptiles: evaluation of the Cholodny-Went theory through effects of auxin application and decapitation. Plant Cell Physiol. **36**(2): 361–367.

Im, K.H., Chen, J.G., Meeley, R.B., and Jones, A.M. 2000. Auxin-binding protein mutants in maize. Maydica, **45**(4): 319–325.

Jones, A.M. 1990. Location of transported auxin in etiolated maize shoots using 5-azidoindole-3-acetic acid. Plant Physiol. **93**(3): 1154–1161. doi:10.1104/pp.93.3.1154. PMID:16667572.

Jones, A.M., and Herman, E. 1993. KDEL-containing auxin-binding protein is secreted to the plasma membrane and cell wall. Plant Physiol. **101**(2): 595–606. PMID:12231715.

Jones, A.M., and Venis, M.A. 1989. Photoaffinity labeling of indole-3-acetic acid-binding proteins in maize. Proc. Natl. Acad. Sci. U.S.A. **86**(16): 6153–6156. doi:10.1073/pnas.86.16.6153. PMID:16594060.

Jones, A.M., Lamerson, P.M., and Venis, M.A. 1989. Comparison of site I auxin binding and a 22-kilodalton auxin-binding protein in maize. Planta, **179**(3): 409–413. doi:10.1007/BF00391088.

Jones, A.M., Cochran, D.S., Lamerson, P.M., Evans, M.L., and Cohen, J.D. 1991. Red light-regulated growth. I. Changes in the abundance of indoleacetic acid and a 22-kilodalton auxin-binding protein in the maize mesocotyl. Plant Physiol. **97**(1): 352–358. doi:10.1104/pp.97.1.352. PMID:11538374.

Jones, A.M., Im, K.H., Savka, M.A., Wu, M.J., DeWitt, G., Shillito, R., and Binns, A.N. 1998. Auxin-dependent cell expansion mediated by overexpressed auxin-binding protein 1. Science, **282**(5391): 1114–1117. doi:10.1126/science.282.5391.1114. PMID:9804548.

Keller, C.P., and Van Volkenburgh, E. 1996. The electrical response of *Avena* coleoptile cortex to auxins. Evidence in vivo for activation of a Cl^- conductance. Planta, **198**(3): 404–412. doi:10.1007/BF00620057.

King, J.J., Stimart, D.P., Fisher, R.H., and Bleecker, A.B. 1995. A mutation altering auxin homeostasis and plant morphology in Arabidopsis. Plant Cell, **7**(12): 2023–2037. PMID:12242367.

Leblanc, N., David, K., Grosclaude, J., Pradier, J.M., Barbier-Brygoo, H., Labiau, S., and Perrot-Rechenmann, C. 1999. A novel immunological approach establishes that the auxin-binding protein, Nt-abp1, is an element involved in auxin signaling at the plasma membrane. J. Biol. Chem. **274**(40): 28314–28320. doi:10.1074/jbc.274.40.28314. PMID:10497189.

Liu, X., Cohen, J.D., and Gardner, G. 2011. Low-fluence red light increases the transport and bioynthesis of auxin. Plant Physiol. **157**(2): 891–904. doi:10.1104/pp.111.181388. PMID:21807888.

Löbler, M., and Klämbt, D. 1985. Auxin-binding protein from coleoptile membranes of corn (*Zea mays* L.). I. Purification by immunological methods and characterization. J. Biol. Chem. **260**(17): 9848–9853. PMID:2991266.

Lomax, T.L., Muday, G.K., and Rubery, P.H. 1995. Auxin transport. *In* Plant hormones: physiology, biochemistry and molecular biology. *Edited by* P.J. Davies. Kluwer Academic Publishers, Dordrecht, the Netherlands. pp. 509–530.

Maher, E.P., and Bell, C.J. 1990. Abnormal responses to gravity and auxin in mutants of *Arabidopsis thaliana*. Plant Sci. **66**(1): 131–138. doi:10.1016/0168-9452(90)90178-Q.

Marten, I., Lohse, G., and Hedrich, R. 1991. Plant growth hormones control voltage-dependent activity of anion channels plasma membrane of guard cells. Nature, **353**(6346): 758–762. doi:10.1038/353758a0.

Murashige, T., and Skoog, A. 1962. A revised medium for rapid growth and bio assays with tobacco tissue cultures. Physiol. Plant. **15**(3): 473–497. doi:10.1111/j.1399-3054.1962.tb08052.x.

Nagashima, A., Suzuki, G., Uehara, Y., Saji, K., Furukawa, T., Koshiba, T., Sekimoto, M., Fujioka, S., Kuroha, T., Kojima, M., et al. 2008. Phytochromes and cryptochromes regulate the differential growth of *Arabidopsis* hypocotyls in both a PGP10-dependent and a PGP19-independent manner. Plant J. **53**(3): 516–529. doi:10.1111/j.1365-313X.2007.03358.x. PMID:18086281.

Napier, R.M., Venis, M.A., Bolton, M.A., Richardson, L.I., and Butcher, G.W. 1988. Preparation and characterization of monoclonal and polyclonal antibodies to maize membrane auxin-binding protein. Planta, **176**(4): 519–526. doi:10.1007/BF00397659.

Napier, R.M., David, K.M., and Perrot-Rechenmann, C. 2002. A short history of auxin-binding proteins. Plant Mol. Biol. **49**(3–4): 339–348. doi:10.1023/A:1015259130955. PMID:12036258.

Naqvi, S.M. 1975. Kinetics of auxin transport in light and in dark grown *Zea mays* L. coleoptile segments. Zeitschrift Pflanzenphysiol. **76**(5): 379–383.

Palme, K., Hesse, T., Campos, N., Garbers, C., Yanofsky, M.F., and Schell, J. 1992. Molecular analysis of an auxin binding protein gene located on chromosome 4 of *Arabidopsis*. Plant Cell, **4**(2): 193–201. PMID:1321684.

Pěnčík, A., Rolčík, J., Novák, O., Magnus, V., Barták, P., Buchtík, R., Salopek-Sondi, B., and Strnad, M. 2009. Isolation of novel indole-3-acetic acid conjugates by immunoaffinity extraction. Talanta, **80**(2): 651–655. doi:10.1016/j.talanta.2009.07.043. PMID:19836533.

Perrot-Rechenmann, C. 2010. Cellular responses to auxin: division versus expansion. Cold Spring Harb. Perspect. Biol. **2**(5): a001446. doi:10.1101/cshperspect.a001446. PMID:20452959.

Philippar, K., Fuchs, I., Lüthen, H., Hoth, S., Bauer, C.S., Haga, K., Thiel, G., Ljung, K., Sandberg, G., Böttger, M., Becker, D., and Hedrich, R. 1999. Auxin-induced K^+ channel expression represents an essential step in coleoptile growth and gravitropism. Proc. Natl. Acad. Sci. U.S.A. **96**(21): 12186–12191. doi:10.1073/pnas.96.21.12186. PMID:10518597.

Ray, P.M., Dohrmann, U., and Hertel, R. 1977. Specificity of auxin-binding sites on maize coleoptile membranes as possible receptor sites for auxin action. Plant Physiol. **60**(4): 585–591. doi:10.1104/pp.60.4.585. PMID:16660143.

Rayle, D.L., and Cleland, R.E. 1972. The in-vitro acid-growth response: relation to in-vitro growth responses and auxin action. Planta, **104**(4): 282–296. doi:10.1007/BF00386312.

Rayle, D.L., and Cleland, R.E. 1980. Evidence that auxin-induced growth of soybean hypocotyls involves proton excretion. Plant Physiol. **66**(3): 433–437. doi:10.1104/pp.66.3.433. PMID:16661450.

Rayle, D.L., and Cleland, R.E. 1992. The acid growth theory of auxin-induced cell elongation is alive and well. Plant Physiol. **99**(4): 1271–1274. doi:10.1104/pp.99.4.1271. PMID:11537886.

Robert, S., Kleine-Vehn, J., Barbez, E., Sauer, M., Paciorek, T., Baster, P., Vanneste, S., Zhang, J., Simon, S., Čovanová, M., Hayashi, K., Dhonukshe, P., Yang, Z., Bednarek, S.Y., Jones, A. M., Luschnig, A.M., Aniento, F., Zažímalová, E., and Friml, J. 2010. ABP1 mediates auxin inhibition of clathrin-dependent enocytosis in *Arabidopsis*. Cell, **143**(1): 111–121. doi:10.1016/j.cell.2010.09.027. PMID:20887896.

Sauer, M., and Kleine-Vehn, J. 2011. AUXIN BINDING PROTEIN1: the outsider. Plant Cell, **23**(6): 2033–2043. doi:10.1105/tpc.111.087064. PMID:21719690.

Sawers, R.J.H., Linley, P.J., Farmer, P.R., Hanley, N.P., Costich, D.E., Terry, M.T., and Brutnell, T.P. 2002. *Elongated mesocotyl1*, a phytochrome-deficient mutant of maize. Plant Physiol. **130**(1): 155–163. doi:10.1104/pp.006411. PMID:12226496.

Scherer, G.F.E. 2011. AUXIN-BINDING-PROTEIN1, the second auxin receptor: what is the significance of a two-receptor concept in plant signal transduction? J. Exp. Bot. **62**(10): 3339–3357. doi:10.1093/jxb/err033. PMID:21733909.

Schwob, E., Choi, S.-Y., Simmons, C., Migliaccio, F., Ilag, L., Hesse, T., Palme, K., and Söll, D. 1993. Molecular analysis of three maize 22 kDa auxin-binding protein genes—transient promoter expression and regulatory regions. Plant J. **4**(3): 423–432. doi:10.1046/j.1365-313X.1993.04030423.x. PMID:7693132.

Shi, J.H., and Yang, Z.B. 2011. Is ABP1 an auxin receptor yet? Mol. Plant, **4**(4): 635–640. doi:10.1093/mp/ssr050. PMID:21715649.

Shimomura, S., Inohara, N., Fukui, T., and Futai, M. 1988. Different properties of two types of auxin-binding sites in membranes from maize coleoptiles. Planta, **175**(4): 558–566. doi:10.1007/BF00393079.

Sidler, M., Hassa, P., Hasan, S., Ringli, C., and Dudler, R. 1998. Involvement of an ABC transporter in a developmental pathway regulating hypocotyl elongation in the light. Plant Cell, **10**(10): 1623–1636. PMID:9761790.

Sitbon, F., and Perrot-Rechenmann, C. 1997. Expression of auxin-regulated genes. Physiol. Plant. **100**(3): 443–455. doi:10.1111/j.1399-3054.1997.tb03048.x.

Teale, W.D., Paponov, I.A., and Palme, K. 2006. Auxin in action: signalling transport and the control of plant growth and development. Nat. Rev. Mol. Cell Biol. **7**(11): 847–859. doi:10.1038/nrm2020. PMID:16990790.

Tepperman, J.M., Zhu, T., Chang, H.S., Wang, X., and Quail, P.H. 2001. Multiple transcription-factor genes are early targets of phytochrome A signaling. Proc. Natl. Acad. Sci. U.S.A. **98**(16): 9437–9442. doi:10.1073/pnas.161300998. PMID:11481498.

Thomine, S., Lelièvre, F., Boufflet, M., Guern, J., and Barbier-Brygoo, H. 1997. Anion-channel blockers interfere with auxin responses in dark-grown *Arabidopsis* hypocotyls. Plant Physiol. **115**(2): 533–542. doi:10.1104/pp.115.2.533. PMID:9342869.

Tian, Q., and Reed, J.W. 2001. Molecular links between light and auxin signaling pathways. J. Plant Growth Regul. **20**(3): 274–280. doi:10.1007/s003440010022.

Tromas, A., and Perrot-Rechenmann, C. 2010. Recent progress in auxin biology. C. R. Biol. **333**(4): 297–306. doi:10.1016/j.crvi.2010.01.005. PMID:20371104.

Tromas, A., Braun, N., Muller, P., Khodus, T., Paponov, I.A., Palme, K., Ljung, K., Lee, J.-Y., Benfey, P., Murray, J.A.H., Scheres, B., and Perrot-Rechenmann, C. 2009. The AUXIN BINDING PROTEIN 1 is required for differential auxin responses mediating root growth. PLoS ONE, **4**(9): e6648. doi:10.1371/journal.pone.0006648. PMID:19777056.

Van Overbeek, J. 1936. Growth hormone and mesocotyl growth. Recueil. Trav. Bot. Neerl. **33**: 333–340.

Vanderhoef, L.N., and Briggs, W.R. 1978. Red light-inhibited mesocotyl elongation in maize seedlings. Plant Physiol. **61**(4): 534–537. doi:10.1104/pp.61.4.534. PMID:16660331.

Vanneste, S., and Friml, J. 2009. Auxin: a trigger for change in plant development. Cell, **136**(6): 1005–1016. doi:10.1016/j.cell.2009.03.001. PMID:19303845.

Walton, J.D., and Ray, P.M. 1981. Evidence for receptor function of auxin binding sites in maize. Red light inhibition of mesocotyl elongation and auxin binding. Plant Physiol. **68**(6): 1334–1338. doi:10.1104/pp.68.6.1334. PMID:16662103.

Xu, T., Wen, M., Nagawa, S., Fu, Y., Chen, J.-G., Wu, M.-J., Perrot-Rechenmann, C., Friml, J., Jones, A.M., and Yang, Z. 2010. Cell surface- and Rho GTPase-based auxin signaling controls cellular interdigitation in *Arabidopsis*. Cell, **143**(1): 99–110. doi:10.1016/j.cell.2010.09.003. PMID:20887895.

Zažímalová, E., Murphy, A.S., Yang, H., Hoyerová, K., and Hošek, P. 2010. Auxin transporters—why so many? Cold Spring Harb. Perspect. Biol. **2**(3): a001552. doi:10.1101/cshperspect.a001552. PMID:20300209.

Zimmermann, S., Thomine, S., Guern, J., and Barbier-Brygoo, H. 1994. An anion current at the plasma membrane of tobacco protoplasts shows ATP-dependent voltage regulation and is modulated by auxin. Plant J. **6**(5): 707–716. doi:10.1046/j.1365-313X.1994.6050707.x.

Fig.1-Suppl.

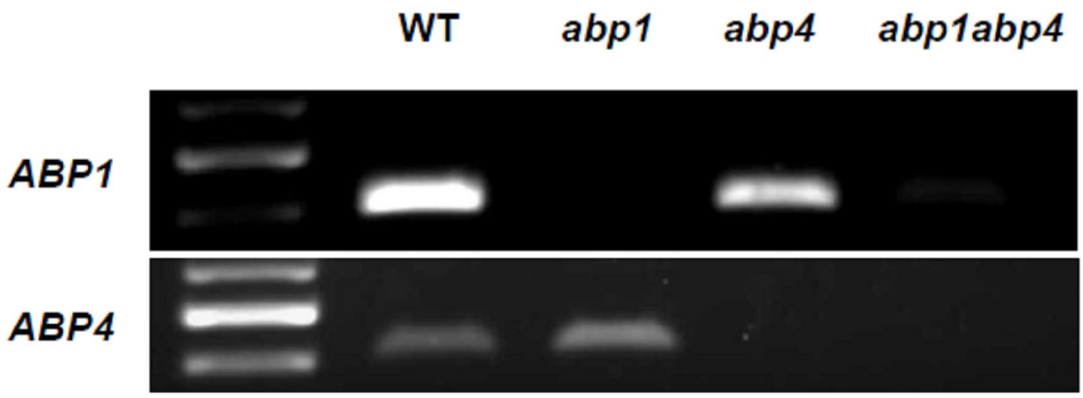

Supplemental Fig. 1, RT-PCR analysis of the absence and/or presence of *ABP1* and *ABP4* transcripts in knockout maize single mutants *abp1*, *abp4* and double mutant *abp1abp4*, and in the corresponding WT. Seedlings were grown in darkness in a growth chamber for one week. The procedures of RNA purification, cDNA synthesis and RT-PCR were the same as described by Fellner et al. (2006) with slight modification mentioned in Material and Methods. Using specific primers, PCR products (ABP1 and ABP4, both 403 bp in size) were size fractionated by electrophoresis in a 1% (w/v) agarose gel stained with ethidium bromide.